

# University of Alberta

Mechanistic Insight Into the Role of FABP7 in Malignant Glioma

by

Michael Beaulieu

A thesis submitted to the Faculty of Graduate Studies and Research in  
partial fulfillment of the requirements for the degree of

Master of Science

in

Experimental Oncology

Department of Oncology

©Michael Beaulieu

Fall 2012

Edmonton, Alberta

Permission is hereby granted to the University of Alberta Libraries to reproduce single copies of this thesis and to lend or sell such copies for private, scholarly or scientific research purposes only.

Where the thesis is converted to, or otherwise made available in digital form, the University of Alberta will advise potential users of the thesis of these terms.

The author reserves all other publication and other rights in association with the copyright in the thesis and, except as herein before provided, neither the thesis nor any substantial portion thereof may be printed or otherwise reproduced in any material form whatsoever without the author's prior written permission.

*For Bunkey*

## **ABSTRACT**

Malignant gliomas (MG) are the most common and aggressive brain cancers. FABP7 is an intracellular lipid trafficking molecule whose expression correlates with reduced MG patient survival. FABP7 has been shown to increase the migratory behaviour of MG cells. Moreover, the migratory behaviour of FABP7-positive MG cells is mediated by ligands of FABP7. We hypothesize that FABP7 plays a central role in stabilizing the aggressive behaviour of MG cells in a manner that is dependent on the COX-2 pathway.

Here, we demonstrate that FABP7 alters the gene expression profile of MG cells, and the expression of potent inflammatory mediators. We provide evidence for a ligand-specific interaction between FABP7 and PPAR- $\beta/\delta$ , which could have consequences in mediating FABP7-dependent gene expression. We also demonstrate a role for FABP7 in modulating the AA and DHA content of nuclear phospholipid classes, and suggest that DHA maybe useful for treatment of MG.

# Table of Contents

<b>CHAPTER 1: INTRODUCTION.....</b>	<b>1</b>
1.1 MALIGNANT GLIOMA .....	2
1.1.1 Standard of care for MG.....	2
1.1.2 Molecular analysis of MG .....	5
1.1.3 MG: cell of origin .....	8
1.2 FATTY ACID-BINDING PROTEINS .....	12
1.2.1 FABPs: structure and ligand binding.....	16
1.2.2 Functional roles for FABPs.....	19
1.2.3 FABP7 in cancer.....	21
1.3 FATTY ACIDS.....	24
1.3.1 Essential fatty acids in cell signaling.....	24
1.3.2 EFAs in cancer.....	27
1.4 PEROXISOME PROLIFERATOR-ACTIVATED RECEPTORS (PPARs).....	28
1.4.1 Fatty acids, FABPs and PPARs .....	30
1.4.2 PPARs in cancer .....	31
1.5 CYCLOOXYGENASE (COX).....	33
1.5.1 Regulation of COX-1 and COX-2 .....	36
1.5.2 Ligands for COX.....	40
1.5.3 COX-2 in MG.....	41
1.6 WORKING HYPOTHESIS .....	45
<b>CHAPTER 2: MATERIALS AND METHODS .....</b>	<b>47</b>
2.1. STABLE TRANSFECTION OF U87 CELLS .....	48
2.2 CELL CULTURE .....	48
2.3 PREPARATION OF FATTY ACIDS.....	48
2.4 GENE EXPRESSION MICROARRAY ANALYSIS .....	49
2.5 REVERSE TRANSCRIPTION-PCR (RT-PCR) ANALYSIS OF MICROARRAY DATA .....	49
2.6 WESTERN BLOT ANALYSIS .....	51
2.7 CO-IMMUNOPRECIPITATIONS (CO-IP) .....	52
2.8 ENZYME-LINKED IMMUNOSORBENT ASSAY (ELISA).....	53
2.9 LIVE CELL IMAGING OF PGE <sub>2</sub> -TREATED U87B CELLS .....	53
2.10 ISOLATION OF NUCLEI FROM U87C AND U87B.....	54
2.11 ISOLATION OF LIPIDS FROM CELLS AND NUCLEI .....	55
2.12 PHOSPHOLIPID ANALYSIS.....	56
<b>CHAPTER 3: RESULTS .....</b>	<b>57</b>
3.1 GENE EXPRESSION ANALYSIS OF FABP7(-) VERSUS FABP7(+) U87 MG CELLS .....	58
3.1.1 Stable expression of FABP7 alters the gene expression profile of U87 cells.....	58
3.1.2 RT-PCR analysis of U87C versus U87B cell lines identifies potential mechanisms of FABP7-dependent MG cell migration .....	58
3.1.3 A potential ligand-dependent interaction between FABP7 and PPAR-β/δ.....	67
3.2 COX-2 EXPRESSION AND ACTIVITY IN U87C AND U87B MG CELLS .....	70
3.2.1 FABP7 increases COX-2 expression and activity in U87 MG cells .....	70
3.2.2 The effect of PGE <sub>2</sub> treatment on U87B cells.....	74
3.3.1 AA AND DHA INCORPORATION INTO THE PHOSPHOLIPIDS OF U87C VERSUS U87B CELLS .....	76
3.3.2 AA and DHA incorporation into the nuclear phospholipids of U87C versus U87B cells.....	82

<b>CHAPTER 4: DISCUSSION</b> .....	<b>90</b>
4.1 DISCUSSION.....	91
4.1.1 <i>Malignant Glioma: Picking up the pieces</i> .....	91
4.1.2 <i>FABP7 provides insight into MG tumour behaviour</i> .....	93
4.1.3 <i>AA and DHA content of phospholipid classes in U87C and U87B MG cells</i> .....	104
4.1.4 <i>Future directions</i> .....	110
4.1.5 <i>Conclusions</i> .....	113
4.1.6 <i>References</i> .....	115

## List of Tables

<b>Table:</b>	<b>Title</b>	<b>Page</b>
<b>1.1:</b>	Original and numerical naming systems for FABPs .....	15
<b>3.1:</b>	A selection of genes that are differentially expressed in U87C compared to U87B MG cells based on cDNA microarray data .....	60

## List of Figures

Figure: Title	Page
1.2.1: Crystal structure of FABP7 bound to DHA .....	17
1.5.1: COX activity in the cell .....	34
3.1.1: Differential expression of PPAR- $\beta/\delta$ and PPAR- $\gamma$ in FABP7-expressing U87 MG cells .....	62
3.1.2: Differential expression of COX-1, COX-2, PLA2G4A and PLA2G4C in FABP7-expressing U87 MG cells .....	63
3.1.3: Increased expression of MMPs in FABP7-expressing U87 MG cells .....	65
3.1.4: Differential gene expression profile in U87C versus U87B MG cell lines..	66
3.1.5: Potential ligand-dependent interaction of FABP7 and PPAR- $\beta/\delta$ in U87 MG cells.....	69
3.2.1: COX-2 levels and PGE <sub>2</sub> production are up-regulated upon FABP7 expression in U87 MG cells .....	71
3.2.2: PLA2G4A levels are elevated in U87B compared to U87C MG cells .....	73
3.2.3: The response of U87B cells to PGE <sub>2</sub> .....	75
3.3.1: DHA and AA content of phospholipids purified from U87C and U87B MG cells treated with BSA .....	78
3.3.2: The DHA and AA content of phospholipid classes is increased in both U87C and U87B MG cells when treated with DHA and AA .....	79
3.3.3: Effect of DHA and AA treatment on DHA and AA content, respectively, of PS in U87C and U87B cells .....	80
3.3.4: Effect of DHA and AA treatment on DHA and AA content, respectively, of PE in U87C and U87B cells .....	81
3.3.5: DHA and AA content of phospholipid classes in nuclei of U87C and U87B MG cells treated with BSA .....	84
3.3.6: The DHA and AA content of nuclear phospholipid classes is increased in U87C and U87B MG cells treated with DHA or AA .....	85
3.3.7: Effect of DHA and AA treatment on DHA and AA content, respectively, of PS in U87C and U87B nuclei .....	87
3.3.8: Effect of DHA and AA treatment on DHA and AA content, respectively, of PE in U87C and U87B nuclei .....	88
3.3.9: FABP7-dependent changes in DHA and AA content of nuclear PC .....	89
4.1.1: Potential role for FABP7 in stabilizing multiple positive feedback loops for COX-2-mediated glioma growth, survival and migration .....	102
4.1.2: Model of the role of FABP7 in COX-2 signaling in malignant glioma cells .....	109

## List of Abbreviations

<u>Abbreviation</u>	<u>Full name</u>
<b>AA</b>	arachidonic acid
<b>aa</b>	amino acid
<b>AD</b>	adenylate cyclase
<b>ATX</b>	autotaxin
<b>BCNU</b>	bis-chloroethylnitrosourea
<b>BF3</b>	boron trifluoride
<b>BSA</b>	bovine serum albumin
<b>cAMP</b>	cyclic adenosine monophosphate
<b>cc</b>	cubic centimeter
<b>CDH18</b>	cadherin 18
<b>cDNA</b>	complementary deoxyribonucleic acid
<b>CNS</b>	central nervous system
<b>COX</b>	cyclooxygenase
<b>CREB</b>	cAMP response element-binding protein
<b>CSC</b>	cancer stem cell
<b>DC</b>	dendritic cell
<b>DHA</b>	docosahexaenoic acid
<b>DIC</b>	differential interference contrast
<b>DMEM</b>	Dubelcco's modified essential medium
<b>DNA</b>	docosahexaenoic acid
<b>DTT</b>	dithiothreitol
<b>ECL</b>	enhanced chemiluminescence
<b>EFA</b>	essential fatty acid
<b>EGFR</b>	epidermal growth factor receptor
<b>ELISA</b>	enzyme-linked immunosorbent assay
<b>EPA</b>	eicosapentaenoic acid
<b>ER</b>	endoplasmic reticulum
<b>ERAD</b>	endoplasmic reticulum associated degradation
<b>ERK1/2</b>	extracellular regulated kinase 1/2
<b>FABP</b>	fatty acid-binding protein
<b>FCS</b>	fetal calf serum
<b>FFA</b>	free fatty acid
<b>GBM</b>	glioblastoma multiforme
<b>GFAP</b>	glial fibrillary acidic protein

<b>GFP</b>	green fluorescent protein
<b>GSC</b>	glioma stem cell
<b>Gy</b>	Gray
<b>HDAC</b>	histone deacetylase
<b>HIF1a</b>	hypoxia-inducible factor 1a
<b>HLA-DMA</b>	human lymphocyte antigen DMA
<b>HSL</b>	hormone sensitive lipase
<b>HTH</b>	helix-turn-helix
<b>IDH1</b>	isocitrate dehydrogenase 1
<b>INK4A</b>	cyclin-dependent kinase inhibitor 2A
<b>IP</b>	immunoprecipitation
<b>IP3</b>	inositol 1,4,5-trisphosphate
<b>ITC</b>	isothermal titration calorimetry
<b>JAK2</b>	Janus kinase 2
<b>Da</b>	dalton
<b>KO</b>	knock out
<b>L1CAM</b>	L1 cellular adhesion molecule
<b>LCFA</b>	long chain fatty acid
<b>LOH</b>	loss of heterozygosity
<b>LPA</b>	lysophosphatidate
<b>LPC</b>	lysophosphatidylcholine
<b>M</b>	molar
<b>MAPK</b>	mitogen-activated protein kinase
<b>MG</b>	malignant glioma
<b>MGMT</b>	O-6-methylguanine-DNA methyltransferase
<b>MHC II</b>	major histocompatibility complex II
<b>MMP</b>	matrix metalloproteinase
<b>MRG</b>	mammary-derived growth inhibitor
<b>MRI</b>	magnetic resonance imaging
<b>mRNA</b>	messenger ribonucleic acid
<b>NFI</b>	nuclear factor 1
<b>NFkB</b>	nuclear factor kB
<b>NPC</b>	neural progenitor cell
<b>NSAID</b>	non-steroidal anti-inflammatory drug
<b>OPC</b>	oligodendrocyte precursor cell
<b>PBS</b>	phosphate-buffered saline
<b>PC</b>	phosphatidylcholine
<b>PE</b>	phosphatidylethanolamine

<b>PGE2</b>	prostaglandin E2
<b>PI</b>	phosphatidylinositol
<b>PI3K</b>	phosphatidylinositol 3-kinase
<b>PKA</b>	protein kinase A
<b>PKC</b>	protein kinase C
<b>PLA2G4A</b>	phospholipase A2 group 4A
<b>PLA2G4C</b>	phospholipase A2 group 4C
<b>PLC</b>	phospholipase C
<b>PLSCR4</b>	phospholipid scramblase 4
<b>PMSF</b>	phenylmethanesulfonylfluoride
<b>PP</b>	peroxisome proliferator
<b>PPAR</b>	peroxisome proliferator-activated receptor
<b>PPRE</b>	peroxisome proliferator-responsive element
<b>PRKCZ</b>	protein kinase C zeta
<b>PS</b>	phosphatidylserine
<b>PTEN</b>	phosphatase and tensin homolog
<b>PTGER</b>	prostaglandin E2 receptor
<b>PUFA</b>	polyunsaturated fatty acid
<b>rpm</b>	revolutions per minute
<b>RT</b>	radiation therapy
<b>RTK</b>	receptor tyrosine kinase
<b>RT-PCR</b>	reverse transcription-polymerase chain reaction
<b>RXR</b>	retinoic acid receptor
<b>SD</b>	standard deviation
<b>SDS</b>	sodium dodecylsulphate
<b>STAT</b>	signal transducer and activator of transcription
$\tau_{1/2}$	half life
<b>TAA</b>	tumour-associated antigen
<b>Th</b>	helper T cell
<b>TMZ</b>	temazolamide
<b>TNBC</b>	triple-negative breast cancer
<b>TNFR</b>	tumour necrosis factor receptor
<b>TPA</b>	12-0-tetradecanoylphorbol-13-acetate
<b>Tr</b>	regulatory T cell
<b>UV</b>	ultraviolet
<b>VEGF</b>	vascular endothelial growth factor
<b>WHO</b>	World Health Organization

# **CHAPTER 1**

## **Introduction**

## 1.1 Malignant Glioma

Tumours that arise from the central nervous system (CNS) are a particularly deadly set of malignancies that vary widely in their characteristics and behaviour. Gliomas are the most common type of primary brain tumour and represent approximately 60% of all CNS malignancies. While these tumours have a relatively low yearly incidence (~3.0/100,000 persons in North America; Easaw *et al.*, 2011), they pose some of the greatest challenges for cancer survival.

It is estimated that more than 80% of glial tumours are astrocytomas - a name that reflects the morphological similarities of the tumour cells to astrocytes of the CNS. The use of several histological criteria: cytological atypia, mitotic index, anaplasia, microvascular proliferation and necrosis, guide the grading of astrocytic tumours into low-grade astrocytomas (WHO grades I and II) and high-grade astrocytomas (WHO grades III and IV; Louis *et al.*, 2007). Grades III and IV astrocytomas (anaplastic astrocytoma and glioblastoma multiforme (GBM), respectively) are referred to as malignant glioma (MG) and are among the most aggressive cancers. In accordance with this, current treatment strategies for MG aim to be equally aggressive.

### 1.1.1 Standard of care for MG

The current standard of care for persons >18 years of age who are diagnosed with either grade III or grade IV astrocytoma is surgical

resection followed by adjuvant radiation and chemotherapy. Initially, surgical resection of the tumour mass is used to obtain symptom relief and tissue for a more refined diagnosis. Though it is a topic for debate, maximal resection of the tumour mass is preferred to biopsy alone as it tends to increase the overall quality of life of patients (Tsitlakidis *et al.*, 2010). For patients with newly diagnosed GBM, adjuvant chemo- and radiation therapy is highly recommended following surgery. In fact, delaying the time between diagnosis and receiving radiotherapy (RT) by as little as one week is associated with shorter survival times (Irwin *et al.*, 2007). The current standard for RT is 60 Gy to the local tumour mass over a period of six weeks. Radiation doses as high as 90 Gy have been tested, but there has been no significant increase in overall survival in patients receiving more than 60 Gy (Chan *et al.*, 2002). Despite the fact that surgery and RT can increase quality of life and prolong survival, these treatments are rarely curative in MG. As a result, most patients with MG also undergo chemotherapy.

The advantages of chemotherapy over surgery and RT are based on the ability of chemotherapeutic agents to target cancer cells that may be distal to the primary tumour mass. In fact, treating MG tumours with alkylating agents, such as temozolomide (TMZ), has led to improvements in patient survival. Esteller *et al.* showed that methylation of the promoter region of the gene, O<sup>6</sup>-methylguanine-DNA methyltransferase (*MGMT*) is a predictor of MG tumour responsiveness to alkylating agents (Esteller *et*

*al.* 2000). Alkylating agents add bulky adducts to the DNA, which causes mutations in the DNA. As a consequence, the DNA repair mechanisms of a cell can be overwhelmed, forcing it to undergo apoptosis. MGMT removes these bulky adducts from the DNA, reducing the mutation frequency of the DNA sequence. Hence, MGMT minimizes the amount of DNA damage that can occur in a cancer cell in response to alkylating agents. A randomized phase II clinical trial comparing GBM patients receiving RT + TMZ versus RT alone showed that the overall one year survival time was increased in the TMZ-treated group compared to those who received RT alone (56.3% vs. 15.7% respectively; Athanassiou *et al.* 2005). In a large-scale phase III clinical trial, GBM patients receiving RT + TMZ achieved a 5-year overall survival rate of 9.8% compared to 1.9% in patients receiving RT alone; however, progression-free survival at 5 years was low in both groups (4.1% in the RT + TMZ group compared to 1.3% in the RT group; Stupp *et al.*, 2009). These data were further stratified based on *MGMT* methylation status and this showed that patients whose *MGMT* promoter was unmethylated had higher survival rates than those with methylated *MGMT* (Stupp *et al.*, 2009). However, as all patients benefited to some extent from TMZ treatment, RT + TMZ is highly recommended for the treatment of MG regardless of *MGMT* methylation status. Nevertheless, determination of *MGMT* methylation status is still of prognostic value.

Despite these aggressive treatment strategies, the prognosis for MG remains dismal, with the majority of patients succumbing to their disease by 5 years (Stupp *et al.*, 2009). This lethality is thought to be due to the infiltrative nature of MG cells. Interestingly, even low-grade gliomas have a tendency to infiltrate surrounding brain tissue and almost always recur as MG (Louis, DN., 2006). As such, a distinction is made between 'secondary' MG that arise from low-grade astrocytomas and 'primary' MG (~90% of all GBM), which occur without previous indication of disease (Furnari *et al.*, 2007). The importance of this distinction was not immediately recognized since these tumours appear to be identical. In Watanabe *et al.* (1996), it was shown that mutually exclusive genetic lesions were associated with primary versus secondary MG (Watanabe *et al.* 1996). These data are further supported by genomic and transcriptomic analyses (Maher *et al.*, 2006 and Tso *et al.*, 2006) and it is now recognized that primary and secondary MG have different pathologies. The ability to distinguish between subtypes of MG may suggest new treatment strategies, or identify groups of patients who are more likely to benefit from certain treatment modalities. This highlights the importance of identifying molecular subtypes of MG.

### *1.1.2 Molecular analysis of MG*

Large-scale genomic analyses have shown that MG are very heterogeneous in their genetics and response to therapy. In fact, MG even

show distinct genetic aberrations at different locations within the same tumour (Bonavia *et al.*, 2011a). As such, it has been difficult to identify key pathways in their tumorigenesis and progression. Some early success in identifying these pathways has been obtained through cytologic and genetic analysis, and these studies are now being complemented by large-scale genomic analysis.

Loss of phosphatase-tensin homology (*PTEN*) function is a common genetic lesion observed in primary MG. *PTEN* is a phosphatase that antagonizes the phosphoinositide-3-kinase (PI3K) pathway. *PTEN* dephosphorylates the secondary messenger phosphatidylinositol-(3,4,5)-triphosphate (IP<sub>3</sub>), a substrate for Akt, and thereby supports apoptosis. Loss of *PTEN* function results in uncontrolled IP<sub>3</sub> production by PI3K, and this activates cell survival signals through Akt (Franke *et al.*, 1997, Salmena *et al.*, 2008). In a large-scale analysis of GBM tumours, homozygous deletions of *PTEN* were reported in 16/143 cases, whereas high-throughput sequencing analysis of 91 primary GBM showed that 29/91 tumours contained somatic mutations in *PTEN*, confirming that inactivating mutations in *PTEN* are more common in MG than deletion of the gene (TCGA, 2008).

The most common genetic alteration in primary MG is over-expression of the epidermal growth factor receptor (*EGFR*; TCGA, 2008). *EGFR* is a member of the receptor tyrosine kinase (RTK) family of proteins that transmit growth signals in the cell via PI3K-Akt signaling

networks. *EGFR* is also frequently mutated in MG where expression of the constitutively active variant, *EGFRvIII*, results in uncontrolled cell proliferation via PI3K-Akt signaling (Huang *et al.*, 1997, Narita *et al.*, 2002). In a recent study, sequencing of 91 primary GBM specimens showed that 38/91 GBM tumours had amplification of *EGFR*. In addition, 80/91 tumours had genetic aberrations in RTK-Ras-PI3K-Akt signaling networks (TCGA, 2008). Given these data, it is likely that this signaling network is important for MG; however, there are many associated difficulties with targeting RTK pathways as a cancer therapy (Huang *et al.*, 2009).

Genomic studies have identified combinations of genes that are commonly altered in MG. Four major molecular subtypes of MG have been identified in humans: proneural (PN), neural (N), classical (CL), and mesenchymal (MES; Verhaak *et al.*, 2010). Impressively, the PN gene signature has been identified by independent studies (Li *et al.*, 2009; Gravendeel *et al.*, 2009; Verhaak *et al.*, 2010). The molecular analysis reported by Verhaak *et al.* (2010) showed that amplifications and mutations in the platelet derived growth factor receptor A (*PDGFRA*) gene were most frequent in the PN subtype. PN tumours are also characterized by their high expression of *PDGFRA*, mutations in isocitrate dehydrogenase 1 (*IDH1*), and their high expression of oligodendrocytic development genes (Verhaak *et al.*, 2010). This genetic background is in contrast to that of the CL subtype. MG classified as CL show high

expression and mutation of *EGFR*. This subclass shows high expression of genes involved in Notch and Sonic hedgehog signaling pathways, as well as markers for neural progenitor and stem cells (Verhaak *et al.*, 2010). From these data it is clear that MG are heterogeneous in their genetics, but it is not clear as to how this diversity came to be. The sub-classification of glioma into molecular subtypes seems to indicate that certain MG tumours arise from very different sources. If we can exploit the properties of the cells that give rise to MG, then it may be possible to undermine the basic nature of MG tumours.

### *1.1.3 MG: cell of origin*

MG rapidly develop resistance to targeted therapies, which is likely a consequence of the diverse molecular profiles of the cells that make up the tumour (Huang *et al.*, 2009; Lei *et al.*, 2011). If we gain a better understanding of the cellular processes that are integral to MG initiation and progression, then we may be able to develop novel treatment strategies for these tumours. Therefore, it is important to understand the origins of this diversity.

The theory of somatic mutation proposes that malignant cells in a tumour are derived from a single replication-competent cell (the cell of origin) that has accumulated mutations in key regulators of the cell cycle. Mutations that accumulate in the cell of origin drive genetic instability, and in doing so, generate a population of cells associated with the malignancy

(Greaves and Maley, 2012). In MG, the cell of origin has long been a topic for debate. Astrocytes were long believed to be the cell of origin in MG since: (i) prior to the discovery of adult neural stem cells, astrocytes were the only cells in the mature brain that were known to be capable of replicating (Chen *et al.*, 2012); (ii) astrocytes and MG cells share remarkably similar morphological characteristics; and (iii) MG express the astrocyte marker, glial fibrillary acidic protein (GFAP; Yang *et al.*, 1994).

More recent studies have demonstrated that gliomas can arise from astrocytes *in vivo*. Uhrbom *et al.* used *Arf/Ink4A* knock-out mice in conjunction with virally-induced oncogenic stimulation of *K-ras* to show that gliomas can develop from either astrocytes or glial progenitor cells, the former giving rise to the more malignant disease (Uhrbom *et al.*, 2005). Despite this evidence, proving that astrocytes are the cell of origin in MG remains difficult. As a case in point, GFAP was originally thought to be expressed only in mature astrocytes, but evidence now shows that precursors to astrocytes also express GFAP (Garcia *et al.*, 2004). Since GFAP is used to track astrocytes in these MG tumour models, it is not clear whether the tumours are directly derived from astrocytes or their precursors.

The presence of another replication-competent cell in the adult mammalian brain raises the possibility of an alternative cell of origin in MG. Neural progenitor cells (NPCs) have self-renewal capacity, the ability to differentiate along multiple lineages, and a natural advantage for

accumulating oncogenic mutations as they are proliferative (Zhu *et al.*, 2005; Zhao *et al.*, 2008; Chen *et al.*, 2012). Alcantara Llaguno *et al.* used a conditional knock-out system in mouse brain to show that the disruption of a set of tumour suppressors in NPCs results in MG formation (Alcantara Llaguno *et al.*, 2009). Interestingly, this effect was not observed when these tumour suppressors were altered in non-neurogenic brain tissue (Alcantara Llaguno *et al.*, 2009). Similar results from other groups support the idea that genetic alterations in NPCs are necessary and sufficient for MG formation (Jacques *et al.*, 2010; Liu *et al.*, 2011).

In further dissecting the role of NPCs in MG, Liu *et al.* used mosaic analysis with double markers to trace cell lineages and showed that a subset of NPCs, the oligodendrocyte precursor cells (OPCs), consistently gave rise to MG tumours (Liu *et al.*, 2011). In light of these findings, it is reasonable to suppose that the MG cell of origin is a common precursor to astrocytes and oligodendrocytes. In fact, Godbout *et al.* showed that MG tumours and cell lines that express a NPC marker, brain fatty acid-binding protein (FABP7; B-FABP), also express the astrocyte marker *GFAP* (Godbout *et al.*, 1998). This implicates a radial glial cell as the cell of origin in MG.

Radial glial cells are the precursors to neurons, astrocytes and oligodendrocytes, and are essential for CNS development. *FABP7*-positive radial glia form long processes that infiltrate the brain tissue, and acts as a scaffold for migrating neurons (Feng *et al.*, 1994; Patten *et al.*,

2006). The mechanisms underlying the formation of these processes are complex, involving both physical and biochemical interactions (Hatten *et al.*, 1985; Feng and Heintz, 1995; Patten *et al.*, 2006). Interestingly, Notch signaling has been shown to positively regulate FABP7 expression in radial glia, which is required for radial glial process formation and regulation of radial glial differentiation (Anthony *et al.*, 2005; Feng *et al.*, 1994; Patten *et al.*, 2003; Patten *et al.*, 2006). In regards to glioma, overexpression of various components of the Notch pathway is associated with secondary GBM, and downregulation of *Notch1* inhibits glioma formation in mice (Stockhausen *et al.*, 2012; Mei *et al.*, 2011). Furthermore, FABP7-positive cells are located at infiltrating margins of MG tumours, and expression of FABP7 in MG cell lines is associated with the formation of radial glia-like processes and increased cell migration (Mita *et al.*, 2007). Notch and FABP7 also appear to be associated with EGFR in MG (Stockhausen *et al.*, 2012; Patten *et al.*, 2003; Liang *et al.*, 2006). The interrelation of these pathways in glioma is characteristic of their interactions in radial glia during normal CNS development. It is also remarkable that the invasive properties of radial glia are in-line with the behaviour of MG cells. In fact, invasion of MG cells is thought to precede tumour mass formation, which further supports the naturally invasive radial glial cell being the cell of origin of MG tumours (Sampetean *et al.*, 2011).

The cellular heterogeneity found in MG tumours can also be explained by the cancer stem cell (CSC) hypothesis. The underlying tenet

of the CSC hypothesis is that only a small fraction of the tumour cell population has the ability to form a tumour *de novo*, and that CSCs are responsible for maintaining the tumour cell diversity. Glioma stem cells (GSCs) were one of the first CSCs observed in solid tumours. Singh *et al.* showed that as few as 100 CD133<sup>+</sup> cells isolated from a human MG were capable of forming a tumour in the brains of immunocompromised mice (Singh *et al.*, 2004). In contrast, 100,000 of the CD133<sup>-</sup> cells were unable to form MG tumours (Singh *et al.*, 2004). There is also evidence showing that GSCs are responsible for the recurrence of MG and its resistance to treatment, which suggests that GSCs may be crucial targets for future therapies (Bao *et al.*, 2006; Beier *et al.*, 2011; Kim *et al.*, 2011). In fact, there are already new lines of therapeutic approaches to MG based on GSCs (Piccirillo *et al.*, 2006; Gil-Ranedo *et al.*, 2011; Wang *et al.*, 2012; Yang *et al.*, 2012). These are novel treatment strategies, but unfortunately, our progress in developing these therapies has been hindered by our understanding of GSC biology (Chen *et al.*, 2012). Thus, the hope remains that the 'cells of origin' in MG could be exploited, leading to new options for MG therapy.

## **1.2 Fatty Acid-binding Proteins**

Fatty acids are essential components of cell membranes and are used by the cell for metabolic energy, signaling and regulation of gene expression. Structurally, they consist of a carboxylic acid 'head' group and

a hydrophobic 'tail' of carbon atoms, which imparts fatty acids with an overall hydrophobic character. From the cell's perspective, this presents a problem. How is a cell able to transport these important hydrophobic molecules through a hydrophilic environment like the cytosol? This is the role of fatty acid-binding proteins (FABPs). FABPs are, in a sense, the intracellular chaperones for fatty acids. The expression of 10 members of the FABP family have been documented in mammals (Hauerland and Spener, 2004; Liu *et al.*, 2008), and a combination of FABPs are expressed in nearly every tissue (Hauerland and Spener, 2004). Originally, FABPs were named according to the tissues from which they were first isolated or in which they were predominantly expressed (i.e. A-FABP in adipose tissue, B-FABP in brain), but it is now known that the expression of a particular FABP is not limited to just one tissue. Accordingly, a numerical naming system has been introduced to avoid confusion (Hertzel and Bernlohr, 2000; Storch and Thumser, 2010) (Table 1.1). Moreover, FABPs exhibit a wide range of spatio-temporal expression patterns, which suggests that they may be key regulators of processes including, but not limited to: metabolism, gene expression, and cell signaling.

Little is known about the genetic regulation of FABPs. Their specific tissue distribution patterns have led to speculation that the presence of a particular FABP is a reflection of the lipid-metabolizing capacity of the tissue in which it is found. Indeed, FABPs make up between 1% and 5%

of the soluble cytosolic fraction in liver, heart and adipose tissue and these values increase during lipid influx (Hauerland and Spener, 2004). There have been some reported successes in linking fatty acid metabolism to FABP expression. The peroxisome proliferator-activated receptor (PPAR) family of transcription factors appears to regulate the lipid-dependent expression of FABPs in certain tissues and most FABP genes contain PPAR regulatory elements in their promoter region (see 1.2.2 and 1.4). These FABP properties are in contrast to those observed for FABP7.

FABP7 is highly expressed in the brain during neuronal development even though lipid catabolism is not the primary source of energy in this tissue (Feng and Heintz, 1995; Thorens, 2012). Various pathways and transcription factors have been shown to regulate FABP7 expression, including: PAX6, Notch, OCT1/6, BRN2 (Liu *et al.*, 2012; Arai *et al.*, 2005; Anthony *et al.*, 2005; Takaoka *et al.*, 2011). Brun *et al.* showed a complex role for the family of transcription factors, nuclear factor 1 (NFI), in directly regulating *FABP7* expression in MG cell lines (Brun *et al.*, 2009). This control of *FABP7* expression may be further regulated by differential phosphorylation of NFI (Bisgrove *et al.*, 2000). The scope of complexity of *FABP7* expression also extends beyond the transcriptional level, as its expression is both spatially and temporally regulated in some astrocytes (Gerstner *et al.*, 2006; Gerstner *et al.*, 2012). Given these complex patterns of genetic regulation, it is likely that FABP7 plays a very important role in brain function.

<i>Source Tissue</i>	<i>Original Name (Numerical Name)</i>
Liver	L-FABP (FABP1)
Intestinal	I-FABP (FABP2)
Heart	H-FABP (FABP3)
Adipocyte	A-FABP (FABP4)
Epidermal	E-FABP (FABP5)
Ileal	IL-FABP (FABP6)
Brain	B-FABP (FABP7)
Myelin	M-FABP (FABP8)
Testicular	T-FABP (FABP9)
Testicular and retina	FABP12

**Table 1.1 Original and numerical naming systems for FABPs.**

### 1.2.1 FABPs: structure and ligand binding

There is a highly variable degree of amino acid sequence homology among members of the FABP family. Despite this, they share a highly conserved tertiary structure (Figure 1.2.1A). All FABPs are characterized by a  $\beta$ -barrel domain that consists of 2  $\beta$ -sheets that are sandwiched together to form the hydrophobic ligand-binding pocket (Balendiran *et al.*, 2000). It is thought that the variability in the primary structure of FABPs may be indicative of their distinct ligand preferences (Liu *et al.*, 2010). In support of this, crystallographic analysis of FABP7 has shown that unique residues present in the FABP7 binding pocket interact with the distinguishing features of its polyunsaturated fatty acid (PUFA) ligands (Balendiran *et al.*, 2000; Figure 1.2.1B).

The tertiary structure of FABPs also contains a helix-turn-helix (HTH) domain that covers the entrance to the binding pocket. This domain mediates ligand transfer between FABPs and cell membranes (Liou and Storch, 2001; Corsico *et al.*, 2004) and, more recently, has been proposed to be involved in protein-protein interactions. Smith *et al.* (2008) showed that a charge quartet located in the HTH domain of FABP4 is responsible for its physical interaction with hormone sensitive lipase (HSL; Smith *et al.*, 2008). This interaction also appears to be dependent on whether or not FABP4 is bound to its fatty acid ligand (Smith *et al.*, 2008). In addition to these data, the same charge quartet was also shown to be involved in fatty acid-dependent interaction of FABP4 with JAK2 (Thompson *et al.*,

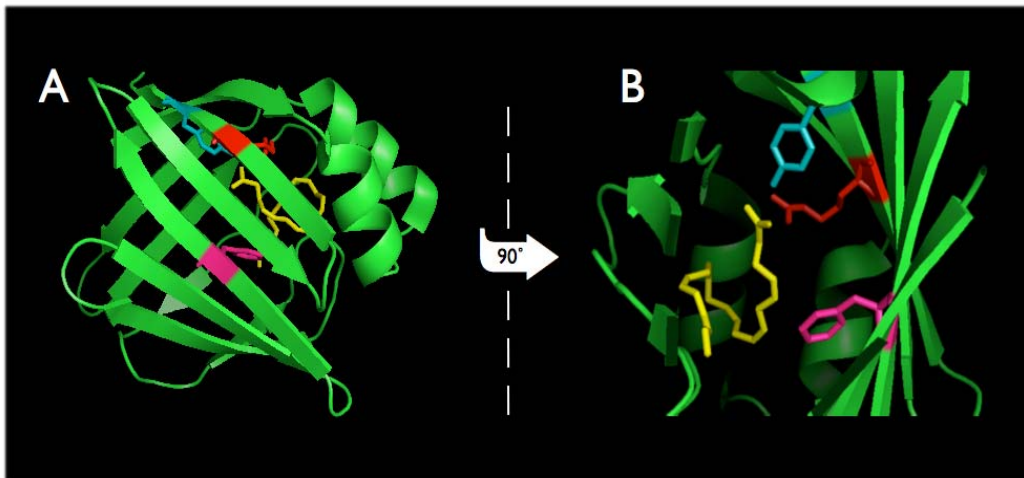


**Figure 1.2.1** Crystal structure of FABP7 bound to DHA, a PUFA (Yellow). (A) FABPs have a characteristic barrel structure capped by a pair of helices. (B) Three residues coordinate the binding of DHA in the binding pocket of FABP7; F104 (Fuschia), R126 (Red), Y128 (Teal). Structural data were obtained from the Protein Data Bank (PDB ID: 1FE3; Balendiran *et al.*, 2000) and rendered using PyMOL.

2009). In light of these findings, it is possible that binding of fatty acids to FABPs alters their conformation in order to manipulate specific FABP functions.

The conserved tertiary structure of FABPs combined with the variability in their primary structure suggests that different FABPs may be better suited to bind different fatty acid ligands. Indeed, this has been confirmed *in vitro* using a wide range of techniques (Xu *et al.*, 1996; Hohoff *et al.*, 1999; Balendiran *et al.*, 2000; Liu *et al.*, 2008). It is important to note that even though the binding constants reported in these papers are not numerically consistent, they do show trends in FABPs binding specific subsets of fatty acids. For example, Balendiran *et al.* used isothermal titration calorimetry (ITC) to show that FABP7 binds the  $\omega$ -3 PUFA docosahexaenoic acid (DHA) and the  $\omega$ -6 PUFA arachidonic acid (AA) with a  $K_D = 0.053 \mu\text{M}$  and  $0.207 \mu\text{M}$ , respectively (Balendiran *et al.*, 2000). When these associations were measured using Lipidex1000 by Xu *et al.* (1996), the observed  $K_D$  was  $0.010 \mu\text{M}$  for DHA and  $0.25 \mu\text{M}$  for AA (Xu *et al.*, 1996). In either case, there is a demonstrated ability for FABP7 to bind DHA and AA at relatively low concentrations. Some FABPs have been shown to exhibit similar binding affinities for the same ligands, and this suggests that these FABPs may have overlapping roles in the cell. In support of FABP binding to specific fatty acids, *Fabp3*-gene ablated mice showed marked deficiencies in their ability to incorporate AA into brain lipids, despite expression of *Fabp5* and *Fabp7* (Murphy *et al.*, 2005). This

*in vivo* evidence suggests that without *Fabp3* there is a deregulation of AA metabolism that is not compensated for by the other FABPs.

### 1.2.2 Functional roles for FABPs

Lipids and fatty acids were long thought to be required solely for formation of cell structure and metabolism, but now are gaining notoriety as key players in regulating gene expression. It has been proposed that FABPs play an important role in fatty acid-dependent gene expression, where they bind their fatty acid ligands and deliver them to fatty acid-activated nuclear receptors (Storch and Corsico, 2008). FABP1 has been shown to interact with the fatty acid-activated transcription factors, peroxisome proliferator-activated receptor alpha (PPAR- $\alpha$ ) and gamma (PPAR- $\gamma$ ) (Wolfrum *et al.*, 2001; Hostetler *et al.*, 2009). It should be noted that both PPAR- $\alpha$  and FABP1 share similar binding constants for the same long chain fatty acids (LCFA; Hostetler *et al.*, 2006; Storch and Corsico, 2008; Hostetler *et al.*, 2009) and that high levels of FABP1 are required for LCFA to activate the transcription of PPARs (Wolfrum *et al.*, 2001). In addition, FABP1 has been found to localize to the nucleus when cells are transfected with FABP1 expression constructs and treated with LCFA (Huang *et al.*, 2002). Taken together with reports showing similar properties for FABP4 and FABP5 (Gillilan *et al.*, 2007; Ayers *et al.*, 2007; Kannan-Thulasiraman *et al.*, 2010; Tan *et al.*, 2002), these data support the idea that FABPs act as chaperones for fatty acids which in turn can

modulate gene expression. It is likely that this mechanism for regulating gene expression applies to the entire family of FABPs, and that differences in ligand specificity and FABP protein-protein interactions can lead to a wide range of outcomes in different tissues. Interestingly, the presence of regulatory elements for PPARs, peroxisome proliferator-responsive elements (PPREs), in the promoter regions of FABP genes (Schachtrup *et al.*, 2004) suggests that FABPs may be involved in regulating their own expression.

FABPs have been implicated in many cellular pathways; however, their physiological roles remain unclear. *In vivo* manipulation of whole organisms has provided significant insight into the roles of FABPs. Knock-out (KO) mice have been generated for most of the FABP family members and, not surprisingly, KO of FABPs results in defects associated with fatty acid metabolism (Hauerland and Spener, 2004; Storch and Corsico, 2008). In contrast to most FABP KO mouse models, the *Fabp7* KO mice show relatively little change in lipid metabolism (Owada *et al.*, 2006). In fact, brains from *Fabp7-null* P0 and P70 mice show no difference in the incorporation of fatty acids into phospholipid subclasses compared to wild-type mice. Furthermore, there was no observed compensatory up-regulation of other FABPs, which is a common consequence of disrupting members of this family. However, there was a significant 5% decrease in the DHA content of the total phospholipid fraction of *Fabp7-null* mice at P0. Interestingly, the *Fabp7-null* P70 mice showed remarkable behavioral

and memory defects in spite of showing little change in membrane fatty acid composition (Owada *et al.*, 2006), suggesting a unique physiological role for FABP7 compared to other FABPs.

### 1.2.3 FABP7 in cancer

The interest in *FABP7* involvement with cancer was sparked by the discovery of a novel tumour growth inhibitor, mammary-derived growth factor inhibitor-related gene (*MRG*). Shi *et al.* sequenced the *MRG* locus and found that *MRG* expression is low in high-grade breast carcinoma, but high in normal breast tissue (Shi *et al.*, 1997). They further showed that over-expression of *MRG* in *MRG*-negative breast cancer cell lines leads to a decrease in tumour cell growth (Shi *et al.*, 1997). Analysis of *MRG* by another group showed that its sequence is 100% identical to *FABP7* (Hohoff and Spener, 1998). *FABP7* has since been reported to be expressed in the mammary gland, and promotes cell differentiation through JAK/STAT signaling (Alshareeda *et al.*, 2012).

Molecular profiling analysis has revealed distinct clinical and molecular subtypes of breast cancer (Perou *et al.*, 2000; Sørlie *et al.*, 2001). The most aggressive subtype is the basal-like tumours, which are biologically and clinically heterogeneous. Basal-like breast cancers are sometimes referred to as triple-negative breast cancer (TNBC) because they do not express the three major prognostic indicators (estrogen receptor, progesterone receptor and HER2) used for breast cancer. Zhang

*et al.* showed that low FABP7 immunoreactivity is associated with the basal phenotype and that tumours expressing high amounts of FABP7 protein have a better clinical outcome (Zhang *et al.*, 2010). This is in contrast to other studies which show that high *FABP7* expression is associated with the basal-like phenotype (Tang *et al.*, 2010; Liu *et al.*, 2012). These discrepancies highlight the heterogeneity of breast cancers even within molecular subtypes. Thus, the prognostic value of FABP7 in these tumours may also reside in its downstream effectors. A recent study published by Liu *et al.* shows that high levels of *FABP7* and *RXR $\beta$* , a nuclear receptor for DHA, are adverse prognostic indicators in TNBC (Liu *et al.*, 2012). The subcellular localization of *FABP7* to the nucleus has been found to be associated with basal-like breast cancer (Alshareeda *et al.*, 2012). In light of these findings, it will be important for future studies to consider the pathways involved with *FABP7* function as these may give clearer insight into the role of *FABP7* in the tumour.

*FABP7* has also been shown to be involved in renal cell carcinoma and melanoma (Domoto *et al.*, 2007; Takaoka *et al.*, 2011) and to have prognostic significance in melanoma (Goto *et al.*, 2010). In melanoma, *FABP7* is frequently over-expressed and plays a role in regulating cell proliferation and invasion (Goto *et al.*, 2006; Slipicevic *et al.*, 2008). *FABP7* also plays an important role in the progression of melanoma. Goto *et al.* showed that loss of heterozygosity (LOH) at the locus containing *FABP7* is associated with metastasis of malignant melanoma tumours.

Furthermore, these investigators found poorer overall survival in the cases where *FABP7* expression was maintained in the tumour metastases (Goto *et al.*, 2010).

One striking observation from the studies of *FABP7* in cancer is that they implicate *FABP7* in highly malignant disease. In accordance with this, *FABP7* is expressed in MG tumour biopsies and a subset of MG cell lines, and is associated with poor survival in MG (Godbout *et al.*, 1998; Liang *et al.*, 2005; Kaloshi *et al.*, 2007). Specifically, nuclear *FABP7* is associated with infiltrative GBM that over-express *EGFR* (Liang *et al.*, 2006). These data indicate an important role for nuclear *FABP7* in MG biology. Mita *et al.* stably transfected a *FABP7* expression construct into the *FABP7*-negative MG cell line, U87, and observed a significant increase in cell proliferation and migration. The reverse effect was seen in the *FABP7*-positive MG cell line, U251, upon stable knock-down of *FABP7* (Mita *et al.*, 2007). These investigators also analyzed human brain tissue biopsies and showed that *FABP7* is localized to infiltrating margins of MG tumours (Mita *et al.*, 2007). These results support the idea that *FABP7* enhances the infiltrative properties of MG tumours; however, little is known about the mechanisms involved. The transcription factors NFI and PAX6 have been shown to regulate *FABP7* expression in MG cells, but there has been no work done relating this to MG cell migration (Bisgrove *et al.*, 2000; Brun *et al.*, 2009; Liu *et al.*, 2012). Thus, further investigations into the role of *FABP7* in MG are warranted.

### 1.3 Fatty Acids

Over the past 50 years our view of the cell membrane has changed dramatically. It was once thought that these membranes were stagnant, homogeneous assemblies of lipids whose function was purely for structure. In many ways, the structure of the cell membrane still dictates its function; however, its content is far from homogeneous, and this has unraveled a myriad of possibilities for its functions in the cell.

#### 1.3.1 Essential fatty acids in cell signaling

Fatty acids are hydrophobic molecules that are essential for cell structure, metabolism, transcriptional regulation and cell signaling. Structurally, they consist of a carboxylic acid 'head' group and a variable length 'tail' of carbon atoms. The length and structure of this carbon tail determines the fate of the fatty acid within the cell. In humans, most fatty acids are synthesized *de novo* in the liver, adipose tissue and mammary glands; however, some fatty acids need to be obtained from the diet - these are the essential fatty acids (EFAs). EFAs are important constituents of cell membranes and have the ability to influence the behaviour of membrane-bound enzymes and receptors (Das *et al.*, 2006). EFAs also play an important role in the developing nervous system, where their bioavailability is tightly controlled (Clandinin, 1999; Belkind-Gerson *et al.*, 2008). AA and DHA, respectively a  $\omega$ -6 and a  $\omega$ -3 PUFA, are the major EFAs found in human brain and their deficiencies are linked with

major neurological disorders (O'Brien and Sampson, 1965; Hamilton *et al.*, 2007). Thus, EFAs are subject to dynamic regulation in the cell and this is controlled in part by their storage in the cell membrane.

Phospholipids are the main constituents of cell membranes and contribute to structural, biochemical and regulatory processes in cells. Structurally, they consist of a polar phosphate group attached to an acylated glycerol moiety. The identity and degree of unsaturation of the fatty acids at these positions has important consequences for cell signaling. For example, AA located at the *sn*-2 position of phospholipids is specifically used to generate prostaglandins, a potent family of signaling molecules involved in homeostasis and inflammation (see Section 1.5). The presence of phospholipids containing DHA is important for stabilizing the activity of rhodopsin in the eye (Bennett and Mitchell, 2008). In the latter case, it is the unique length and degree of unsaturation of DHA that is proposed to enhance cell membrane fluidity by reducing the packing density of lipids. This suggests that altering the fatty acid content of phospholipids could have important consequences on their downstream signaling cascades.

Microdomains of lipids located on the plasma membrane are gaining attention as important components for cell signaling. These lipid rafts are regions of the plasma membrane that are enriched in cholesterol and sphingolipids, and act as platforms that compartmentalize cell signaling at the membrane (Simons and Vaz, 2004). Even though the

physiological relevance of lipid rafts has been questioned, these structures are undoubtedly changing our understanding of the cell membrane. Several proteins are known to associate with lipid rafts, including: src family kinases, the G $\alpha$  subunit of the heterotrimeric G-proteins, Hedgehog, H-Ras, and T-cell receptors (Simons and Toomre, 2000; Simons and Vaz, 2004). These proteins are either acylated with saturated fatty acids or have a strong interaction with the components of lipid rafts. In some cases, lipid raft-protein interactions are stabilized by the presence of phospholipids with unsaturated fatty acids, though the reasons for this have yet to be determined (Simons and Vaz, 2004). It is conceivable that altering the fatty acid composition of sphingolipids, or other phospholipids, with EFAs could alter cell signaling. In fact, the incorporation of DHA into phosphatidylethanolamine (PE) is associated with higher levels of protein kinase C (PKC) at the cell membrane and its increased activity (Giorgione *et al.*, 1995). These results are likely to be cell- or tissue-specific, since others have reported an opposite effect for DHA-containing PE in PKC signaling (Castillo *et al.*, 2005). Furthermore, Schley *et al.* show that treating breast cancer cells with  $\omega$ -3 EFAs alters EGFR signaling by changing the composition of lipid rafts (Schley *et al.*, 2007). This may represent a new avenue for manipulating these signaling pathways in disease.

The presence of fatty acids in the phospholipid molecule has important consequences for its downstream signaling, but so does altering

its overall structure. Enzymes known as phospholipases alter the structure of phospholipids by cleaving them at specific bonds. For example, phospholipase A1 and A2 (PLA<sub>1</sub> and PLA<sub>2</sub>) cleave phospholipids at the *sn*-1 and *sn*-2 position, respectively, to generate free fatty acids (FFA) that can be used for the regulation of gene expression or cell signaling (see Sections 1.4 and 1.5). The other cleavage products generated in these reactions are the lysophospholipids, which are extremely important for cell signaling. Lysophosphatidate (LPA) is generated from lysophosphatidylcholine (LPC) by the action of autotaxin (ATX), and can affect cell migration, proliferation and apoptosis (Okudaira *et al.*, 2010; Samadi *et al.*, 2008).

### 1.3.2 EFAs in cancer

Given the extensive roles of lipids and fatty acids in regulating developmental processes, gene expression and cell signaling, it is not surprising that their deficiency, or their over-abundance, is involved with disease. In mouse models of breast cancer, it has been shown that  $\omega$ -3 and  $\omega$ -6 fatty acids have opposite effects on tumours with  $\omega$ -3 EFAs suppressing, and  $\omega$ -6 EFAs promoting tumour cell growth and metastasis (Rose *et al.*, 1995). Interestingly, Martin *et al.* showed that the AA composition of human MG tumour tissue is much higher than that of normal brain (Martin *et al.*, 1996). This is in contrast to the DHA levels, which are lower in MG tumours (Martin *et al.*, 1996). These findings are

paralleled by findings in MG cells. Mita *et al.* showed that AA increases and DHA decreases the migration of MG cells (Mita *et al.*, 2010). Moreover, this effect on cell migration appears to be dependent on the subcellular localization of FABP7 (Mita *et al.*, 2010). Given the involvement of FABP7 in MG, this suggests that the ligands for FABP7 may also play a role in mediating MG cell behaviour.

It has been suggested that EFAs could be used as adjuvants to chemotherapy (Biondo *et al.*, 2008; Spencer *et al.*, 2009). For example, DHA has been shown to induce apoptosis in human melanoma cell lines (Serini *et al.*, 2012). The involvement of FABP7 in this process has yet to be determined; however, given the role of AA and DHA in modulating FABP7-dependent cell migration in MG, we should consider the FABP7 expression status of tumours as this may predict a response to DHA treatment. The activity of other downstream effectors for fatty acids may also generate insight when considering treatments with DHA or other EFAs. Thus, we may be able to develop new strategies for treating cancers by examining the relationship between FABPs and pathways that mediate the effects of fatty acids in the cell.

#### **1.4 Peroxisome proliferator-activated receptors (PPARs)**

PPARs are members of the nuclear receptor superfamily which function as ligand-activated transcription factors (Kota *et al.*, 2005). There are three members of the PPAR family, PPAR- $\alpha$ , - $\beta/\delta$ , - $\gamma$ , with each

member displaying similar structural features. Despite their overall structural similarities, PPARs demonstrate a range of expression patterns and affinities for ligands (Kota *et al.*, 2005). Peroxisome proliferators (PPs), as the name suggests, are a class of compounds that increase the number of peroxisomes in a cell. PPARs display differential binding affinities to certain classes of PPs and mediate their proliferative effects in the cell (Kota *et al.*, 2005).

The thiazolidinediones (TZDs) are exogenous PPs that function primarily by inducing the transcriptional activity of PPAR- $\gamma$  (Lehmann *et al.*, 1996; Wilson *et al.*, 1996). These exogenous ligands for PPARs were discovered long before their physiological counterparts were recognized. The endogenous ligands for PPARs include saturated fatty acids, PUFAs, and derivatives of prostaglandins (Kota *et al.*, 2005). The binding of these ligands also sheds light on the physiological roles of PPARs in the cell. For instance, PPAR- $\alpha$  is activated by several classes of fatty acids, which is in-line with the essential role of PPAR- $\alpha$  in regulating lipid homeostasis (Pyper *et al.*, 2010). PPAR- $\beta$  and - $\gamma$  have also been shown to regulate a number of physiological processes. PPAR- $\gamma$  expression is highest in adipose tissue where it plays an essential role in regulating adipocyte differentiation, and is also required for development of cardiac and placental tissue (Lehrke and Lazar, 2005; Chawla *et al.*, 1994; Rosen *et al.*, 1999; Barak *et al.*, 1999). PPAR- $\beta$  is expressed at high levels in skin, skeletal muscle, and inflammatory cells, and is involved in regulating lipid

homeostasis (Wagner and Wagner, 2010). PPAR- $\beta$  is also involved in regulating differentiation of muscle cells, neurons, and epithelial cells (Bonala *et al.*, 2012; D'Angelo *et al.*, 2011; Peters *et al.*, 2012).

#### 1.4.1 Fatty acids, FABPs and PPARs

The DNA-binding domain of PPAR is well-conserved and mediates DNA binding by interacting with PPAR-responsive elements (PPREs) in the promoter regions of PPAR target genes (Zhou and Waxman, 1999). The mechanism of this process is well understood in general terms. After binding ligand, PPARs undergo a conformational change that causes them to lose their interaction with histone deacetylase (HDAC) co-repressors and heterodimerize with other nuclear receptors (Peters *et al.*, 2012). This PPAR complex recruits RNA polymerase II and several co-activators to the PPRE, and together they remodel local chromatin structure and increase transcription (Peters *et al.*, 2012).

Retinoid-X-receptor (RXR) is a family of fatty acid-activated nuclear receptors that heterodimerize with PPARs. Kliewer *et al.* have shown that RXR- $\alpha$  enhances the binding of PPAR- $\alpha$  to PPREs, and promotes the transcription of several genes associated with peroxisomal  $\beta$ -oxidation of fatty acids (Kliewer *et al.*, 1992). These effects are further enhanced by addition of the ligands for RXR- $\alpha$  (Kliewer *et al.*, 1992). Researchers have also shown that PPAR- $\alpha$  and - $\gamma$  undergo nucleo-cytoplasmic shuttling upon binding to their ligands (Umemoto and Fujiki, 2012). FABPs display

this same activity, and could potentially be involved in delivering ligands to PPARs in the cytoplasm. This idea is supported by the fact that FABPs enhance PPAR activity by delivering fatty acids directly to PPARs (See 1.2.2). The significance of this interaction occurring in the cytoplasm, followed by re-localization of PPAR to the nucleus, has yet to be determined. Interestingly, when PPAR- $\beta/\delta$  is not bound to a ligand, it may repress transcription of PPAR- $\alpha$  and PPAR- $\gamma$  (Shi *et al.*, 2002; Peters *et al.*, 2012). These combined data highlight the complexity of fatty acids, FABPs and PPARs in regulating gene transcription. This level of complexity indicates that this pathway plays an intricate role in the cell, and that deregulation of FABPs and PPARs in cancer may provide targets for new therapies.

#### 1.4.2 PPARs in cancer

All members of the PPAR family are associated with cancer. Even before PPARs were discovered, the PPAR- $\alpha$  agonist, Wy-14,643, had been shown to induce hepatocellular carcinomas (HCC) in rats (Reddy *et al.*, 1980). Peters *et al.* showed that this was dependent on PPAR- $\alpha$  as *Ppara* *-/-* mice did not develop HCC in response to long-term exposure to Wy-14,643 (Peters *et al.*, 1997). PPAR- $\beta/\delta$  has also been implicated in many different types of cancers; however, its mechanism of action remains controversial. Wagner *et al.* showed that PPAR- $\beta/\delta$  is expressed at high levels in liposarcoma cell lines, and that this expression promotes

cell migration and proliferation (Wagner *et al.*, 2011). These observed effects were dependent on the presence of PPAR- $\beta/\delta$  binding elements in the promoter region of the leptin gene. Leptin is an adipose tissue secretory factor that inhibits cell migration and proliferation in liposarcomas (Wagner *et al.*, 2011). PPAR- $\beta/\delta$  acts as a transcriptional repressor of leptin, and thereby inhibits the anti-proliferative and anti-migratory effects of leptin (Wagner *et al.*, 2011). Yang *et al.* showed that in colon cancer, PPAR- $\beta/\delta$  may be an inhibitor to carcinogenesis and tumour progression (Yang *et al.*, 2010). Furthermore, ligand activation of PPAR- $\beta/\delta$  inhibits skin tumorigenesis (Bility *et al.*, 2010). These findings indicate opposite roles for PPAR- $\beta/\delta$  in different cancers. This presents a problem at the clinical level, as it's not clear whether PPAR- $\beta/\delta$  activity should be inhibited or activated in cancer treatment. Given the functional relationship between FABPs and PPARs, characterization of FABPs and fatty acids may shed light on whether specific cancers should be treated with inhibitors or activators of PPAR- $\beta/\delta$ .

PPAR- $\gamma$  agonists are generally thought to prevent cancer formation in breast and colon tissue, and have been shown to inhibit cell growth and invasion through  $\beta$ -catenin in a panel of MG cell lines (Peters *et al.*, 2012; Wan *et al.*, 2011). A retrospective analysis of diabetic MG patients using PPAR- $\gamma$  agonists has suggested that those who used PPAR- $\gamma$  agonists were less likely to develop high grade gliomas (Grommes *et al.*, 2010). 15-Deoxy-Delta-(12,14)-Prostaglandin J(2) (15d-PGJ2), an agonist of PPAR-

$\gamma$ , has also been shown to inhibit growth of CD133+ glioma stem cells (Chearwae and Bright, 2008). Mita *et al.* found a possible relationship between EFAs (DHA, AA), FABP7, PPAR- $\beta/\delta$  and PPAR- $\gamma$  in MG (Mita *et al.*, 2010). These authors showed that knock-down of PPAR- $\gamma$  prevents FABP7-mediated inhibition of cell migration by DHA. This suggests that FABP7 bound to DHA acts through PPAR- $\gamma$  to inhibit cell migration in MG cells that express FABP7 (Mita *et al.*, 2010). Furthermore, it appears as though AA and FABP7-mediated increases in cell migration are not inhibited by restricting FABP7 localization to the cytoplasm, but perhaps are mediated through PPAR- $\beta/\delta$  and cyclooxygenase (COX; Mita *et al.*, 2010). It is then possible that PPAR- $\beta/\delta$  acts to promote cell migration, or other tumorigenic properties, through FABP7 and metabolites of AA.

### **1.5 Cyclooxygenase (COX)**

COX are enzymes that catalyze the committed step in prostaglandin (PG) biosynthesis (Yuan *et al.*, 2009). There are two isoforms, COX-1 and COX-2, that function as homodimers to convert fatty acid substrates into prostaglandin H<sub>2</sub> (PGH<sub>2</sub>; Vecchio *et al.*, 2010; Figure 1.5.1). This process occurs in two major steps at the inner luminal membrane of the endoplasmic reticulum (ER; Mbonye *et al.*, 2008). The substrate enters the COX homodimer through a hydrophobic channel and binds to the active site of one of the partnered COX monomers (Thuresson *et al.*, 2001; Yuan *et al.*, 2009). This allosterically induces the

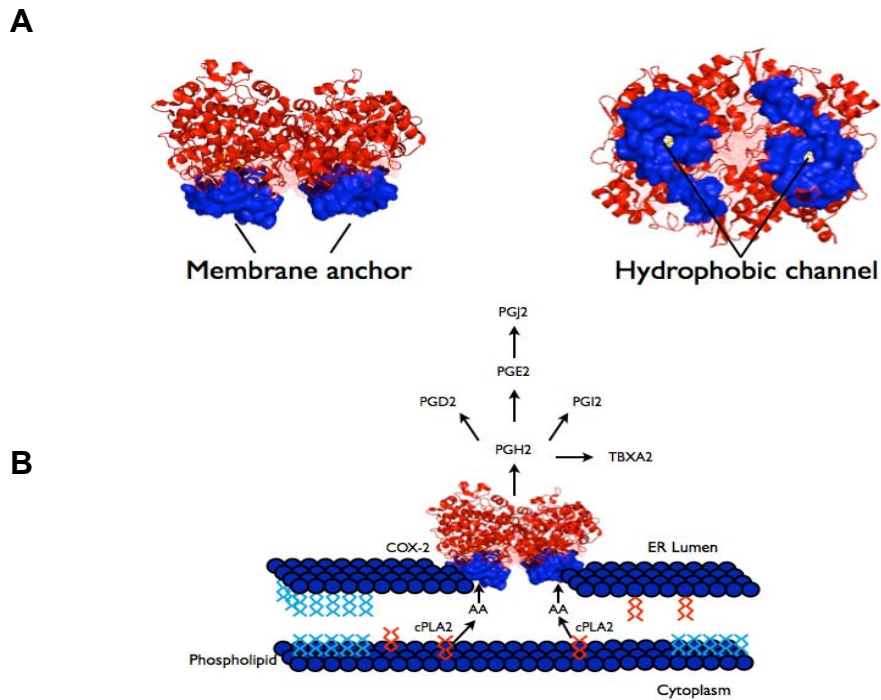


**Figure 1.5.1 COX activity in the cell.** (A) The COX enzyme consists of homodimers that are anchored to the inner luminal membrane of the ER. A hydrophobic channel in the membrane binding domain of COX allows entry of ligands into the hydrophobic binding pocket located in proximity to the active site. (B) COX activity is the rate limiting step in the production of all prostaglandins. Structural data were obtained from the Protein Data Bank (PDB ID: 1CVU; Kiefer *et al.*, 2000) and rendered using PyMOL.

other COX monomer to carry out the catalytic activity (Yuan *et al.*, 2009). The first catalytic step is oxygenation, which effectively adds two O<sub>2</sub> to the backbone of the substrate (Yuan *et al.*, 2009). This step is followed by cyclization of the O<sub>2</sub> group with the substrate backbone, and is catalyzed by the peroxidase activity of COX (Yuan *et al.*, 2009). This gives the PGs their characteristic ring structure and, in the case when AA is the substrate, is called PGH<sub>2</sub>.

The major substrate for COX is AA (Wada *et al.*, 2007; Yuan *et al.*, 2009). AA, located at the *sn*-2 position of phospholipids, is preferentially cleaved by phospholipase A<sub>2</sub> (PLA<sub>2</sub>) and used as substrate for COX (Strokin *et al.*, 2003). While the activity of PLA<sub>2</sub> can affect the expression of COX-2 through PPAR-γ (Pawliczak *et al.*, 2004), the production of PGs is limited by the amount of PGH<sub>2</sub> that can be produced from substrates of COX. Data obtained from non-steroidal anti-inflammatory drugs (NSAIDs) has led to the suggestion that COX isoforms have some non-overlapping physiological roles. NSAIDs have been shown to inhibit activity of both COX isoforms (Laneuville *et al.*, 1994). Interestingly, NSAIDs that bind to both COX-1 and COX-2 can inhibit inflammation, but are also associated with potentially severe side-effects (Snowden *et al.*, 2011). Significant differences in the amino acid sequences of COX-1 and COX-2 (~60% identity; Tanabe and Tohnai, 2002), combined with the differential expression of COX-1 and COX-2, suggest unique roles for these two proteins.

### 1.5.1 Regulation of COX-1 and COX-2

COX-1 is constitutively expressed in most cell types and plays a role in maintaining tissue homeostasis (Tanabe and Tohnai, 2002). There is also evidence that COX-1 expression may be inducible in certain cell types, where it could play a role in regulating cell differentiation (Mroske *et al.*, 2000). On the other-hand, COX-2 is generally an inducible enzyme whose expression is affected by several growth factors, tumour promoters and cytokines (Tanabe and Tohnai, 2002; Vecchio *et al.*, 2010). The transcriptional regulation of COX-2 plays a significant role in regulating PG production in the cell. The nuclear transcription factor kappa B (NF $\kappa$ B) pathway has been shown to regulate COX-2 transcription in several systems (Inoue *et al.*, 2000; Nadjar *et al.*, 2005). Interestingly, PPAR- $\gamma$  plays a role in negatively regulating COX-2 expression through NF $\kappa$ B (Inoue *et al.*, 2000). The over-production of PGD<sub>2</sub> caused by high expression of COX-2 activates PPAR- $\gamma$ , which then inhibits NF $\kappa$ B-mediated COX-2 expression (Inoue *et al.*, 2000). Growth factors such as EGFR have also been shown to affect the transcription of COX-2 through p38 mitogen-activated protein kinase (MAPK)-dependent activation of the Sp1/Sp3 transcription factors, a process that is dependent on protein kinase C- $\delta$  (PKC- $\delta$ ; Xu *et al.*, 2007; Xu *et al.*, 2009). In addition to gene regulation mechanisms, there are inherent features of COX-1 and COX-2 mRNAs that determine their expression levels.

A key difference between *COX-1* and *COX-2* mRNA is the presence of instability elements in the *COX-2* mRNA. AU-rich elements have been shown to destabilize mRNA and this plays an important role in regulating the expression of inducible proteins (Chen *et al.*, 1994). The 3'-untranslated region (UTR) of *COX-2* mRNA has a series of AUUUA-repeats that serve as flags for exonuclease cleavage (Tanabe and Tohnai, 2002). In contrast, the 3'-UTR of *COX-1* mRNA does not contain these AU-rich repeats, which help to explain its stability compared to that of *COX-2* mRNA (Mbonye *et al.*, 2008). In fact, the stability of *COX-1* has generated concern as to the biological relevance of altering *COX-1* expression.

Work by Mroske *et al.* has demonstrated that *COX-1* is expressed upon differentiation of the megakaryocytic cell line, MEG-01 (Mroske *et al.*, 2000), consistent with the fact that PGs produced by *COX-1* in platelets play a major role in activating thrombosis. Platelets are anucleate and so they lack the ability to transcribe the *COX-1* gene; hence, *COX-1* must be obtained from their precursors, the megakaryocytes (Mroske *et al.*, 2000). Megakaryocytic cell lines can undergo differentiation into platelets when treated with 12-*O*-tetradecanoylphorbol-13-acetate (TPA). Treatment of MEG-01 with TPA results in a 1.8 fold increase in *COX-1* transcript levels (Mroske *et al.*, 2000). *COX-1* transcription can also be induced by HDAC inhibitors in human astrocytes (Taniura *et al.*, 2002). These examples demonstrate that *COX-1* transcription can indeed be

modified, albeit under highly specific conditions. When Duquette and Laneuville treated MEG-01 cells with TPA they not only observed an increase in *COX-1* mRNA, but also lagged increase in *COX-1* protein expression (Duquette and Laneuville, 2002). Further work by this group revealed that the 3'-UTR of *COX-1* mRNA contains a conserved 20 nucleotide (nt) sequence that regulates *COX-1* expression at the post-transcriptional level (Duquette and Laneuville, 2002).

Other structural features of *COX* mRNA control its fate in the cell. For example, *COX-1* expression is regulated by secondary structures in its 5'-UTR (Bunimov *et al.*, 2007; Bunimov and Laneuville, 2010). HuR is a stabilizing factor for mRNAs with AU-rich sequences (Doller *et al.*, 2008). Although HuR has not yet been implicated in *COX-1* post-transcriptional regulation, HuR which has been phosphorylated by PKC- $\delta$  has been shown to bind the AU-rich region of *COX-2* mRNA and promote its nuclear export (Doller *et al.*, 2008). From these studies it is clear that *COX* expression is tightly controlled at multiple levels.

The half-life ( $\tau_{1/2}$ ) of *COX-1* in murine NIH/3T3 fibroblasts is greater than 12 hours, whereas the  $\tau_{1/2}$  for *COX-2* in these cells is 2 hours (Mbonye *et al.*, 2006). This group showed that by inhibiting the 26S proteasome, they could increase the  $\tau_{1/2}$  of *COX-2* (Mbonye *et al.*, 2006). The same trends are observed for *COX-1* and *COX-2* in HEK293 cells ( $\tau_{1/2}$  is 24 hours and 5 hours, respectively; Mbonye *et al.*, 2006). While the primary structures of *COX-1* and *COX-2* are similar, they differ in that

COX-2 has an extra 19 amino acid (aa) cassette in its C-terminus (Mbonye *et al.*, 2006). Deletion of the 19 aa does not interfere with COX-2 subcellular localization or activity, but does increase the  $\tau_{1/2}$  of COX-2 (Mbonye *et al.*, 2006). Specifically, the 19 aa cassette was shown to target COX-2 to the endoplasmic reticulum-associated degradation (ERAD) system (Mbonye *et al.*, 2006). This helps to explain the higher turnover of COX-2 protein in relation to COX-1.

Of note, two distinct pathways for COX-2 degradation have been described and the one that is used depends on the activity of COX-2 (Mbonye *et al.*, 2008). The first mechanism involves a 27 aa 'instability' motif that regulates post-translational N-glycosylation of Asn-594 and occurs at a constant rate (Mbonye *et al.*, 2008). The second pathway is initiated by substrate binding to COX-2 (Mbonye *et al.*, 2008). Using NIH/3T3 cells, researchers showed that COX-2 degradation increases when AA is added to the cells, and this effect subsides when COX-2 is inhibited using flurbiprofen or NS-398 (Mbonye *et al.*, 2008). It should also be noted that proteasome and lysosomal protease inhibitors do not affect COX-2 degradation through this pathway, which suggests that ligand-mediated suicide inactivation of COX-2 is an important mechanism for controlling COX-2 activity (Mbonye *et al.*, 2008). Proteins have been identified that can regulate COX-2 activity by interfering with its degradation. As an example, integrin-mediated cell adhesion has been shown to promote COX-2 activity by inhibiting its degradation by

lysosomes, while simultaneously increasing its transcription through Src, PI3K, ERK1/2, and p38 MAPK (Zaric and Ruegg, 2005).

### 1.5.2 Ligands for COX

COX isoforms share ~60% amino acid identity and their crystal structures are virtually superimposable; however, they show remarkable differences in the structure of their active sites (Vecchio *et al.*, 2010). In fact, a highly conserved I523V substitution in the COX-2 isoform makes its binding pocket ~20% larger than the pocket in COX-1 (Kurumbail *et al.*, 1996; Vecchio *et al.*, 2010). COX-1 and COX-2 have a similar binding affinity for AA, but they differ in their catalytic efficiency (Wada *et al.*, 2007; Yuan *et al.*, 2009). Wada *et al.* have shown that COX-2 is able to oxygenate AA ~30% more efficiently than COX-1 (Wada *et al.*, 2007). The fatty acid eicosapentaenoic acid (EPA) has also been shown to bind COX enzymes, albeit with lesser affinity than AA (Wada *et al.*, 2007). COX-2 oxygenates EPA at ~30% efficiency compared to AA, whereas COX-1 oxygenation of EPA is <5% as efficient as that of AA (Wada *et al.*, 2007). It has been proposed that the residue Leu-531 in the COX-2 active site is responsible for COX-2 being able to bind a wider range of fatty acids compared to COX-1 (Vecchio *et al.*, 2010). The flexibility of Leu-531 is thought to stabilize the larger binding pocket in COX-2 and may allow larger substrates to access its active site (Vecchio *et al.*, 2010). Thus, COX-2 may be able to generate a more diverse array of PGs, which helps

to explain its involvement in a wide variety of physiological processes and diseases.

### 1.5.3 COX-2 in MG

Pro-inflammatory signaling can induce angiogenesis, cell proliferation and invasion in cancer cells (Hanahan and Weinberg, 2011). As such, there is great interest in targeting inflammatory pathways as a cancer therapy. In accordance with the role of inflammation in tumour progression, increased COX-2 expression and activity have been observed in many cancers from different origins, including: skin (Amirnia *et al.*, 2012); digestive tract (Thiel *et al.*, 2011); liver (Xu *et al.*, 2006); breast (Holmes *et al.*, 2011); and brain (Shono *et al.*, 2001). For example, COX-2 is estimated to be expressed in ~40% of all breast cancers and its expression correlates with larger tumours, metastases to lymph nodes and bone, and reduced overall survival (Singh *et al.*, 2006; Holmes *et al.*, 2011). High COX-2 expression is generally an indicator of poor prognosis and is associated with resistance to chemo- and radiation therapy (Xu *et al.*, 2009).

COX-2 is also involved in MG. Shono *et al.* showed that high levels of COX-2 are associated with clinically more aggressive MG, and is a strong predictor of poor overall survival (Shono *et al.*, 2001). In an analysis of 83 cases of grades II, III and IV astrocytomas, Perdiki *et al.* found that COX-2 was expressed in 79 cases, with higher expression in the grades

III and IV astrocytomas (Perdiki *et al.*, 2007). COX-2 expression has also been shown to correlate with the proliferative activity of MG tumour cells, total vascular area, and levels of vascular endothelial growth factor (VEGF) and hypoxia inducible factor (HIF)-1 $\alpha$  (Perdiki *et al.*, 2007). Despite these correlations, elucidating the mechanisms that are responsible for the clinical behaviour of MG in relation to COX-2 has been difficult as COX-2 is constitutively expressed in normal brain (Herrmann *et al.*, 2005). These difficulties are further compounded by clinical findings showing that high levels of PGE<sub>2</sub>, a product of the COX-2 pathway, correlate with increased patient survival in GBM (Lalier *et al.*, 2007).

Work by Xu *et al.* has demonstrated that EGFR is capable of inducing COX-2 expression in glioma cell lines, and that this induction is mediated by p38 MAPK and PKC- $\delta$  (Xu *et al.*, 2009). The constitutively active *EGFRvIII* has been shown to regulate glioma angiogenesis and growth through NF $\kappa$ B, which controls the *in vivo* expression of Cox-2 in normal rat brain (Bonavia *et al.*, 2011b; Nadjjar *et al.*, 2005), as well as COX-2 expression in CD133<sup>+</sup> U87 glioblastoma cells (Annabi *et al.*, 2009). Interestingly, when U87 cells were sorted by CD133 status, the CD133<sup>+</sup> cells grew as neurospheres and expressed higher levels of COX-2 (Annabi *et al.*, 2009). As MG stem cells have been shown to be resistant to therapy, this raises the question as to what role COX-2 plays in mediating GSC resistance to therapy.

One potential role that COX-2 may be playing in MG cells is in modulating the ability of the immune system to recognize and destroy tumour cells. Dendritic cells (DCs) are professional antigen presenting cells that can process tumour-associated antigens (TAAs) and display TAA epitopes on their cell surface using the major histocompatibility complex (MHC)-I and -II (Akasaki *et al.*, 2004). CD4<sup>+</sup> T cells only recognize epitopes on the MHC-II receptors, and can initiate lysis of malignant cells. This effect is also controlled by regulatory T cells (Tr) and helper T cells (Th), which can suppress or enhance T cell-mediated cell lysis (Akasaki *et al.*, 2004). Patients with MG display a broad suppression of cell-based immunity (Dix *et al.*, 1999). PGE<sub>2</sub> has long been known to have immunosuppressive functions, and has been shown to inhibit DC function and T cell response (Harizi *et al.*, 2002). U87 MG cells that express high levels of COX-2 induce a CD4<sup>+</sup> Tr cell response via CD11c<sup>+</sup> DCs that suppresses T cell-mediated lysis (Akasaki *et al.*, 2004). Conditioned medium from U251 MG cells can induce PGE<sub>2</sub> production in macrophages, in further support of the idea that MG tumours interact with immune cells to control immune system function through COX-2 (Nakano *et al.*, 2006).

Although the mechanisms controlling COX-2 expression in MG remain to be investigated, there is evidence that PPARs can regulate COX-2 transcription in other tumours. Xu *et al.* have shown that PPAR-β/δ induces COX-2 expression in hepatocellular carcinoma (Xu *et al.*, 2006).

This is a 'feed-forward' mechanism whereby PPAR- $\beta/\delta$  activation of COX-2 activity results in phosphorylation of cPLA<sub>2</sub> $\alpha$ , which further activates PPAR- $\beta/\delta$  and promotes tumour growth (Xu *et al.*, 2006). PGE<sub>2</sub> can also promote tumour progression through PPARs in other systems (Inoue *et al.*, 2000; Han *et al.*, 2004; Han and Roman, 2004; Xu *et al.*, 2006). Given the involvement of COX-2 with fatty acids and PPARs, and the involvement of FABPs with fatty acids and PPARs, it is possible that FABPs play a role in regulating COX-2 activity. U87 MG cells transfected with a FABP7 expression construct express elevated levels of COX-2 RNA and protein compared to the FABP7-negative U87 cells (Mita *et al.*, 2010). Furthermore, increased COX-2 expression is associated with a ~6-fold increase in PGE<sub>2</sub> levels (Mita *et al.*, 2010). In light of the demonstrated and proposed roles for FABPs, PPARs and COX-2 in MG, it is possible that targeting a fatty acid-FABP-PPAR-COX-2 axis could lead to successful strategies for treating MG tumours.

COX-2 has been shown to interact with p53 and interfere with p53-dependent transcription and apoptosis (Corcoran *et al.*, 2005). Choi *et al.* also showed that COX-2 regulates p53 activity and is capable of inhibiting DNA damage-induced apoptosis (Choi *et al.*, 2005). This interaction has been demonstrated *in vivo* and is inhibited by NS-398 (Choi *et al.*, 2005). Human glioblastoma cells treated with a COX-2 specific inhibitor, celecoxib, harbour higher levels of DNA damage and undergo p53-dependent G1 cell cycle arrest, and p53-dependent autophagy (Kang *et*

*al.*, 2009). The COX-2 inhibitor E-6087 enhances the effects of radiotherapy in orthotopic models of glioma in mice (Wagemakers *et al.*, 2009), suggesting that it might be useful to treat MG patients undergoing radiotherapy with COX-2 inhibitors. Interestingly, NS-398 was shown to inhibit glioma cell proliferation in monolayer cultures of U87 and U251 MG cell lines, and inhibit tumour growth and outgrowth of spheroids derived from U87 and U251 cells (Joki *et al.*, 2000). What is striking about these results is that the effects were much more pronounced in U251 compared to U87 cells. U251 cells express FABP7 whereas U87 cells do not express this protein (Mita *et al.*, 2007). In agreement with these data, a reduction in cell migration was observed when FABP7-transfected U87 cells were treated with the COX-2-specific inhibitor, NS-398 (Mita *et al.*, 2010). No effect on cell migration was observed in FABP7-negative U87 control cells. Even though FABP7-positive MG tumours have been associated with poor survival in MG, these data indicate that FABP7-positive tumours may respond better to treatment with COX-2 inhibitors. It is possible that COX-2 inhibitors could magnify the effects of DHA and FABP7 on MG cell migration, thereby targeting the infiltrative tumour cells.

## **1.6 Working Hypothesis**

We propose that FABP7 and its fatty acid ligands play a central role in regulating the expression of factors involved with MG tumour progression. We further propose that *FABP7*-positive MG cells are

inherently migratory and infiltrative, properties mediated in part by the activity of COX-2.

## **CHAPTER 2**

### **Materials and methods**

### *2.1. Stable transfection of U87 cells*

U87 is a FABP7-negative [FABP7(-)] human MG cell line that was obtained from Dr. Jorgen Fogh (Sloane Kettering Institute, Rye, NY, USA; Godbout *et al.*, 1998). U87 cells were stably transfected with either empty pREP4 vector or a pREP4-FABP7 expression construct as described in Mita *et al.* (2007). From this point forward, U87C will refer to the FABP7(-) cell line that was clonally derived from U87 cells stably transfected with control vector (as described in Mita *et al.*, 2007). Similarly, U87B will refer to the FABP7(+) cell line that was clonally derived from U87 cells stably transfected with the pREP4-FABP7 expression construct. Stably transfected cells were selected in 50 µg/ml hygromycin B.

### *2.2 Cell culture*

Cells were cultured in Dulbecco's Modified Essential Medium (DMEM) supplemented with 10% fetal calf serum (FCS), 100 µg/mL streptomycin and 100 U/mL penicillin. Cells were maintained at 37°C in a humidified 5% CO<sub>2</sub> atmosphere. Prior to lipid extraction, U87C and U87B cultures were supplemented with either 60 µM BSA, 60 µM AA, or 60 µM DHA for 24 hours. Cells were harvested and pellets were stored at -80°C.

### *2.3 Preparation of fatty acids*

Fatty acids (Sigma) were dissolved in 100% ethanol, then complexed to fatty acid-free BSA (Sigma) over a constant stream of nitrogen gas. Residual ethanol accounted for <0.1% of total volume.

#### *2.4 Gene expression microarray analysis*

Microarray analysis was carried out using RNAs prepared from 3 independent cultures of U87C (U87C1, U87C2, U87C3) and three independent cultures of U87B (U87B1, U87B2, U87B3). Total RNA was isolated from each of these cell lines using the Qiagen RNeasy Plus kit according to the manufacturer's protocol. Only high quality RNA was used in these experiments (RNA integrity number >8.5/10) as measured by a Bioanalyzer 2100 (Agilent technologies). The RNA was then labeled and used to probe Agilent whole genome arrays (Liu *et al.*, 2011).

#### *2.5 Reverse transcription-PCR (RT-PCR) analysis of microarray data*

RT-PCR was carried out as described (Liu *et al.*, 2011) using RNA isolated from U87C1, U87C2, U87C3, U87B1, U87B2 and U87B3 cell lines. The following oligonucleotides were used in the RT-PCR analysis: FABP7, forward 5' -TGG AGG CTT TCT GTG CTA C- 3', reverse 5' -TAG GAT AGC ACT GAG ACT TG- 3'; PPAR- $\alpha$ , forward 5' -ATT CGC CAT GCT GTC TTC TG- 3', reverse 5' -CTC CTT TGT AGT GCT GTC AG- 3'; PPAR- $\beta/\delta$ , forward 5' -AGC CTC AAC ATG GAG TGC C- 3', reverse 5' -ATG TCG TGG ATC ACA AAG GG- 3'; PPAR- $\gamma$ , forward 5'- CAG GAG

ATC ACA GAG TAT GC- 3', reverse 5' -CAA CTG GAA GAA GGG AAA TG- 3'; COX1, forward 5' -TGT TTG GGC TGC TTC CTG G- 3', reverse 5'- ATT CCT CCA ACT CTG CTG C- 3'; COX-2, forward 5' -TCC TGT GCC TGA TGA TTG C- 3', reverse 5' -TGG AAC AAC TGC TCA TCA CC- 3'; PLA2G4A, forward 5' -GCC TCT GGA TGT CAA AAG TA- 3', reverse 5' -GCT TTC AAC CAT GGC TTC TT- 3'; PLA2G4C, forward 5' -CCT GTT CAA CAT AGA TGC CT- 3', reverse 5' -CCT TCT TCT GAA TGA CGC TA- 3'; L1CAM, forward 5' -CCC ACT CAG CCA CAA CGG- 3', reverse 5' -GAT GAA GCA GAG GAT GAG C- 3'; CDH18, forward 5' -GGC GGA GGA GAT TTA GTC G- 3', reverse 5' -AGA GTC ATA AGG GGG AAC G- 3'; MMP2, forward 5' -TAC AGC CTG TTC CTC GTG G- 3', reverse 5' -TGC TCC AGT TAA AGG CGG C- 3'; MMP3, forward 5' -CCA CTC ACA TTC TCC AGG CT- 3', reverse 5' -GCT AGT AAC TTC ATA TGC GGC- 3'; MMP12, forward 5' -CCT GGA GAT GAT GCA CGC A- 3', reverse 5' -TGT CAT CAG CAG AGA GGC G- 3'; MMP 14, forward 5' -GCA GGC CGA CAT CAT GAT CT- 3', reverse 5' -CAG TGT TGA TGG ACG CAG G- 3'; MMP15, forward 5' -GGT ACG AGT GAA AGC CAA CC- 3', reverse 5' -GGT ACC GTA GAG CTG CTG G- 3'; PLSCR4, forward 5' -CGG TAT CAG CCT GGC AAA TA- 3', reverse 5' -CAT GGC CCA CGA ACT CTC- 3'; PRKCZ, forward 5' -CAG GAG AAG AAA GCC GAA TC- 3', reverse 5' -CAT CCA TCC CAT CGA TAA CTG- 3'; ENPP2, forward 5' -GTC TGT TGT CAT CCC TCA CG- 3', reverse 5' -CGT GAG ATT GGC AAT AAT GGC- 3'; HLA-DMA, forward 5' -AAC CAC ACA TTC CTG CAC AC- 3',

reverse 5' -GTG TAG CGG TCA ATT TCG TG- 3';  $\beta$ -actin, forward 5' - CTG GCA CCA CAC CTT CTA C- 3', reverse 5'- CAT ACT CCT GCT TGC TGA TC- 3'. PCR products were separated on a 1% agarose gel, stained with ethidium bromide and visualized under UV light.

## 2.6 Western blot analysis

Whole cell lysates were prepared by incubating cells on ice for 20 min in buffer B: 50 mM Tris-HCl pH 7.5, 150 mM NaCl, 1% NP-40, 0.5% sodium deoxycholate, 0.1% SDS, 1X protease inhibitor cocktail (Roche), 1 mM PMSF, 2 mM DTT. For the analysis of PLA2G4A, cell lysates were prepared using either buffer B or buffer A (buffer B + 2 mM sodium fluoride, 2 mM sodium orthovanadate, 25 mM sodium pyrophosphate). Lysates were centrifuged at 14,000 x g for 15 minutes, and the supernatant was collected and stored at -80°C. Protein concentration was measured using the Bradford assay. Fifty  $\mu$ g of whole cell lysate were separated by electrophoresis in a 13.5% SDS-polyacrylamide gel followed by electroblotting onto nitrocellulose membranes. Membranes were immunostained with rabbit anti-FABP7 antibody (1:500 dilution) (Godbout *et al.*, 1998), goat anti-COX-2 antibody (1:500 dilution) (sc-1747; Santa Cruz) or rabbit anti-PLA2G4A antibody (1:1000 dilution) (ab73406; Abcam), and detected with horseradish peroxidase-conjugated secondary antibodies (Jackson ImmunoResearch Biotech) using the ECL detection system (GE Healthcare).

## 2.7 Co-immunoprecipitations (co-IP)

U87B cells were cultured to ~70% confluency and then treated with either 60  $\mu$ M BSA, AA, or DHA for 24 hours. Following this treatment, the cells were washed in PBS and cell pellets were used to prepare protein extracts. For the standard co-IP, immunoprecipitation assay buffer [50 mM Tris-HCl pH 7.5, 150 mM NaCl, 0.5% sodium deoxycholate, 1% NP-40, 2 mM PMSF, 1 mM DTT, 1X protease inhibitor cocktail (Roche)] was used to prepare fresh U87B whole cell lysate. A total of 750  $\mu$ g cell lysate were pre-cleared by adding 40  $\mu$ l of washed recombinant Protein A Sepharose beads (GE Healthcare) to the cell lysate in an Eppendorf tube, followed by a 3 hour incubation at 4°C. The supernatant was removed by centrifuging tubes in a microcentrifuge for 2 minutes at 4,000 rpm. Five  $\mu$ l goat anti-PPAR- $\beta/\delta$  (GenScript) was added to the supernatant and incubated at 4°C for 3 hours. Fifty  $\mu$ l of bead slurry (50% beads, 50% immunoprecipitation buffer, by volume) was added to the tubes containing PPAR- $\beta/\delta$  antibody and incubated overnight at 4°C. The following morning, the tubes were centrifuged at 4,000 rpm for 2 minutes and the supernatant stored at -20°C for western blotting. The bead fraction was washed 3 times with 500  $\mu$ l of immunoprecipitation assay buffer and analysed by western blotting.

The procedure for cross-linked co-IP is a modification of Thompson *et al.*, (2009). Briefly, cultured U87B cells supplemented with BSA, AA, or DHA were washed once in PBS, then cross-linked with 0.5% formaldehyde for 10 minutes at room temperature. The cross-linking

reaction was terminated by adding 125 mM glycine to the cells and incubating at room temperature for 5 minutes. Cells were harvested by scraping directly in immunoprecipitation assay buffer (50 mM Tris-HCl pH 7.5, 50 mM NaCl, 0.1% sodium deoxycholate, 0.5% NP-40, 1 mM PMSF, 2 mM DTT, 1X protease inhibitor cocktail) and sonicated at 30% power, 3 times for 15 seconds at 4°C using a Model 300 V/T ultrasonic homogenizer (BioLogics, Inc). Co-immunoprecipitation was as described previously using either rabbit anti-FABP7 or goat anti-PPAR- $\beta/\delta$  antibody.

### *2.8 Enzyme-linked immunosorbent assay (ELISA)*

PGE<sub>2</sub> levels were measured by ELISA using the protocol supplied by the manufacturer (Amersham Prostaglandin E<sub>2</sub> Biotrak Enzyme Immunoassay System, GE Healthcare). Cells were seeded in triplicate in 96-well plates at 50,000 cells/well and cultured in serum-free medium for 24 hours. Cells were then lysed and PGE<sub>2</sub> was quantified using manufacturer's protocol 8.4. One hundred  $\mu$ l of 1 M H<sub>2</sub>SO<sub>4</sub> were added to each well following substrate incubation and the plates were read at 450 nm using a microplate reader (FLUOstar OPTIMA, BMG Labtechnologies).

### *2.9 Live cell imaging of PGE<sub>2</sub>-treated U87B cells*

PGE<sub>2</sub> (Sigma P5640) was resuspended in 100% ethanol and diluted to 1 mM using 10 mM KH<sub>2</sub>PO<sub>4</sub> pH 7.22. Fifty thousand U87B cells

were plated on 35-mm culture dishes with a glass coverslip embedded in the bottom of the dish. Cells were cultured under standard conditions for 24 hours and then washed twice with PBS. Following these washes the medium was replaced with serum-free DMEM. Cells were incubated for 1 hour at 37°C in a humidified 5% CO<sub>2</sub> chamber attached to an Axiovert 200M microscope (Zeiss) set up for phase contrast microscopy with a 20X objective lens. The cells were then treated with either 10 μM KH<sub>2</sub>PO<sub>4</sub> pH 7.2 or 10 μM PGE<sub>2</sub>. Metamorph *version 7.7.0 (Molecular Devices, LLC)* was used to capture a single differential interference contrast (DIC) image every minute for 2 hours. Data were exported to Imaris x64 *version 7.5.0* for video and image processing (Bitplane).

#### *2.10 Isolation of nuclei from U87C and U87B*

All reagents were kept on ice. Nuclear extracts were prepared using a modification of Gorski *et al.* (1986). Cell pellets from 2 150-mm tissue culture plates of either U87C or U87B cells, treated with 60 μM BSA, 60 μM AA or 60 μM DHA, were washed in PBS and kept on ice for 10 minutes prior to homogenization. Cells were homogenized using a 7 mL dounce homogenizer in a modified Gorski homogenization buffer (HB; 10 mM HEPES pH 7.6, 25 mM KCl, 1 mM EDTA, 0.15 mM spermine, 0.5 mM spermidine, 0.2 mM PMSF, 5% glycerol, 2 M sucrose). HB containing no sucrose was also prepared and used to dilute the 2 M sucrose HB to generate a sucrose gradient (0 M, 0.3 M, 1.5 M and 2.0 M sucrose). The

following were added to all HB immediately prior to use: 0.15 mM spermine, 0.5 mM spermidine and 0.2 mM PMSF. Cell pellets were resuspended in 3 mL of 0.3 M sucrose HB and homogenized 5 times using a loose pestle, followed by 100 strokes (U87B) or 150 strokes (U87C) using a tight pestle. The volume was doubled by adding 3 mL of 2 M sucrose HB and the homogenate layered in 50 cc Beckman polyallomer tubes containing 10 ml of a 1.5 M sucrose HB cushion. Tubes were centrifuged in a HB6 rotor at 9000 rpm for 2.5 hours at 4°C. The supernatant was removed using a glass pipet and the walls were wiped down using tissue. The cell pellets were stored at -80°C prior to lipid extraction.

### *2.11 Isolation of lipids from cells and nuclei*

Lipids were extracted from cells or nuclei using a modified Folch procedure in detergent-free glass tubes. Chloroform:methanol extraction in the presence of 10 mM KCl was used to isolate the total lipid fraction from U87C and U87B whole cells or nuclei. Tubes were left overnight at 4°C to allow for phase and debris separation. The following morning, the tubes were centrifuged at 2,000 rpm for 2 minutes and the organic phase was transferred into detergent-free glass vials using a glass Pasteur pipette. The vials were held under a steady stream of nitrogen gas to evaporate the solvent. The remaining lipid pellet was resuspended in 100 µl hexane and stored at -80°C.

### 2.12 Phospholipid analysis

Phospholipid subclasses were separated from total lipid extracts by thin layer chromatography on 10 X 10 cm HPK silica gel plates (Whatman) using a chloroform:methanol:2-propanol:0.25% KCl (w/v):triethylamine solvent system (60:18:50:12:36 by volume), as previously described (Bradova *et al.* 1990). Separated phospholipids were visualized with 8-anilino-1-naphthalene-sulfonic acid (Sigma) and identified under UV light using appropriate standards as references (Supelco). Phosphatidylcholine (PC), phosphatidylethanolamine (PE), phosphatidylinositol (PI), and phosphatidylserine (PS) fatty acid methyl esters were prepared from the scraped silica bands using 14% (w/v) BF<sub>3</sub>/methanol reagent (Sigma). Fatty acid methyl esters were separated by automated gas liquid chromatography (Varian CP-3800) on an SGE BP20 column (60 mm x 0.25 mm internal diameter). The analytical conditions were designed to separate all saturated, mono-, di-, and polyunsaturated fatty acids from 14 to 24 carbons in chain length. The relative amount of AA or DHA in each phospholipid subclass was determined by calculating the area of the peak corresponding to AA or DHA, divided by the total area under the gas chromatogram.

## **CHAPTER 3**

### **Results**

### **3.1 Gene expression analysis of FABP7(-) versus FABP7(+) U87 MG cells**

#### *3.1.1 Stable expression of FABP7 alters the gene expression profile of U87 cells*

Previous work has shown that stable expression of FABP7 in U87 cells increases their motility and cell migration (Mita *et al.*, 2007). The effect of FABP7 on cell migration was dependent on whether FABP7-expressing cells were cultured in AA-enriched or DHA-enriched medium (Mita *et al.*, 2010). As transfection of FABP7 into U87 cells affected their growth properties and FABPs had previously been shown to play a role in the regulation of gene expression, we used whole genome gene expression (cDNA) microarrays to examine the expression profiles of U87B and U87C cells. Over 1,000 genes were differentially expressed in U87B cells compared to U87C cells, including families of genes involved in cell adhesion, cell migration, inflammation and immune modulation. These results were consistent among all three independent preparations of U87C and U87B MG cells. A subset of genes that are differentially expressed in U87C versus U87B MG cells is highlighted in Table 3.1.

#### *3.1.2 RT-PCR analysis of U87C versus U87B cell lines identifies potential mechanisms of FABP7-dependent MG cell migration*

In order to elucidate the potential mechanisms for FABP7-dependent MG cell migration, RT-PCR was used to confirm the differential

**Table 3.1 A selection of genes that are differentially expressed in U87C compared to U87B MG cells based on cDNA microarray data.**

PGE<sub>2</sub> receptor (EP1, 2, 3, 4); adenylate cyclase 8 (ADCY8); interleukin-1 $\beta$  (IL-1 $\beta$ ); sphingosine-1-phosphate receptor 1 and 2 (S1PR1/2) lysophosphatidic acid receptor 1 (LPA1); ectonucleotide pyrophosphatase/phosphodiesterase (ENPP1 ,4, 5); autotaxin (ATX); tumor necrosis factor receptor superfamily member (TNFRSF); chemokine (C-X-C) receptor (CXCR4, 12); No change (NC); p-values were calculated using a two-tailed students t test, n=6.

Gene	Fold change with FABP7 expression	p value
PPAR- $\alpha$	NC	-
PPAR- $\beta/\delta$	+2.5	p<0.0001
PPAR- $\gamma$	-8.2	p<0.0001
COX-1	-42	p<0.0001
COX-2	+11.2	p<0.0001
c-PLA <sub>2</sub> $\alpha$	+27	p<0.0001
i-PLA <sub>2</sub>	-3.7	p=0.008
EP1	NC	-
EP2	-2	p=0.0002
EP3	-2.1	p=0.049
EP4	NC	-
ADCY8	+96.3	p<0.0001
IL-1 $\beta$	+13	p<0.0001
S1PR1	+14.2	p=0.00016
LPA1	-2.3	p=0.001
S1PR2	+4.1	p=0.01
ENPP1	+3.4	p<0.0001
ATX	+4.9	p<0.0001
ENPP4	+4.5	p<0.0001
ENPP5	+213	p<0.0001
PKC $\zeta$	-25	p<0.0001
TNFRSF11B	-16.6	p=0.0012
TNFRSF19	+4.8	p<0.0001
CXCR4	-46	p<0.0001
CXCR12	+2	p=0.024

expression of a subset of genes from the microarray data. As some FABPs have been shown to interact with PPARs and alter PPAR transcriptional activity, we examined the effect of FABP7 on PPAR- $\alpha$ , PPAR- $\beta/\delta$ , and PPAR- $\gamma$  expression in U87C versus U87B MG cells (Figure 3.1.1). While *PPAR- $\alpha$*  RNA levels were similar in U87C and U87B cells, there was an increase in *PPAR- $\beta/\delta$*  RNA levels, and a decrease in *PPAR- $\gamma$*  RNA levels, in FABP7-positive U87 cells compared to FABP7-negative U87 cells.

Mita *et al.* demonstrated that AA could increase MG cell migration in U87B, but not in U87C cells, and that this effect was independent of FABP7 nuclear localization (Mita *et al.*, 2010). Since PPARs regulate COX expression and FABP7 is associated with increased *PPAR- $\beta/\delta$*  expression in U87 cells, we examined the expression of *COX-1* and *COX-2* in U87C versus U87B MG cells. There was a significant decrease in *COX-1* expression in U87B cells compared to U87C cells. In contrast, an increase in *COX-2* RNA levels was observed upon FABP7 expression in U87 cells (Figure 3.1.2). In accordance with these findings, upstream mediators of the AA/COX pathway were also affected by FABP7 expression. We observed an increase in *PLA2G4A* expression in the U87B cells, whereas another *PLA<sub>2</sub>G* family member (*PLA2G4C*) showed decreased expression in U87B cells (Figure 3.1.2).

The tumour microenvironment plays an important role in the maintenance of CSCs and MG tumour progression. We observed that

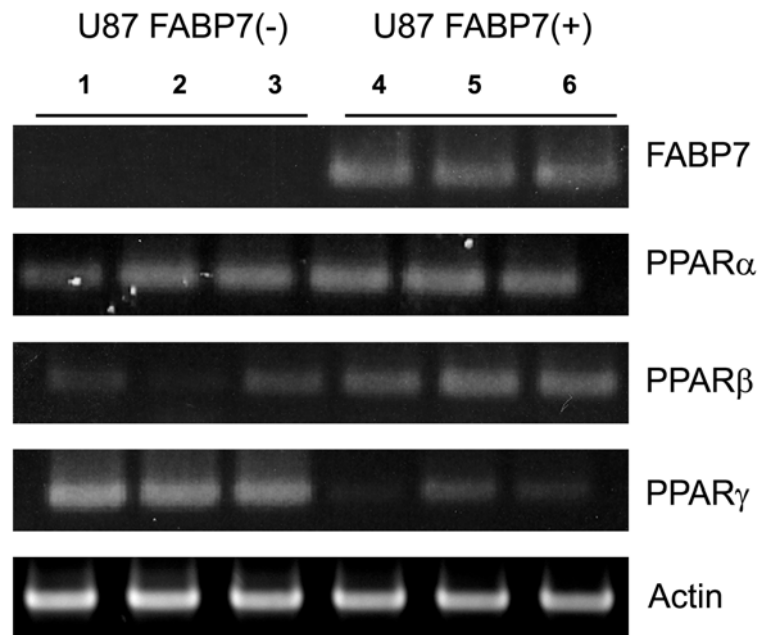


**Figure 3.1.1 Differential expression of PPAR- $\beta/\delta$  and PPAR- $\gamma$  in FABP7-expressing U87 MG cells.** RNAs isolated from 3 independent preparations of FABP7-negative U87C cells (lanes 1, 2, 3) and 3 independent preparations of FABP7-positive U87B MG cells (lanes 4, 5, 6) were reverse-transcribed to generate the corresponding cDNAs. The expression patterns of PPAR family members was examined by semi-quantitative RT-PCR using primers specific to *PPAR- $\alpha$* , *- $\beta/\delta$*  or *- $\gamma$* . RT-PCR reactions using  $\beta$ -actin primers served as controls for amount of RNA present in each reaction. PCR products were electrophoresed in 1% agarose gels and stained with ethidium bromide.

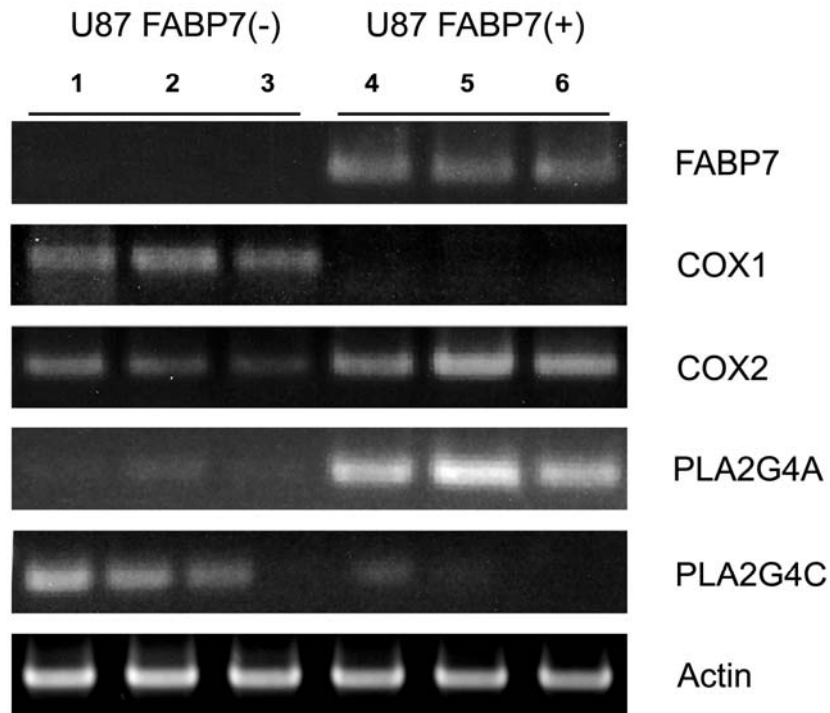


**Figure 3.1.2 Differential expression of COX-1, COX-2, PLA2G4A and PLA2G4C in FABP7-expressing U87 MG cells.** RNA from 3 independent preparations of U87C cells (lanes 1, 2, 3) and 3 independent preparations of FABP7-positive U87B MG cells (lanes 4, 5, 6) was converted into cDNA using a reverse transcriptase. The expression patterns of the indicated genes were determined by semi-quantitative RT-PCR using primers specific to COX-1, COX-2, PLA2G4A or PLA2G4C. RT-PCR reactions using  $\beta$ -actin primers served as controls for amount of RNA present in each reaction. PCR products were electrophoresed in 1% agarose gels and stained with ethidium bromide.

several members of the matrix metalloproteinase (MMP) family (*MMP2*, *MMP3*, *MMP14*, *MMP15*) were over-expressed in U87B cells (Figure 3.1.3). Several other interesting molecules displayed differential expression in U87C versus U87B cells. For example, levels of protein kinase C zeta (*PRKCZ*) and L1 cellular adhesion molecule (*L1CAM*) were reduced in U87B cells. In contrast, phospholipid scramblase 4 (*PLSCR4*), ectonucleotide pyrophosphatase/phosphodiesterase 2 (*ENPP2*), cadherin 18 type 2 (*CDH18*) and major histocompatibility complex class II DM alpha (*HLA-DMA*) all showed increased expression in U87B cells (Figure 3.1.4).

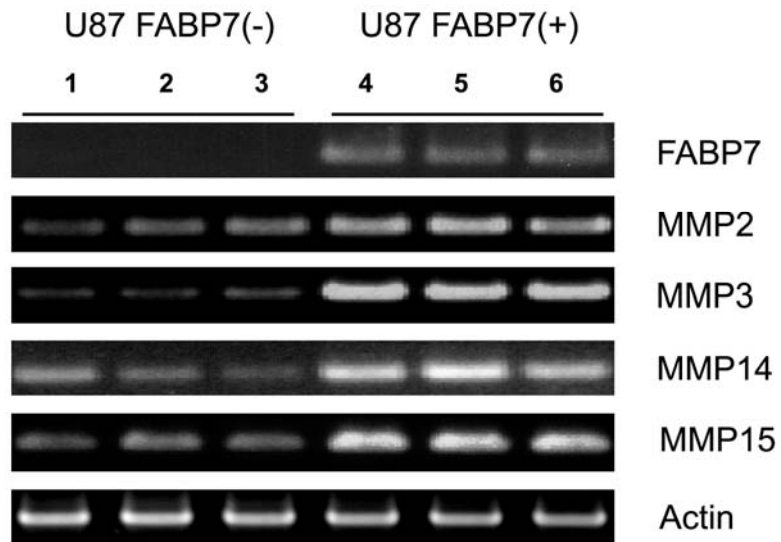


**Figure 3.1.3 Increased expression of MMPs in FABP7-expressing U87 MG cells.** RNAs isolated from 3 independent preparations of FABP7-negative U87C cells (lanes 1, 2, 3) and 3 independent preparations of FABP7-positive U87B MG cells (lanes 4, 5, 6) were converted to cDNAs using reverse transcriptase. Expression patterns were examined by semi-quantitative RT-PCR using primers specific to MMP2, MMP3, MMP14 or MMP15. RT-PCR reactions using  $\beta$ -actin primers served as controls for amount of RNA present in each reaction. PCR products were electrophoresed in 1% agarose gels and stained with ethidium bromide.

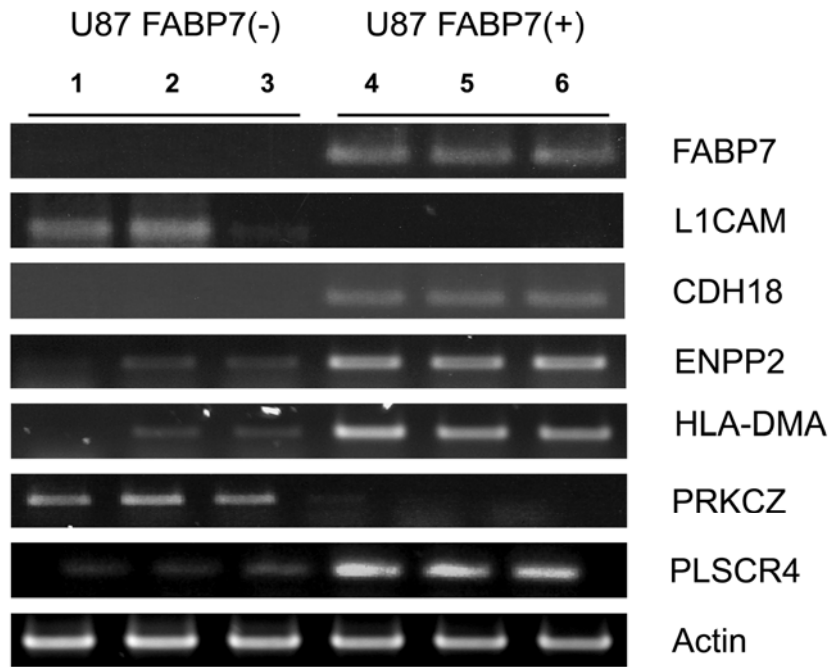


**Figure 3.1.4 Differential gene expression profiles in U87C versus U87B MG cell lines.** RNAs isolated from 3 independent preparations of FABP7-negative U87C cells (lanes 1, 2, 3) and 3 independent preparations of FABP7-positive U87B MG cells (lanes 4, 5, 6) were converted to cDNAs using reverse transcriptase. The expression patterns of the genes were examined by semi-quantitative RT-PCR using primers specific to L1CAM, CDH18, ENPP2, HLA-DMA, PRKCZ or PLSCR4. RT-PCR reactions using  $\beta$ -actin primers served as controls for amount of RNA present in each reaction. PCR products were electrophoresed in 1% agarose gels and stained with ethidium bromide.

### 3.1.3 A potential ligand-dependent interaction between FABP7 and PPAR- $\beta/\delta$

It is well-established that some FABPs deliver fatty acid ligands to PPARs, which in turn activates PPAR and thereby alters the expression of PPAR target genes. We hypothesize that there is a direct interaction between FABP7 and PPARs in U87B cells, which may mediate the effects of FABP7 on gene expression. Initially, we attempted co-immunoprecipitation (co-IP) of FABP7 and PPAR- $\beta/\delta$  using a standard co-IP protocol; however, no interaction was detected in these co-IPs using either FABP7 or PPAR- $\beta/\delta$  antibodies (data not shown).

It is possible that the hydrophobic conditions under which the co-IP were carried out interfered with fatty acid-FABP7 interaction, which in turn may have affected FABP7-protein interactions. In light of this conjecture, we used low concentrations of formaldehyde in an attempt to physically cross-link FABP7, an approach previously used to demonstrate a fatty acid-dependent interaction between FABP4 and JAK2 (Thompson *et al.*, 2009). Through a series of experiments to optimize co-IP conditions, we were able to obtain preliminary data supporting ligand-dependent interaction between FABP7 and PPAR- $\beta/\delta$  in U87B cells cultured in serum-free DMEM supplemented with either 60  $\mu$ M BSA, 60  $\mu$ M AA or 60  $\mu$ M DHA for 24 hours (Figure 3.1.5). A weak band was observed when 5  $\mu$ l of PPAR- $\beta/\delta$  antibody was used to co-immunoprecipitate PPAR- $\beta/\delta$  from cross-linked U87B cells, suggesting PPAR- $\beta/\delta$  interaction with

FABP7 in a ligand-dependent manner (Figure 3.1.5A). This effect was enhanced with the addition of 10  $\mu$ l PPAR- $\beta/\delta$  antibody (Figure 3.1.5B). The signal obtained with U87B cells treated with 60  $\mu$ M BSA was stronger in both experiments. Interestingly, there was a differential interaction of FABP7 and PPAR- $\beta/\delta$  in the AA-treated cells compared to the DHA-treated cells, with the AA treatment resulting in less interaction than the DHA-treated cells.

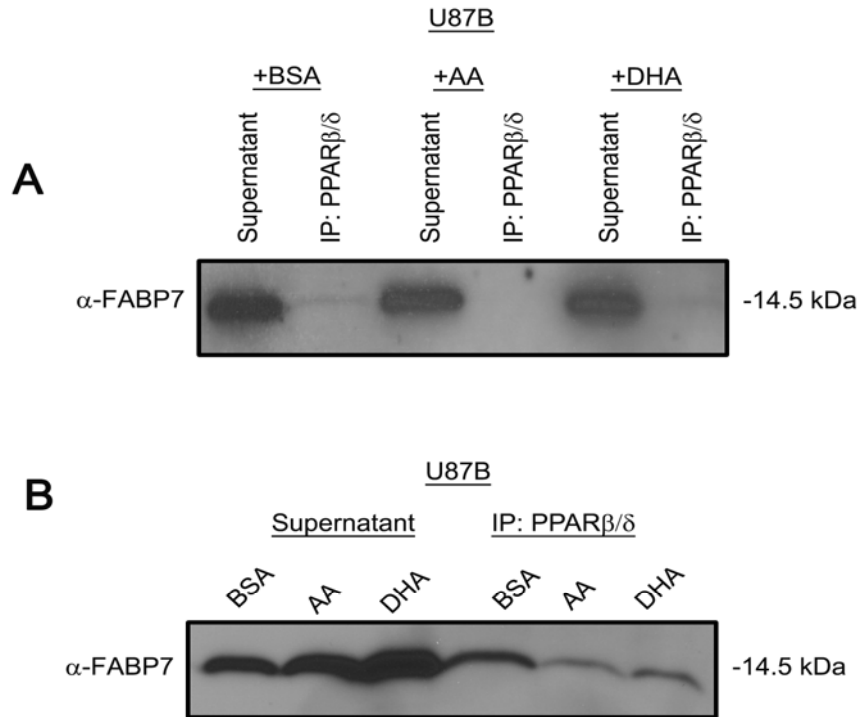


**Figure 3.1.5 Potential ligand-dependent interaction of FABP7 and PPAR-β/δ in U87 MG cells.** U87B cells were cultured in DMEM in the absence of fetal calf serum and treated with either 60 μM BSA, 60 μM AA or 60 μM DHA every 8 hours for a total of 24 hours. Cells were cross-linked in 0.5% formaldehyde and whole cell lysates were prepared. Five hundred μg of whole cell lysates were used for co-immunoprecipitation with 5 μl (A) or 10 μl (B) anti-PPAR-β/δ antibody. Co-immunoprecipitated FABP7 was detected by immunoblotting the supernatant and bead fractions of immunoprecipitation reactions on a nitrocellulose membrane. FABP7 was detected by immunostaining with anti-FABP7 antibody followed by horseradish-peroxidase-conjugated secondary antibody.

## 3.2 COX-2 expression and activity in U87C and U87B MG cells

### 3.2.1 FABP7 increases COX-2 expression and activity in U87 MG cells

COX-2 is over-expressed in many cancers, including MG (Perdiki *et al.*, 2007). AA is the main substrate for COX-2 and the conversion of AA into prostaglandins (e.g. PGE<sub>2</sub>) by COX-2 has been shown to play a role in many cellular processes, including migration of cancer cells (Mita *et al.*, 2010). Western blot analysis of COX-2 expression in U87C compared to U87B cells showed that COX-2 is over-expressed in U87B cells (Figure 3.2.1A). In accordance with this, U87B cells showed a 6-fold increase in PGE<sub>2</sub> levels based on an ELISA assay (Figure 3.2.1B).

Cytosolic phospholipase cPLA2 releases AA from phospholipids in the cell membrane. AA released by cPLA2 is generally used to generate inflammatory mediators. Based on our gene expression microarray data (Table 3.1) and RT-PCR analysis (Figure 3.1.2), *PLA2G4A* RNA levels are increased upon FABP7 expression in U87 cells. Western blot analysis indicates increased levels of PLA2G4A protein in U87B compared to U87C cells (Figure 3.2.2A). However, bands were observed at ~45 kDa rather than the predicted ~100 kDa.

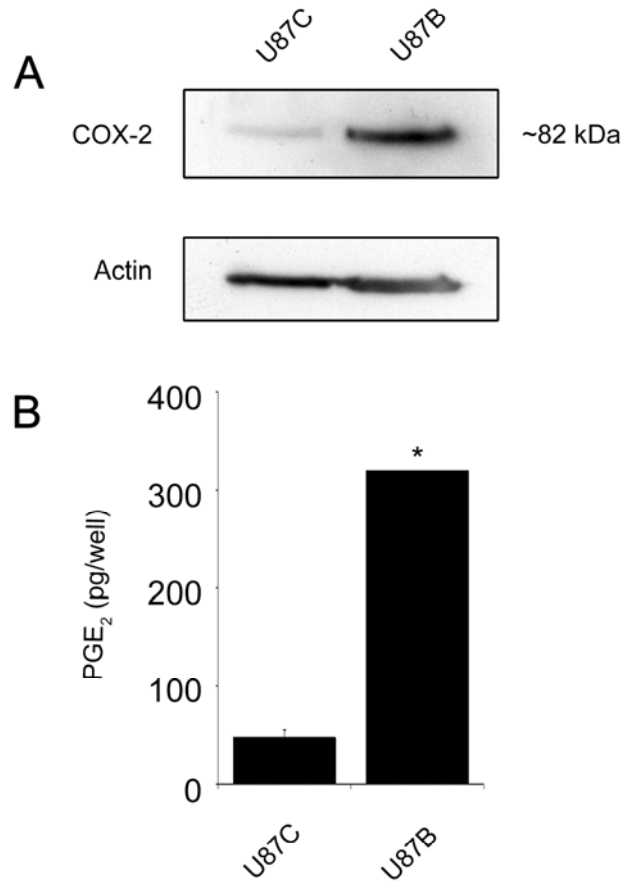
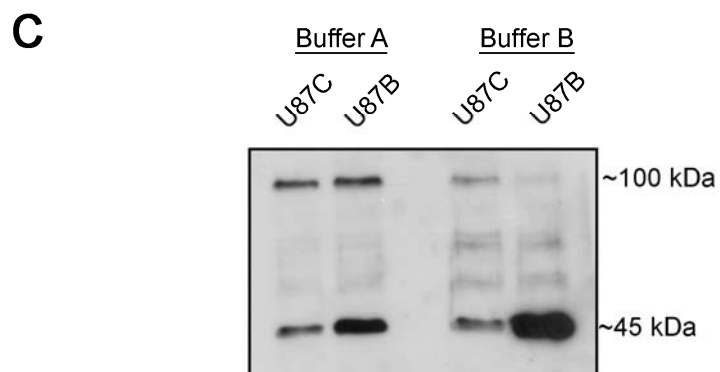
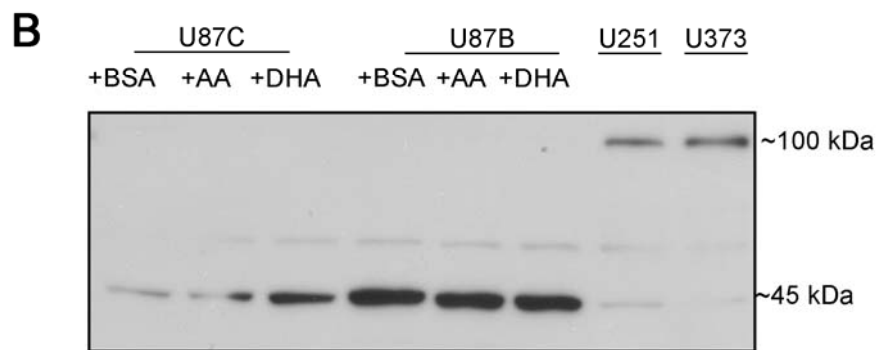
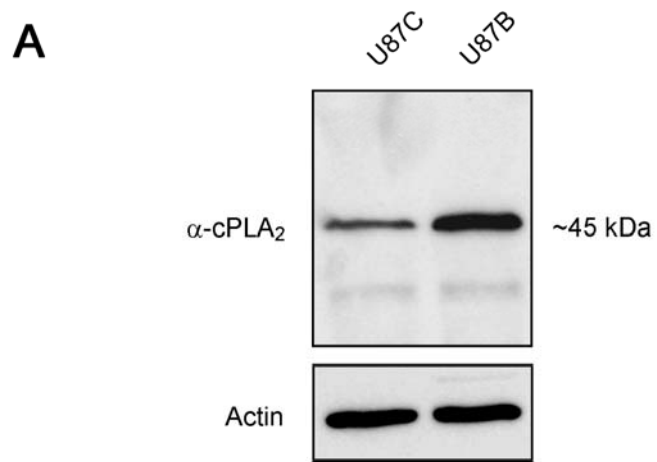


**Figure 3.2.1 COX-2 levels and PGE<sub>2</sub> production are up-regulated upon FABP7 expression in U87 MG cells.** (A) Western blot analysis of whole cell lysates (25 µg/lane) prepared from U87C and U87B MG cells. Nitrocellulose membranes were sequentially immunostained with goat anti-COX-2 and mouse anti-actin antibody, and the signal detected using horseradish peroxidase-conjugated secondary antibodies. (B) ELISA was used to measure PGE<sub>2</sub> levels in U87C and U87B cells. The data were obtained from two independent experiments measured in triplicate. No error bars are shown for U87B as all the wells were saturated for PGE<sub>2</sub>. A version of this figure was published in Mita *et al.* (2010).

**Figure 3.2.2 PLA2G4A levels are elevated in U87B compared to U87C MG cells.** (A) Western blot analysis of whole cell lysates (25  $\mu$ g/lane) prepared from U87C and U87B MG cells. Nitrocellulose membranes were sequentially immunostained with rabbit anti-PLA2G4A and mouse anti-actin antibody, and the signal detected using horseradish peroxidase-conjugated secondary antibodies. (B) U87C and U87B cells were serum starved for 24 hours in the presence of 60  $\mu$ M BSA, 60  $\mu$ M AA, or  $\mu$ M DHA. Whole cell lysates (25  $\mu$ g/lane) from each culture, along with lysates from U251 and U373 MG cells, were electrophoresed in 13.5% polyacrylamide gels and blotted onto nitrocellulose membranes. Membranes were immunostained with rabbit anti-PLA2G4A antibody. (C) U87C or U87B cells were harvested in either buffer A or buffer B (see Materials and Methods) and electrophoresed (25  $\mu$ g cell lysates/lane) in 13.5% polyacrylamide gels, blotted onto a nitrocellulose membrane and immunostained with a rabbit anti-PLA2G4A antibody.



To further investigate the identity of the 45 kDa protein, we treated U87C and U87B cells with either 60  $\mu$ M BSA, 60  $\mu$ M AA or 60  $\mu$ M DHA. Treatment with fatty acids did not affect the size of the band detected with anti-PLA2G4A antibody in U87 cells. However, bands of the expected size were detected in the two FABP7-positive MG cell lines, U251 and U373 (Figure 3.2.2B). Further analysis revealed a relation between the 45 kDa and 100 kDa bands. In whole cells lysates of U87C and U87B cells prepared with buffer A (no phosphatase inhibitors) (see Section 2.6), we observed higher levels of the 100 kDa PLA2G4A band in relation to the 45 kDa product in both U87C and U87B cells, with slightly higher levels of the 100 kDa band in the U87B cells (Figure 3.2.2C). When U87C and U87B cells were lysed in buffer B (containing phosphatase inhibitors), we observed a significant reduction in the levels of the 100 kDa PLA2G4A band in U87B cells. This decrease was accompanied by a significant increase in the levels of the 45 kDa product (Figure 3.2.2C). These results suggest that the 45 kDa product may be a cleaved form of PLA2G4A.

### 3.2.3 *The effect of PGE<sub>2</sub> treatment on U87B cells*

We also investigated the effects of PGE<sub>2</sub> treatment on U87B cells *in vivo*. Based on our live cell imaging analysis, there were no changes to the behaviour of U87B cells when treated with saturating levels of PGE<sub>2</sub> (Figure 3.2.3).

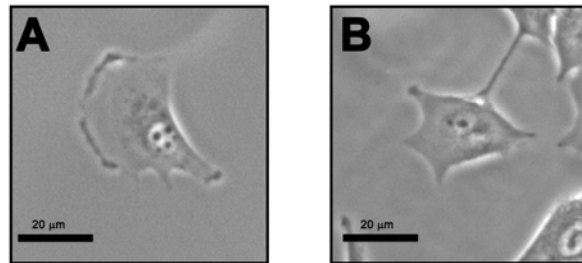


**Figure 3.2.3 The response of U87B cells to PGE<sub>2</sub>.** U87B cells were treated with either 10  $\mu$ M K<sub>2</sub>PO<sub>4</sub> (A) or 10  $\mu$ M PGE<sub>2</sub> (B) in the absence of serum and tracked with DIC microscopy using Metamorph imaging software. Images were exported and processed using Imaris x64 version 7.5.0.

### *3.3.1 AA and DHA incorporation into the phospholipids of U87C versus U87B cells*

Changes in the PUFA content of phospholipids can affect membrane properties and membrane-based signaling pathways. To investigate the mechanisms by which DHA inhibits, and AA promotes cell migration in U87B cells, we treated U87C and U87B cells with BSA, AA or DHA for 24 hours and examined the content of AA and DHA in the phospholipid classes PC, PS, PI and PE. There was no difference in the AA or DHA content of PC, PS, PI and PE in whole cell lipid extracts prepared from BSA-treated U87C and U87B cells (Figure 3.3.1). In these BSA-treated cells, the relative percent AA relative to total fatty acids was lowest in PC and PS and highest in PI and PE. The DHA content relative to total fatty acid content was highest in PE and lowest in PC.

Treatment of U87C and U87B cells with either AA or DHA for 24 hours resulted in significant increases in the relative content of AA or DHA in phospholipids compared to BSA-treated cells (Figure 3.3.2). When U87C and U87B cells were treated with 60  $\mu$ M DHA, we observed ~20-fold, ~7-fold, ~8.5-fold and ~6-fold increases in the DHA content of PC, PS, PI and PE, respectively (Figure 3.3.2A). Similarly, we observed ~8.4-fold, ~2-fold, ~2.6-fold and ~1.5-fold increases in the AA content of PC, PS, PI and PE, respectively, when U87C and U87B cells were treated with 60  $\mu$ M AA compared to BSA (Figure 3.3.2B).

To determine how AA treatment might affect DHA content, and how DHA treatment might affect AA content of phospholipids, we also examined the AA and DHA content of DHA-treated and AA-treated U87C and U87B cells. In AA-treated cells, the percent DHA in PC, PS, PI and PE was similar to that observed in BSA-treated U87C and U87B cells, with no change in PC and slight decreases of ~1.5-fold, ~2.4-fold and ~1.4-fold in PS, PI and PE, respectively (Figure 3.3.2A). We also observed ~1.8-fold, ~1.3-fold, and ~2-fold increases in the AA content of PC, PS and PI, respectively, and an ~2-fold decrease in the AA content of PE in U87C and U87B cells treated with 60  $\mu$ M DHA compared to BSA (Figure 3.3.2B).

Two notable differences were observed in U87C and U87B cells treated with AA versus DHA in terms of relative AA and DHA fatty acid composition in phospholipids. First, there was an ~5-fold increase in the DHA content of PS when cells were treated with DHA compared to BSA, in contrast to an ~2-fold increase in the AA content of PS in cells treated with AA compared to BSA (Figure 3.3.3). Second, there was a ~6-fold increase in the DHA content of PE when U87C and U87B cells were treated with DHA versus BSA, in contrast to the ~1.5-fold increase in the AA content of PE in cells treated with AA versus BSA (Figure 3.3.4).

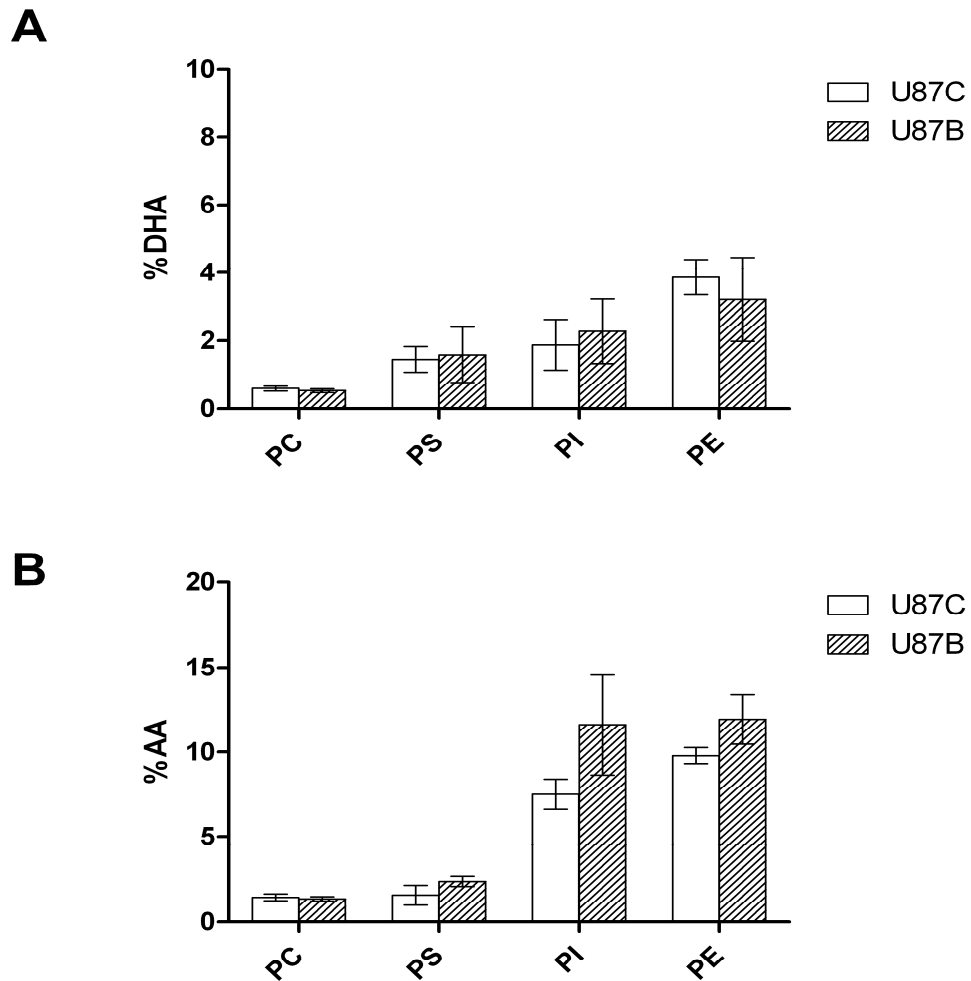


**Figure 3.3.1 DHA and AA content of phospholipids purified from U87C and U87B MG cells treated with BSA.** (A) Percent DHA (relative to total fatty acids) in the indicated phospholipid classes (PC, PS, PI, PE). (B) Percent AA in the indicated phospholipid classes (PC, PS, PI, PE). Data points are percent mean  $\pm$  SD, n=3.

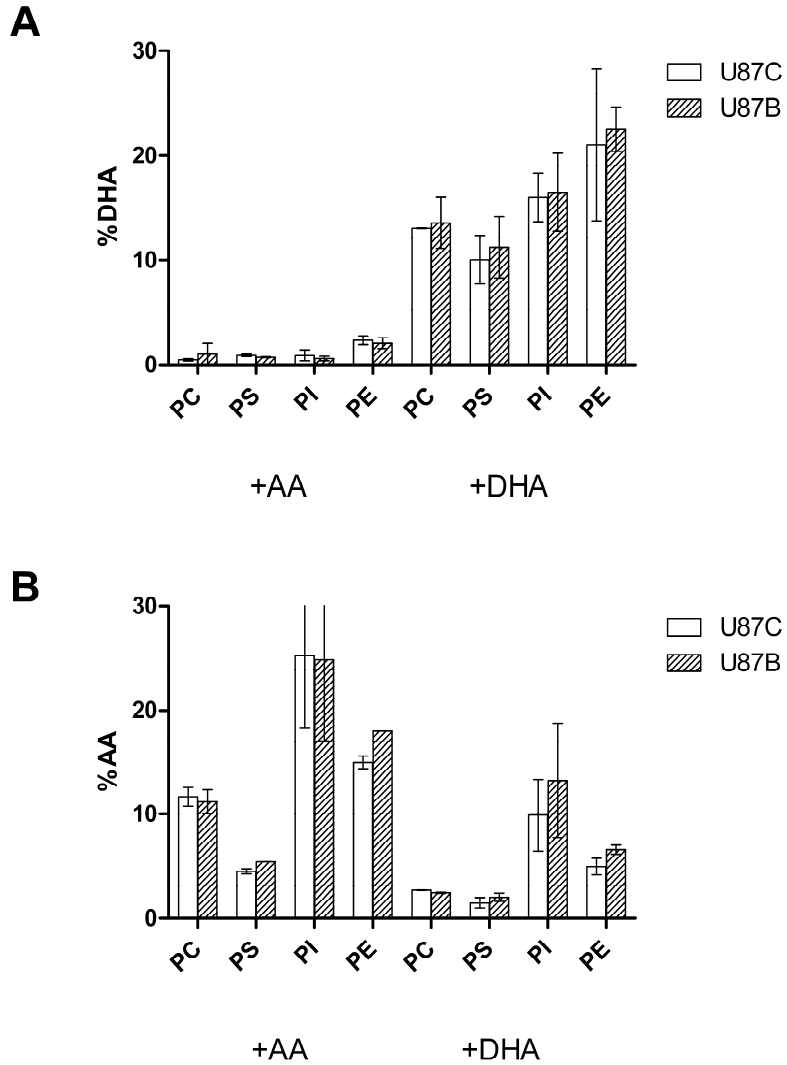


**Figure 3.3.2 The DHA and AA content of phospholipid classes is increased in both U87C and U87B MG cells when treated with DHA and AA.** (A) Percent DHA in the indicated phospholipid classes (PC, PS, PI, PE) purified from U87C and U87B cells treated with either 60  $\mu$ M AA or 60  $\mu$ M DHA for 24 hours. (B) Percent AA in phospholipid classes (PC, PS, PI, PE) purified from U87C and U87B cells treated with either 60  $\mu$ M AA or 60  $\mu$ M DHA for 24 hours. Data points are the percent mean  $\pm$  SD, n=3.

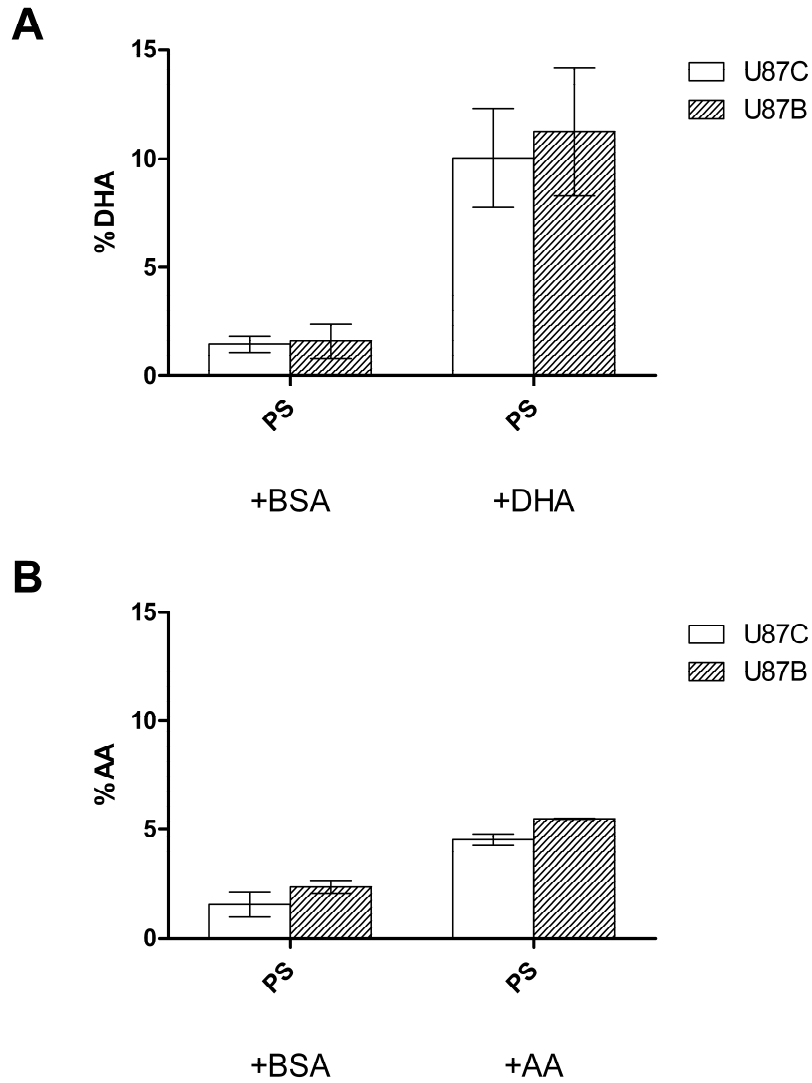


**Figure 3.3.3 Effect of DHA and AA treatment on DHA and AA content, respectively, of PS in U87C and U87B cells.** (A) DHA content of PS purified from U87C and U87B cells treated with either 60  $\mu$ M BSA or 60  $\mu$ M DHA for 24 hours. (B) AA content of PS purified from U87C and U87B cells treated with either 60  $\mu$ M BSA or 60  $\mu$ M AA for 24 hours. Data points are the mean  $\pm$  SD, n=3. \*p<0.05 pooled two-tailed t-test.

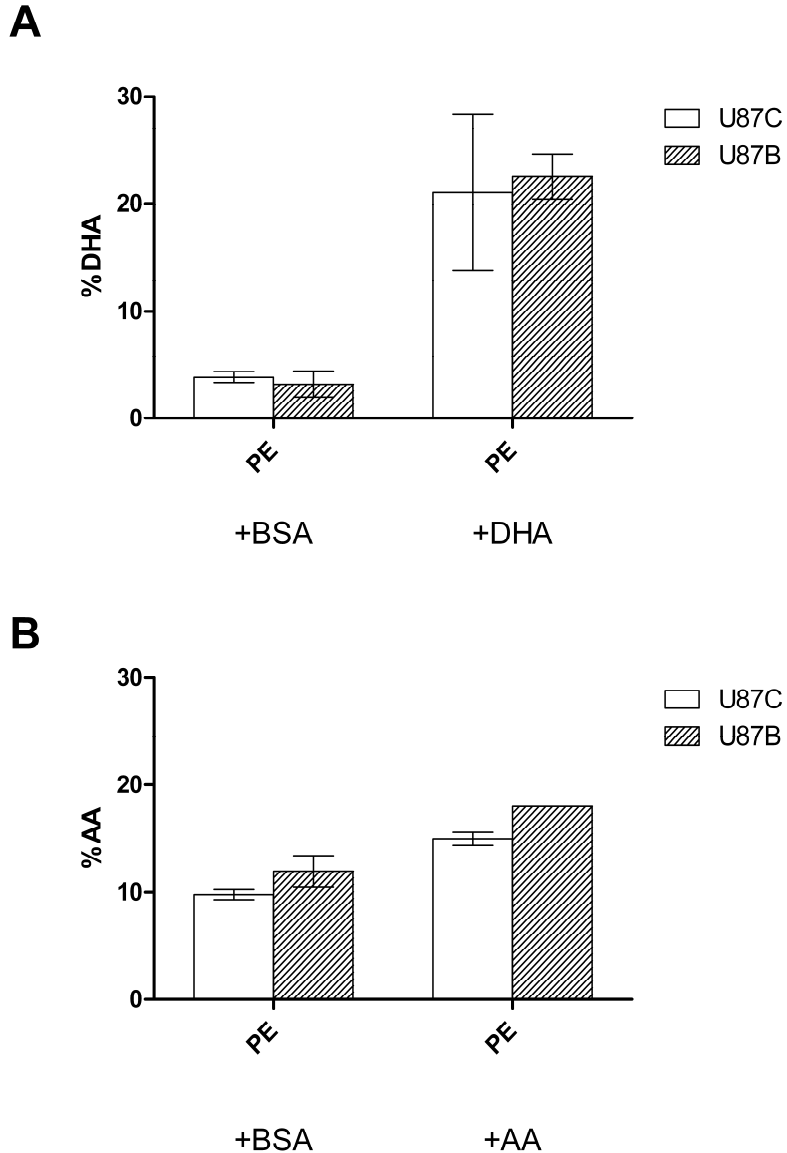


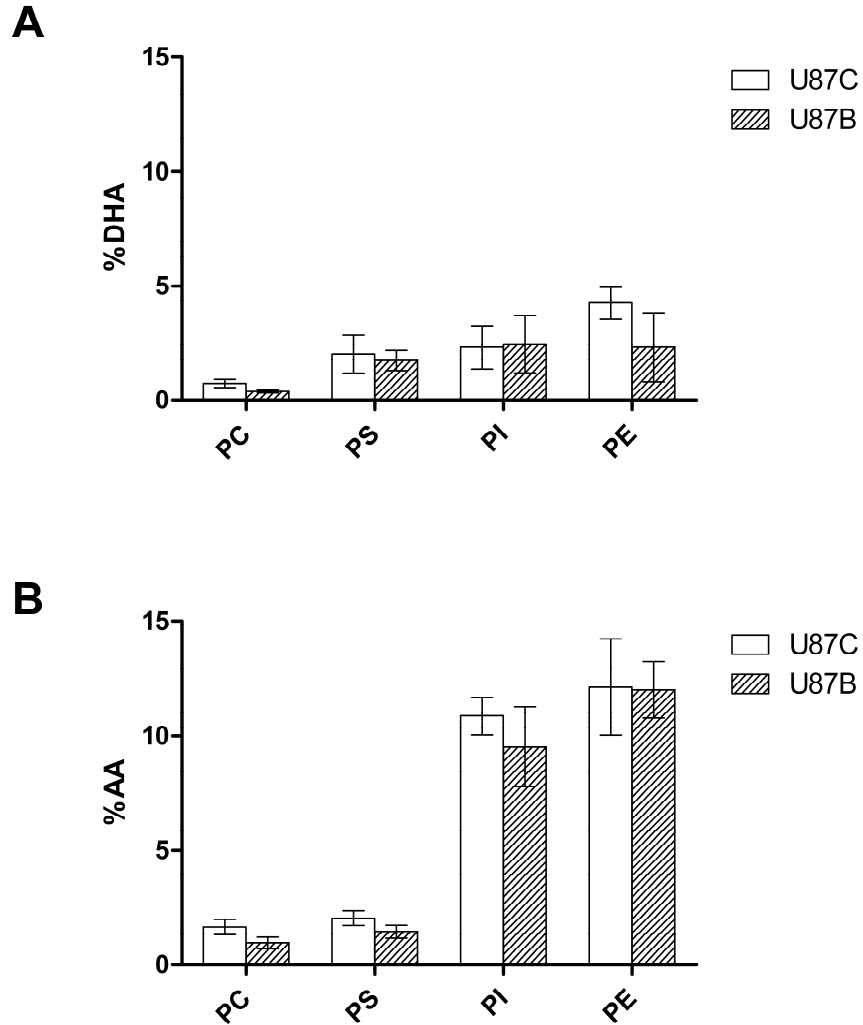
**Figure 3.3.4 Effect of DHA and AA treatment on DHA and AA content, respectively, of PE in U87C and U87B cells.** (A) DHA content of PE purified from U87C and U87B cells treated with either 60  $\mu$ M AA or 60  $\mu$ M DHA for 24 hours. (B) AA content of PE purified from U87C and U87B cells treated with either 60  $\mu$ M AA or 60  $\mu$ M AA for 24 hours. Data points are the mean  $\pm$  SD, n=3. \*p<0.05 pooled two-tailed t-test.

### 3.3.2 AA and DHA incorporation into the nuclear phospholipids of U87C versus U87B cells

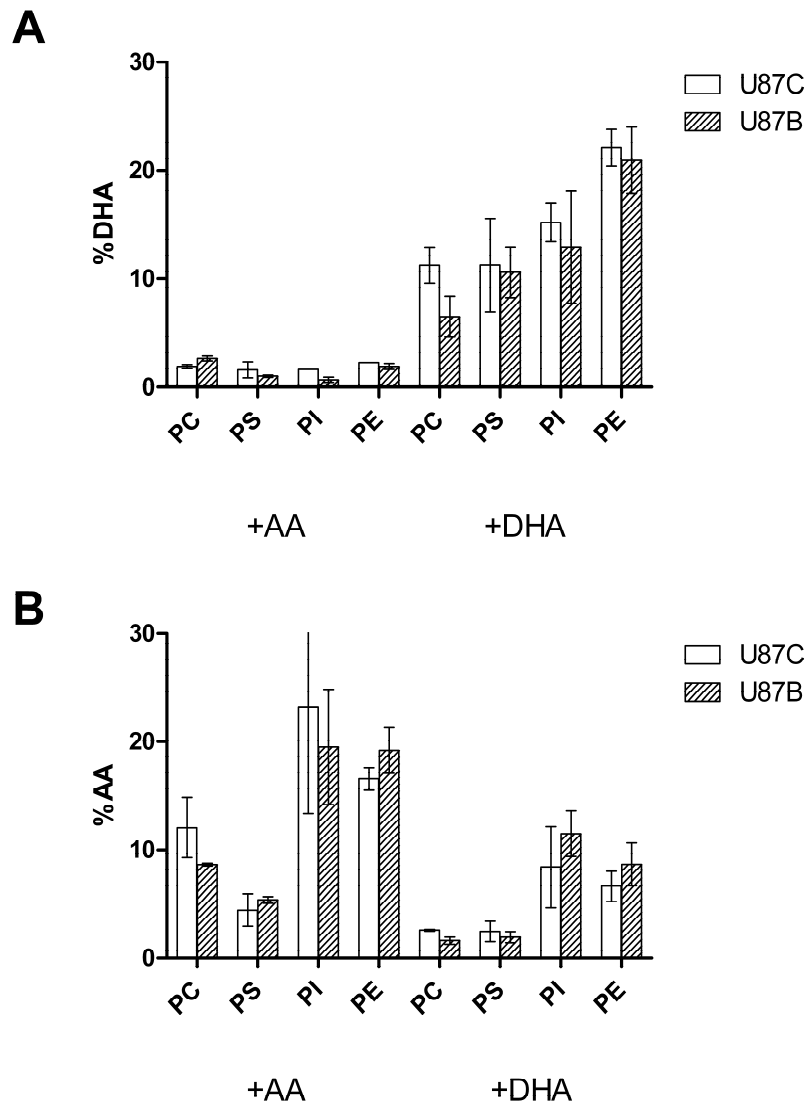
FABP7 is found in both the cytoplasm and nucleus (Mita *et al.*, 2007) and the presence of FABP7 in the nucleus is associated with a worse prognosis in GBM (Liang *et al.*, 2006). To investigate the possibility that the effect of FABP7 on MG growth might be mediated through alterations in the fatty acid composition of nuclear membranes, we purified nuclei from U87C and U87B cells treated with BSA, 60  $\mu$ M AA or 60  $\mu$ M DHA. Lipids were extracted from these nuclei preparations and phospholipids separated by thin layer chromatography.

FABP7 expression in U87 cells treated with BSA was associated with a significant decrease in both the AA and DHA content of PC; however FABP7 expression had no effect on the AA and DHA content of PS, PI or PE (Figure 3.3.5). As previously noted in phospholipids from whole cells, treating U87C and U87B cells with either AA or DHA for 24 hours resulted in a significant increase in the relative content of AA or DHA in nuclear PC, PS, PI and PE compared to BSA-treated cells (Figure 3.3.6). As with whole cell phospholipids, we tested whether or not treatment with 60  $\mu$ M AA or 60  $\mu$ M DHA would change the DHA or AA content, respectively, of nuclear phospholipid classes in U87C and U87B cells. We observed ~1.3-fold, ~1.3-fold, ~2-fold decreases in the DHA content of nuclear PS, PI and PE, respectively, and a ~2.7-fold increase in the DHA content of PE in nuclei prepared from U87C and U87B cells

treated 60  $\mu$ M AA (Figure 3.3.6A). We also observed ~1.6-fold, and ~1.2-fold increases and no change in the AA content of PC, PS and PI, respectively, and a ~1.4-fold decrease in the AA content of PE, when U87C and U87B cells were treated with 60  $\mu$ M DHA (Figure 3.3.6B).

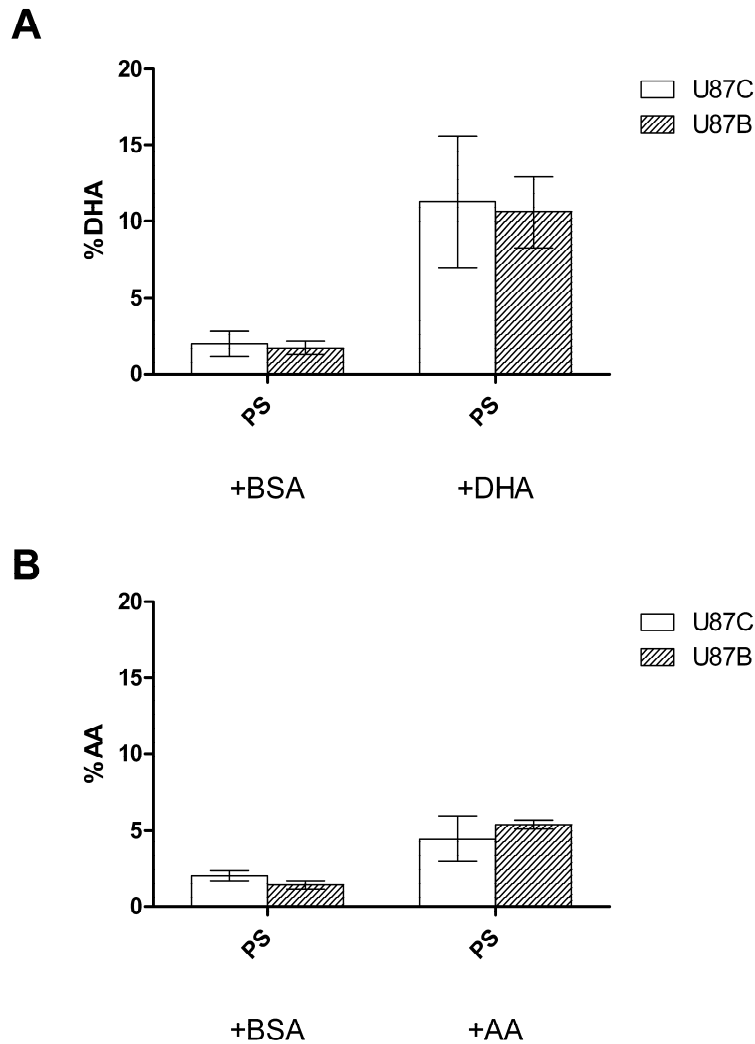


**Figure 3.3.5 DHA and AA content of phospholipid classes in nuclei of U87C and U87B MG cells treated with BSA.** (A) DHA content of phospholipids (PC, PS, PI, PE) purified from nuclei prepared from U87C and U87B cells treated with 60  $\mu$ M BSA for 24 hours. (B) AA content of phospholipids (PC, PS, PI, PE) purified from nuclei prepared from U87C and U87B cells treated with 60  $\mu$ M BSA for 24 hours. Data points are the mean  $\pm$  SD, n=3.

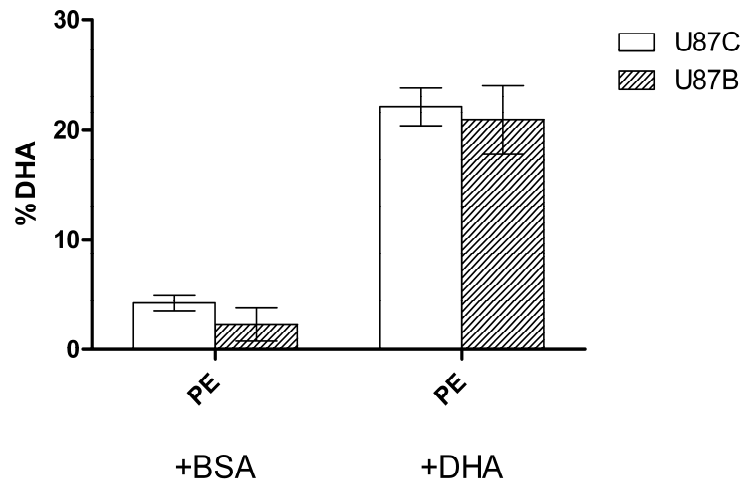
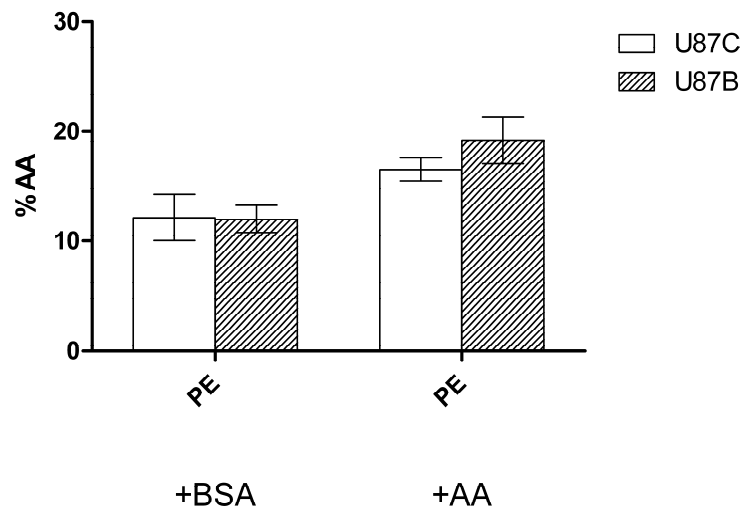


**Figure 3.3.6** The DHA and AA content of nuclear phospholipid classes is increased in U87C and U87B MG cells treated with DHA or AA. (A) DHA content of the indicated phospholipid classes (PC, PS, PI, PE) purified from nuclei prepared from U87C and U87B cells treated with either 60  $\mu\text{M}$  AA or 60  $\mu\text{M}$  DHA for 24 hours. (B) AA content of phospholipid classes (PC, PS, PI, PE) purified from nuclei prepared from U87C and U87B cells treated with either 60  $\mu\text{M}$  AA or 60  $\mu\text{M}$  DHA for 24 hours. Data points are the mean  $\pm$  SD,  $n=3$ .

As with the whole cell phospholipids, we observed a ~5.5-fold increase in the DHA content of nuclear PS when either U87C or U87B were treated with DHA compared to BSA (Figure 3.3.7A). In contrast, the AA content of PS in U87C and U87B only increased ~2-fold upon AA treatment (Figure 3.3.7B). Again, as with the whole cell phospholipids, we observed a ~5.2-fold increase in the DHA content of nuclear PE when either U87C or U87B were treated with DHA compared to BSA (3.3.8A). This is in contrast to the AA content of nuclear PE in U87C and U87B, where only a ~2-fold increase was observed upon treatment with AA (Figure 3.3.8B). Most notable, however, was the significant differences in AA and DHA composition observed in nuclear PC phospholipids purified from U87C versus U87B cells (Figure 3.3.9). Specifically, a ~40-50% reduction in DHA content was observed in U87B cells, compared to U87C cells, treated with BSA and DHA. Furthermore, a reduction in AA content was observed in U87B cells treated with BSA, AA and DHA compared to similarly-treated U87C cells. Thus, FABP7 expression appears to be associated with a general decrease in the AA and DHA content of nuclear PC.



**Figure 3.3.7 Effect of DHA and AA treatment on DHA and AA content, respectively, of PS in U87C and U87B nuclei.** (A) DHA content of PS purified from nuclei prepared from U87C and U87B cells treated with either 60  $\mu$ M BSA or 60  $\mu$ M DHA for 24 hours. (B) AA content of PS purified from nuclei prepared from U87C and U87B cells treated with either 60  $\mu$ M BSA or 60  $\mu$ M AA for 24 hours. Data points are the mean  $\pm$  SD, n=3. \*p<0.05 pooled two-tailed t-test.

**A****B**

**Figure 3.3.8 Effect of DHA and AA treatment on DHA and AA content, respectively, of PE in U87C and U87B nuclei.** (A) DHA content of PE purified from nuclei prepared from U87C and U87B cells treated with either 60  $\mu$ M BSA or 60  $\mu$ M DHA for 24 hours. (B) AA content of PE purified from nuclei prepared from U87C and U87B cells treated with either 60  $\mu$ M BSA or 60  $\mu$ M AA for 24 hours. Data points are the mean  $\pm$  SD, n=3. \*p<0.05 pooled two-tailed t-test.

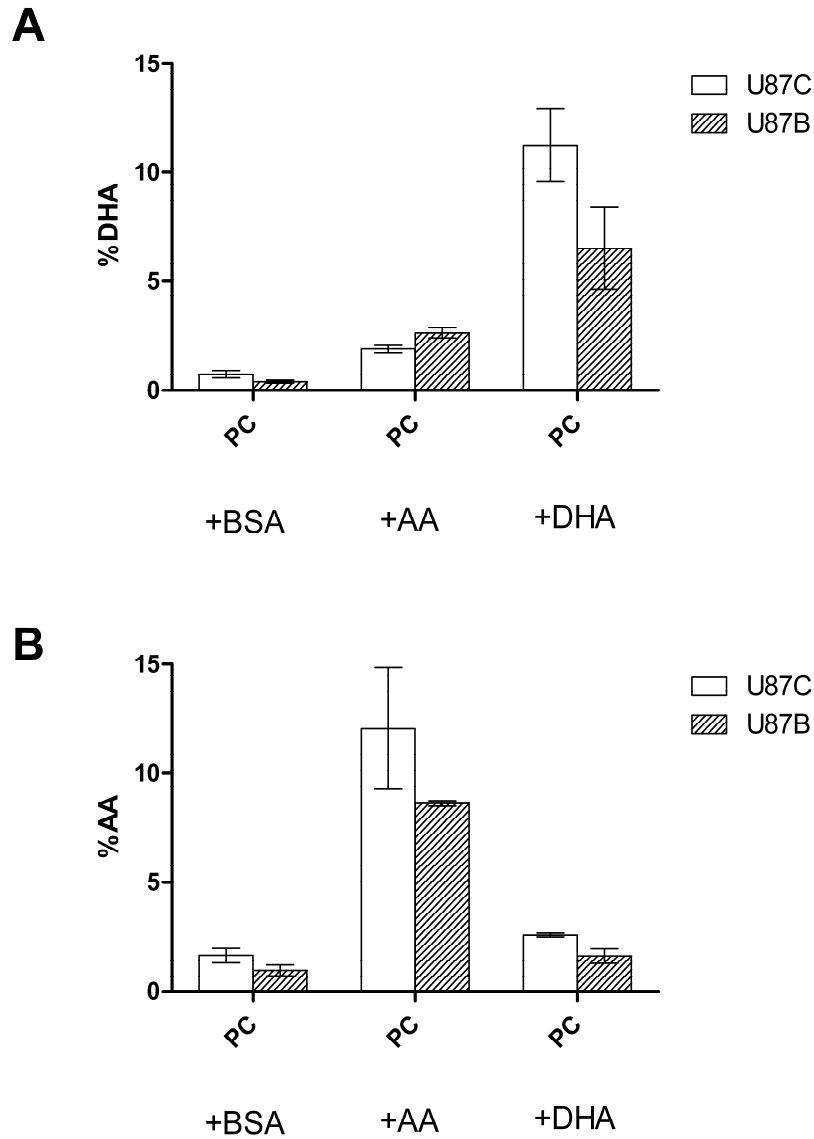


**Figure 3.3.9 FABP7-dependent changes in DHA and AA content of nuclear PC.** (A) DHA content of PC isolated from nuclear lipid extracts prepared from U87C and U87B MG cells treated with either 60  $\mu$ M BSA, 60  $\mu$ M AA or 60  $\mu$ M DHA for 24 hours. (B) AA content of PC isolated from nuclear lipid extracts prepared from U87C and U87B MG cells treated with either 60  $\mu$ M BSA, 60  $\mu$ M AA or 60  $\mu$ M DHA for 24 hours. Data points are the mean  $\pm$  SD, n=3. \*p<0.05 two-tailed t-test.

# **CHAPTER 4**

## **Discussion**

## 4.1 Discussion

### 4.1.1 Malignant Glioma: Picking up the pieces

MG are amongst the most aggressive tumours. Although they are relatively rare in comparison to other cancers, they carry a dismal prognosis. Despite an aggressive treatment regimen, patients with GBM rarely survive beyond one year. It is therefore imperative that new strategies be identified for the treatment of MG.

The frontline MG therapy consists of surgical resection and radiation therapy. Though the extent of surgical resection remains a controversial subject in the field, there is evidence suggesting that younger patients (<65 years) whose GBM undergo maximal tumour resection (>98% tumour volume) have improved survival compared to patients with resection levels less than 98% (Kuhnt *et al.*, 2011; Sanai *et al.*, 2011). While achieving such high levels of resection remains difficult, recent improvements in intra-operative magnetic resonance imaging (MRI) have allowed neurosurgeons to achieve greater levels of tumour resection while reducing the risk of damaging healthy brain tissue (Kuhnt *et al.*, 2011).

There have been several attempts at designing dose-escalation trials with radiation therapy that have failed to yield any clear survival benefit to patients with GBM. Nieder and Mehta (2011) provide evidence that certain subsets of GBM may be more resistant to radiotherapy, thus providing a rationale to revisit previous radiation dose-escalation trials

(Nieder and Mehta, 2011). If radiation-sensitive populations of GBM cells can be identified, then perhaps hyper-fractionation regimens of radiation therapy can be used to improve survival in a subset of radiation-sensitive patients. Although these treatment modalities may improve the survival of patients with MG, they have inherent limitations. Both surgery and radiotherapy target local disease, and infiltration of MG cells into surrounding brain tissue, the hallmark of MG tumours, ultimately results in their recurrence. Thus, in order to achieve long-term survival of patients with MG, we must aim to target these infiltrative cells.

The use of chemotherapeutic agents is an attractive option for treating disseminated MG; however, their usefulness can be limited to particular subsets of patients. Furthermore, the use of chemotherapeutic agents is often accompanied by severe side effects and the development of drug resistance. As an example, BCNU wafers that are surgically implanted into the brain have significantly improved patient survival in randomized phase III clinical trials of patients with newly diagnosed GBM (Westphal *et al.*, 2003); however, the side effects associated with these devices are much more severe than originally anticipated (Bock *et al.*, 2010). Thus, there is a need for new chemotherapeutic agents that target MG growth properties associated with tumour progression and tumour recurrence, but which have little to no side effects. To find such a target, we must deconstruct MG tumours to their fundamental pieces, and rebuild our understanding of this disease.

#### 4.1.2 FABP7 provides insight into MG tumour behaviour

In this study we have demonstrated several potential mechanisms for FABP7 affecting the growth of MG cells. Our model system consists of the FABP7-negative GBM cell line (U87C) and its stable FABP7-transfected counterpart (U87B). Previous work has shown that U87B cells exhibit marked differences in cell motility and invasion compared to U87C cells. The role of FABP7 in mediating these processes is dependent on its subcellular localization to the nucleus (Mita *et al.*, 2007; Mita *et al.*, 2010). We have shown by microarray analysis that FABP7 expression is associated with extensive changes in the gene expression profiles of U87C and U87B cells. The experimental design of our microarray analysis ensures the reproducibility of our results. RNA from three independent preparations of both U87C and U87B cells were used to probe a total of six independent microarray chips. We observed remarkably consistent changes in the gene expression profiles of the three independent preparations of U87C and U87B cells.

RT-PCR analysis was used to confirm the relative expression patterns of genes in our cDNA microarrays. In light of the dramatic effects of FABP7 on the gene expression profile of U87B cells, we sought to investigate the potential mechanisms by which FABP7 might alter gene expression in these cells. Several FABPs have been shown to alter gene expression by delivering fatty acids to ligand-activated nuclear receptors (Ayers *et al.*, 2007; Kannan-Thulasiraman *et al.*, 2010; Tan *et al.*, 2002).

We observed an FABP7-dependent effect on the expression profiles of members of the PPAR family of transcription factors, with *PPAR-β/δ* RNA levels increasing and *PPAR-γ* RNA levels decreasing in U87B cells. *PPAR-α* RNA levels were not altered upon FABP7 expression in U87 cells. Work by Mita *et al.* (2010) confirmed these trends at the protein level. While *PPAR-α* is generally thought to be involved in the maintenance of lipid homeostasis (Pyper *et al.*, 2010), *PPAR-β/δ* and *-γ* have been shown to be involved in regulating processes like inflammation and cell differentiation (Chalwa *et al.*, 1994; Bonala *et al.*, 2012; D'Angelo *et al.*, 2011; Peters *et al.*, 2012). Our microarray data suggest that FABP7 expression in U87 is accompanied by changes in factors involved with the immune response and inflammation. Given the involvement of *PPAR-β/δ* in mediating inflammatory processes in various cell types, we investigated whether FABP7 could be affecting inflammation in MG through *PPAR-β/δ*.

We present preliminary evidence showing a potential ligand-dependent interaction between FABP7 and *PPAR-β/δ* in U87B MG cells. We observed an increased interaction between FABP7 and *PPAR-β/δ* when cells were treated with DHA compared to AA. FABP7 binds preferentially to DHA and this may reflect the increased level of interaction compared to AA-treated cells. Strikingly, strongest interaction was detected in cells treated with fatty acid-free BSA. In order to further investigate the ligand-dependent interaction of FABP7 with *PPAR-β/δ*, we serum-starved our cells during fatty acid treatment. Serum starvation was

necessary as the 10% fetal calf serum used to culture our cells contains approximately 4  $\mu\text{M}$  DHA and 11  $\mu\text{M}$  AA. The increased interaction of FABP7 and PPAR- $\beta/\delta$  under these conditions may reflect a starvation response in the cell as PPAR- $\beta/\delta$  has been shown to up-regulate genes associated with lipid metabolism (Wagner and Wagner, 2010). This implicates FABP7 as a metabolic sensor for PPARs.

In order to further validate our findings, we propose to repeat these co-IP experiments in the presence of serum, and with higher concentrations of AA and DHA. This may help to intensify our IP signals and yield more consistent results as FABPs bound to fatty acids may dictate the level of protein-protein interactions. Furthermore, we will have to work out the conditions for immunostaining western blots with anti-PPAR antibodies, as we were not able to verify that PPAR- $\beta/\delta$  was co-immunoprecipitated with FABP7.

Smith *et al.* (2008) have identified a potential 'protein-protein interaction motif' in several FABPs (amino acid sequence: F-Acidic-Acidic-YMKXXGVG). These authors propose that this domain interacts with a corresponding HIYK in other proteins via coordination of a charge quartet (Smith *et al.*, 2008). The FABP7 protein contains the amino acid sequence FDEYMKALGVG, which implies that FABP7 protein-protein interactions may occur through similar mechanisms as FABP4 (Smith *et al.*, 2008, Thompson *et al.*, 2009). Intriguingly, a HIYK motif is located in the C-terminal domains of both PPAR- $\beta/\delta$  and - $\gamma$ , but not in PPAR- $\alpha$ . This

provides a rationale for pursuing these co-IP experiments and extending them further to test interactions between FABP7 and PPARs. To this end, it will be important to determine whether or not FABP7 and its ligands are capable of altering PPAR transcriptional activity. Reporter gene assays using vectors containing PPRES can be used to test whether FABP7 and its ligands can affect PPAR transcriptional activity *in vitro*. I have cloned a putative FABP7 'protein binding mutant' by site-directed mutagenesis to generate FABP7 with the motif FDAAMAALGVG. This construct can be used as a negative control in future co-IPs of FABP7 with PPARs, and as a negative control in PPRE-driven gene reporter assays. Together, these experiments will test to what extent FABP7-PPAR ligand-dependent interactions are affecting gene transcription in our system and may even shed light on the functional roles of FABPs.

RT-PCR analysis of U87C and U87B cells showed that important inflammatory mediators were over-expressed in U87B cells compared to U87C cells. In particular, PLA2G4A (c-PLA<sub>2</sub>α), a cytosolic and calcium-dependent PLA<sub>2</sub>, is up-regulated upon FABP7 expression in U87 cells. This is in contrast to another PLA<sub>2</sub> family member, PLA2G4C (c-PLA<sub>2</sub>γ), a cytosolic calcium-independent PLA<sub>2</sub>, which showed decreased expression in the U87B cells. Together these findings point to a role for both calcium-dependent (through their up-regulation) and calcium-independent PLA<sub>2</sub> (through their down-regulation) in the promotion of MG cell migration in our system.

To further interrogate the hypothesis that PLA<sub>2</sub> is involved in MG cell migration, we examined c-PLA<sub>2</sub>α expression in U87C versus U87B cells. Using an antibody specific to c-PLA<sub>2</sub>α, we observed induction of a ~45-55 kDa band in U87B cells compared to U87C; however, the appropriate size for c-PLA<sub>2</sub>α is ~100 kDa, as detected in cell extracts prepared from the FABP7-positive MG cell lines, U251 and U373. As our RT-PCR data indicate that *PLA2G4A* RNA levels are increased in U87B compared to U87C cells, we were interested in whether or not this smaller protein fragment was related to c-PLA<sub>2</sub>α. By testing buffers that either contained or were devoid of non-specific phosphatase inhibitors, we were able to demonstrate a relationship between the 100 kDa c-PLA<sub>2</sub>α band and the 45-55 band observed in U87C and U87B cells. Interestingly, we observed that in cell extracts prepared in the absence of generic phosphatase inhibitors, there is a loss of the 100 kDa c-PLA<sub>2</sub>α and an increase in the 45 kDa protein in U87B cells. A search of the literature revealed that c-PLA<sub>2</sub>α can undergo proteolytic cleavage by various caspases.

Cleavage of c-PLA<sub>2</sub>α by caspase-3 results in a 70 kDa inactive form of c-PLA<sub>2</sub>α (Adam-Klages *et al.*, 1998; Luschen *et al.*, 1998). Cleavage of c-PLA<sub>2</sub>α at Asn-459 was found to be mediated by caspase-1 and generates a 55 kDa c-PLA<sub>2</sub>α fragment (Luschen *et al.*, 1998). It is possible that these fragments retain some of their lipase activity, which could potentially allow them to remain active in the cell and release more

AA substrate for COX-2. Tumour necrosis factor receptors (TNFRs) have been shown to be involved in the phosphorylation-dependent membrane translocation and activation of c-PLA<sub>2</sub>α. Jupp *et al.* showed that TNFR1 activation results in c-PLA<sub>2</sub>α cleavage (Jupp *et al.*, 2003). Another family member, TNFR2, doesn't appear to be involved in c-PLA<sub>2</sub>α cleavage, but does affect c-PLA<sub>2</sub>α translocation to perinuclear regions of the cell and enhances c-PLA<sub>2</sub>α activity (Jupp *et al.*, 2003). Our microarray analysis showed that various members of the TNFR superfamily are differentially expressed with FABP7. It will be important to clarify to what extent c-PLA<sub>2</sub>α cleavage is dependent on its phosphorylation status and the functional implications of phosphorylation on c-PLA<sub>2</sub>α cleavage products.

Given the relationship between c-PLA<sub>2</sub>α and pro-apoptotic caspases, we performed a FACS analysis of U87C and U87B cells and showed that FABP7 does not appear to induce apoptosis in our system (data not shown). Thus, in light of our findings it will be important to test the relevance of the 45 kDa c-PLA<sub>2</sub>α fragment in MG cell lines that express FABP7. We have preliminary data indicating that the relationship between the 100 kDa and 45 kDa c-PLA<sub>2</sub>α may be calcium-dependent (data not shown). A role for calcium in c-PLA<sub>2</sub>α cleavage is an interesting possibility in light of previous experiments by Casas *et al.* (2005) demonstrating that over-expression of c-PLA<sub>2</sub>α can inhibit high Ca<sup>2+</sup> influx-dependent apoptosis. These researchers showed that the latter is dependent on the Ca<sup>2+</sup> binding ability of c-PLA<sub>2</sub>α (Casas *et al.*, 2005).

Since  $\text{Ca}^{2+}$  binding to c-PLA<sub>2</sub>α results in its translocation to membranes, it will be interesting to test the dependence of these processes on the AA content of the cell membrane. MG tumours are known to contain higher levels of AA compared to healthy brain tissue (Martin *et al.*, 1996), and this relationship between FABP7 and c-PLA<sub>2</sub>α may have important implications for MG cell survival.

We have also analyzed downstream components of the PLA<sub>2</sub> pathway. PLA<sub>2</sub> primarily cleaves AA from the *sn*-2 position of PC in the cell membrane. AA is then converted to prostaglandins by the enzymatic activity of cyclooxygenases (COX). RT-PCR analysis of COX-1 and COX-2 showed that COX-1 RNA expression is significantly decreased upon FABP7 expression in U87 cells, in contrast to COX-2 RNA, which is significantly increased in U87B compared to U87C cells. An analysis of the literature revealed that regulation of COX activity is primarily through degradation of its RNA or protein, or by the presence of one COX isoform over the other. Since COX-1 RNA was not detected in U87B based on our RT-PCR analysis, we selected COX-2 for further analysis by western blotting. This analysis showed that COX-2 protein is more abundant in U87B cells than in U87C cells. These data, in combination with our data showing that PGE<sub>2</sub> levels are increased in U87B compared to U87C cells, support the hypothesis that FABP7 is acting to promote PLA<sub>2</sub>-COX-2-PGE<sub>2</sub> signaling in MG.

The expression of PGE<sub>2</sub> receptors (PTGERS) may also dictate the function of PGE<sub>2</sub> in our system. There are four PTGERS, also called EP receptors, and each is responsible for the effects of PGE<sub>2</sub> on the cell. In our microarray analysis, EP1 and EP4 RNA were both expressed at similar levels in U87C and U87B cells, whereas EP2 and EP3 showed decreased RNA expression in U87B compared to U87C cells. Since the levels of EP1 and EP4 remain constant with FABP7 expression in our system, and the level of EP2 and EP3 are reduced, less PGE<sub>2</sub> will bind to EP2 and EP3; therefore, PGE<sub>2</sub> may preferentially activate EP1 and EP4 receptors in our system. EP1 receptors in the cell membrane bind to extracellular PGE<sub>2</sub>, which causes them to activate phospholipase C (PLC). Activation of PLC is associated with increased diacylglycerol levels and IP<sub>3</sub> production, which activates protein kinase C (PKC) and intracellular Ca<sup>2+</sup> release from the ER, respectively (Rundhaug *et al.*, 2011). EP4 receptors in the cell membrane bind to extracellular PGE<sub>2</sub> and activate adenylate cyclase (AD) and the PI3K/Akt pathway. AD activity generates high intracellular levels of cyclic AMP (cAMP), which activates protein kinase A (PKA). We observed a substantial increase in brain adenylate cyclase (ADCY8) RNA expression in U87B cells compared to U87C, which may indicate that the EP4 receptor may be activated by PGE<sub>2</sub> in our system. In glioma cells, PGE<sub>2</sub> has been shown to induce cAMP response element-binding protein (CREB) transcriptional activity through PKA-mediated inhibition of ERK activity (Bidwell *et al.*, 2010). Together, this

shows how PGE<sub>2</sub> and EP receptors can mediate processes like cell proliferation, survival, inflammation and invasion (Rundhaug *et al.*, 2011).

It is well-established that uncontrolled EGFR-PI3K-Akt signaling plays an important role in GBM (TCGA, 2008). Xu *et al.* (2009) reported a connection between EGFR and COX-2, where EGFR induced COX-2 expression and activity via PKC- $\delta$  signaling. A relationship between EGFR and FABP7 has also been reported in GBM. In particular, Liang *et al.* have shown that nuclear FABP7 is associated with over-expression of EGFR, and correlates with a poor prognosis in GBM (Liang *et al.*, 2006). To date, there have been no reports linking COX-2 expression/activity with EGFR expression in GBM tumours. In light of our results, we propose that FABP7 may be the missing link between EGFR and COX-2 in MG tumours. Mita *et al.* have shown that FABP7-positive cells surround blood vessels and are located at sites of infiltration in the margins of GBM tumours (Mita *et al.*, 2007). This is interesting since COX-2 requires O<sub>2</sub> for its catalytic activity. Thus, FABP7-positive cells located near blood vessels may express higher levels of COX-2, resulting in increased COX-2 activity in regions of the brain where its cofactors (O<sub>2</sub>) are readily available. Together, EGFR, FABP7 and COX-2-expressing cells may be setting up a specialized pro-survival niche within MG tumours where they can migrate away from the primary tumour mass and seed secondary MG tumours (Figure 4.1).

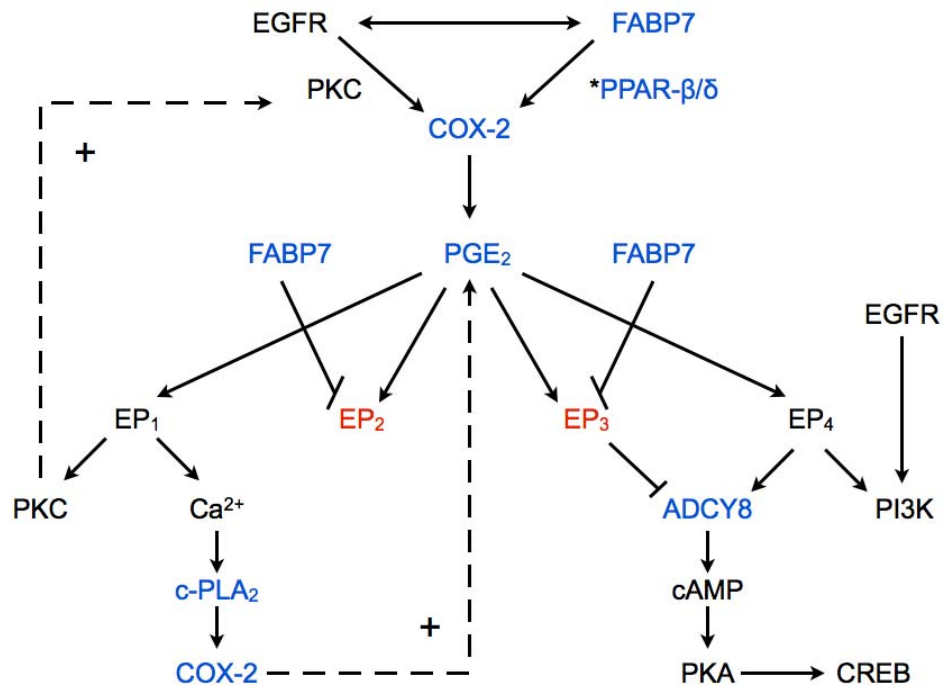


**Figure 4.1 Potential role for FABP7 in stabilizing multiple positive feedback loops for COX-2-mediated glioma growth, survival and migration. Down-regulated (red) or up-regulated (blue); Positive feedback (+).**

Mita *et al.* (2010) demonstrated that inhibition of COX-2 activity reduced the migration of U87B cells compared to U87C, thereby implicating COX-2 and PGE<sub>2</sub> in MG cell migration. Given this role for COX-2 in MG cell migration, and the evidence showing that COX-2 is predictor of poor survival in GBM, it is possible that COX-2 may be a good candidate for glioma therapy. Several inhibitors of COX-2 have been shown to inhibit COX-2 function in human gliomas (King Jr and Khalili, 2001; Joki *et al.*, 2000); however, there are some conflicting results. For example, researchers have shown that increased PGE<sub>2</sub> biosynthesis correlates with patient survival in GBM (Lalier *et al.*, 2007). It is possible that these counter-intuitive results are due to the variety of EP receptors expressed by these patients' tumour cells. In light of our findings for FABP7 and COX-2 in MG cells, and the involvement of FABP7 with EP receptor expression, EGFR/FABP7/COX-2-expressing tumours may respond particularly well to treatments that target FABP7 in combination with COX-2 and other treatment modalities. Mita *et al.* have also shown that DHA treatment of U87B cells results in significantly reduced cell migration (Mita *et al.*, 2010), suggesting that DHA may also be effective in preventing infiltration of FABP7-positive MG cells within the brain. If the cells are no longer migrating, then they may be more susceptible to radiation therapy.

E-6087, an inhibitor of COX-2 activity, enhances the effects of radiotherapy in orthotopic models of MG (Wagemakers *et al.*, 2009).

Another COX-2 inhibitor, celecoxib, induces DNA damage via p53-dependent G1 cell cycle arrest (Kang *et al.*, 2009). COX-2 has also been shown to regulate p53 activity and inhibit DNA damage-induced apoptosis (Choi *et al.*, 2005). This provides a rationale for treating FABP7/COX-2-expressing MG tumours with adjuvant DHA and COX-2 inhibitors. This combined therapy may be especially effective as COX-2 inhibitors may play more than one role in targeting MG cells. Besides their effects in radiosensitizing MG cells, COX-2 inhibitors may inhibit MG cell growth in a manner that is exacerbated by FABP7 expression. In support of this idea, Joki *et al.* showed that NS-398, a COX-2 inhibitor, inhibits tumour growth in monolayer and spheroid cultures of U87 and U251 cells (Joki *et al.*, 2000). Interestingly, the effects of NS-398 were much more pronounced in the U251 cells compared to U87 cells. Since U251 are FABP7-positive and U87 are FABP7-negative, this suggests the interesting possibility that FABP7 and COX-2- positive tumours may respond well to COX-2 inhibitors in combination with DHA.

#### *4.1.3 Fatty acid content of phospholipid classes in MG cells in response to treatment with AA and DHA*

Expression of FABPs is known to enhance the uptake of fatty acids in the cell (Darimont *et al.*, 2000; Burczynski *et al.*, 1999). Our lab has previously shown that FABP7 expression in U87 cells results in an increase in the uptake of the polyunsaturated fatty acids, AA and DHA, but

that AA and DHA treatment of U87C and U87B cells had little effect on incorporation of AA and DHA in total phospholipids (data not shown). The goal of our experiments was to determine whether FABP7 expression in U87 cells affects the AA and DHA composition of the main phospholipid classes. Our results indicate that FABP7 expression by itself does not alter the “steady-state levels” of AA and DHA in PC, PS, PI and PE purified from whole cell lipid extracts. These findings are consistent with those reported for FABP7 KO mice, and together suggest a unique role for FABP7 among the FABP family members.

Our findings using nuclear lipid extracts are in slight contrast to our whole cell lipid data. In nuclear lipid extracts, we observed a FABP7-dependent decrease in both the AA and DHA content of PC. Interestingly, c-PLA<sub>2</sub> $\alpha$  is known to specifically cleave AA at the *sn*-2 position of PC and COX-2 localizes to perinuclear membranes, as opposed to the ER-localized COX-1 (Yazaki *et al.*, 2012). The observed decreases in both the AA and DHA content of PC in nuclear lipid extracts may indicate increased activity of phospholipases and COX-2 at the nuclear membrane. An interesting possibility is that the decrease in COX-1 expression observed upon FABP7 expression in U87 cells acts as a way to increase COX-2 activity by reducing competition for AA. This highlights an important point about our whole cell lipid data. FABP7 may be altering the AA and DHA content of phospholipids in specific subcellular compartments or organelles. By extracting lipids from plasma membrane and mitochondrial

fractions, rather than whole cells, we may be able to find further clues as to the role of FABP7 in MG cell phospholipid metabolism.

Mita *et al.* have shown that the ratio of AA to DHA is important in mediating the effects of AA and DHA on FABP7-dependent MG cell migration (Mita *et al.*, 2010). We therefore tested the effects of AA and DHA treatment on DHA and AA content of phospholipid classes, in both whole cell and nuclear lipid preparations of U87C and U87B cells. In line with our previous data, FABP7 expression did not affect the AA and DHA content of phospholipid classes purified from whole cell lipids. Similarly, the AA content of PC after 24 hour treatment with AA or DHA was similar in nuclear extracts prepared from either U87C or U87B (Figure 3.3.9B). However, there was a FABP7-dependent increase in the DHA content of PC in AA-treated U87C and U87B cells (Figure 3.3.9A). This suggests that under pro-migratory conditions in U87 cells (FABP7-positive, +AA), there is an increased level of DHA in PC of nuclear membranes. One possible explanation for this effect may be that in the presence of high AA, c-PLA<sub>2</sub> $\alpha$  preferentially releases AA from PC, whereas DHA remains in PC. Under conditions where COX-2 is highly expressed, less availability of DHA compared to AA may result in the production of prostaglandins that favour cell survival and migration. It is also possible that a decrease in the availability of DHA leads to a reduction in the amount of anti-inflammatory molecules produced by the cell.

The structural similarities between DHA and AA have led researchers to hypothesize that DHA may be metabolized by some of the same enzymes as AA. Vecchio *et al.* (2010) have shown that precursors of DHA are capable of binding the COX-2 enzyme, and in doing so, it is hypothesized that these molecules antagonize the effects of AA on the cell. This is in-line with evidence that suggests that  $\omega$ -3 PUFAs like DHA have anti-inflammatory effects compared to the pro-inflammatory  $\omega$ -6 PUFAs, such as AA (Weylandt *et al.*, 2012). Recently, molecules derived from EPA and DHA have been shown to play an important role in the resolution of inflammation within the cell. The D-series resolvins are a class of DHA-derived compounds that exhibit anti-inflammatory effects on cells, and are synthesized within the cell by 15-lipoxygenases (15-LOX; Sun, Oh *et al.*, 2007). The mechanisms through which inflammation is resolved by the D1-series resolvins are broad and known to include inhibition of NF- $\kappa$ B activity and down-regulation of COX-2 expression (Spite *et al.*, 2009; Zhao *et al.*, 2011). The balance between the pro-inflammatory COX-2 and the anti-inflammatory 15-LOX may dictate the inflammatory status of cells (Weylandt *et al.*, 2012); however, this may also be mediated by the availability of DHA versus AA. This could potentially implicate FABP7 as a shuttle for AA and DHA to COX-2 and 15-LOX respectively, and further implicates FABP7 in mediating the inflammatory status of cells. In summary, we propose a model where the ratio of AA and DHA in FABP7-positive MG cells may determine

phospholipase specificity, which in turn could effect COX-2 substrate availability, and ultimately change the array of prostaglandins that are secreted by MG cells (Figure 4.2).

We also observed increased levels of AA compared to DHA in the phospholipid classes PS and PE in both nuclei and whole cell lipid preparations of U87C and U87B cells. While it is not known what the consequences of this could be, this may be an important indication that certain phospholipid classes consistently retain a certain level of AA regardless of the AA or DHA content in their environment. This may have important consequences if one is to use DHA in the treatment of MG tumours. Since PE is required for the synthesis of PS, our observation that AA is found at comparatively higher levels in both PE and PS, and in both whole cell and nuclear lipids, suggests a difference in the regulation of PE and PS synthesis in response to AA or DHA. Given that PS externalization mediates interactions with macrophages as a consequence of apoptosis, future experiments should test the effects of DHA versus AA on MG cell growth and survival in relation to PS exposure on the cell surface. It should be noted that our RT-PCR analysis showed that a phospholipid scramblase (PLSCR4) was induced with FABP7 expression. These proteins regulate the distribution of phospholipids in membrane bilayers, and as such, may be a target for PS externalization in FABP7-positive MG cells.

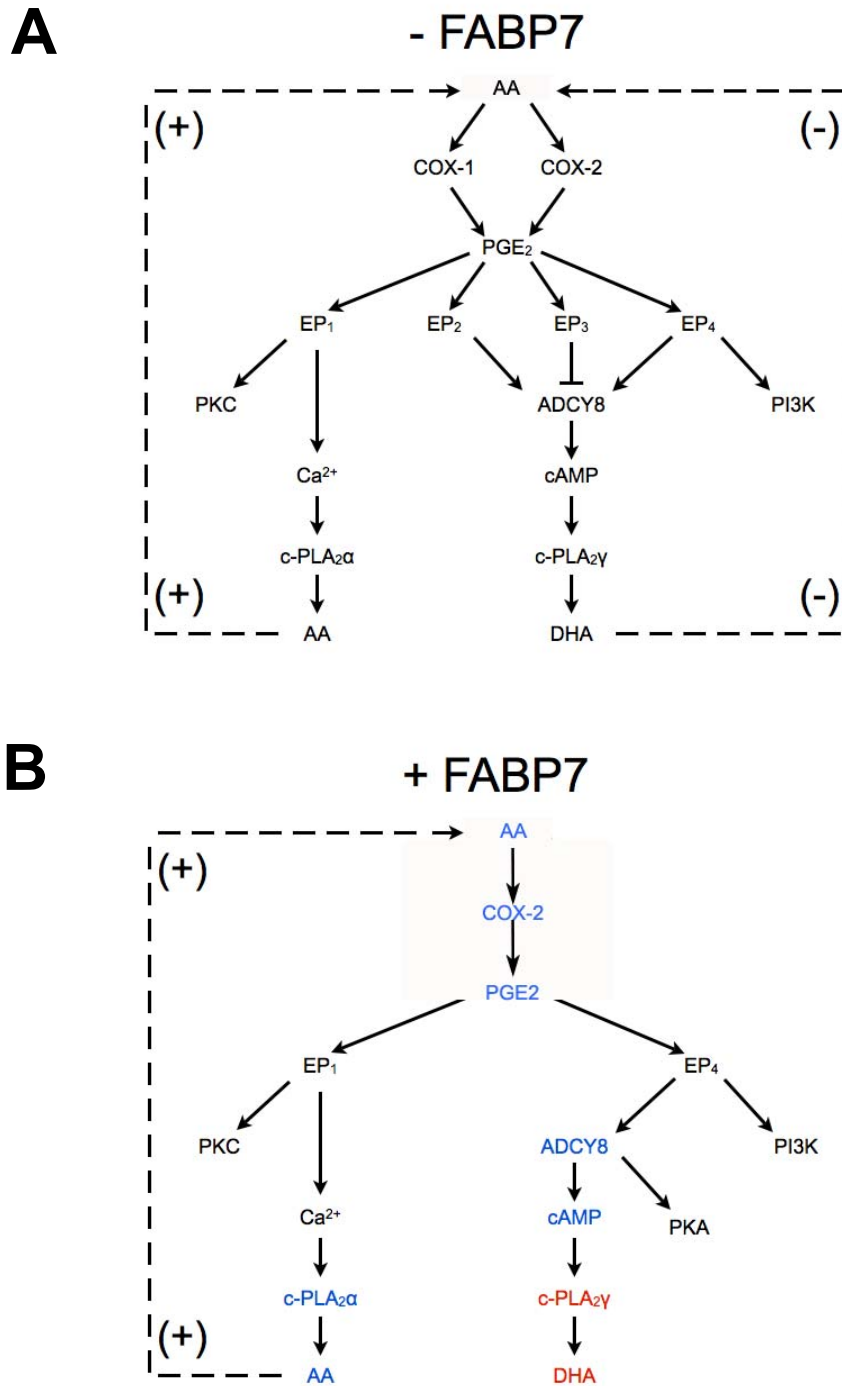


**Figure 4.2 Model of the role of FABP7 in COX-2 signaling in malignant glioma cells.** Down-regulated (red) or up-regulated (blue) with FABP7; Positive feedback (+), negative feedback (-).

Lalier *et al.* have shown that PGE<sub>2</sub> biosynthesis induces Bax-dependent apoptosis, a process that correlates with patient survival in GBM (Lalier *et al.*, 2007). This implies that under certain conditions COX-2 activity induces apoptosis, rather than acting as an inflammatory enzyme. This is interesting in light of experiments which show that COX-2 plays a role in regulating immune cell function in U87 MG cells (Akasaki *et al.*, 2004), and those that implicate PGE<sub>2</sub> in suppression of immune cell function in MG (Harizi *et al.*, 2002; Dix *et al.*, 1999). MG cells may respond differently to PGE<sub>2</sub> depending on which EP receptors they express, and this may form the basis for treating patients with FABP7/COX-2-expressing MG with COX-2 inhibitors. Finally, our microarray data show large increases in the expression of virtually every member of the MHC class II genes in U87B compared to U87C MG cells. CD4<sup>+</sup> T cells recognize MHC class II molecules on the cell surface of their target cells. Thus, FABP7 expression may be marking MG cells for T cell mediated lysis. Inhibition of COX-2 in these cells may limit their immune tolerance and assist in MG cell lysis by T cells.

#### *4.1.4 Future directions*

Although FABPs are relatively simple proteins in terms of their overall structure, their exact roles in the cell remain elusive. Work in our lab has uncovered evidence that implicates FABP7 in regulating cell migration through its fatty acid ligands. While this work has potential

applications to understanding the nature of some aggressive cancers, it also illustrates the complexity of FABPs as a family. In order to gain insight into the functional role of FABP7, we have cloned both C and N-terminal GFP-tagged FABP7 into mammalian expression vectors. These constructs will be used as a tool for investigating the behaviour and kinetics of FABP7-ligand interactions in live cells. In order to gain insight into the role of FABP7 in regulating gene expression or fatty acid incorporation into phospholipids, we propose live cell imaging experiments that track FABP7 subcellular localization over time in response to its ligands. By using specific markers of organelles, we can track the behaviour of FABP7 in real-time. Our lab has also prepared several mutant FABP7 constructs: a ligand binding mutant; a nuclear localization mutant; and a protein binding mutant. Live cell imaging experiments with these GFP-tagged FABP7 mutants will help to explain the functional roles of ligand binding, nuclear localization and protein-protein interactions in living cells. These experiments can also be extended to other FABPs that are expressed in MG cells, and together may reveal a specific coordination between specific fatty acids and FABPs, with cellular processes that promote or inhibit tumour progression.

We have shown evidence that suggests a relationship between FABP7 and PPAR- $\beta/\delta$ , and FABP7 and COX-2. As PPAR- $\beta/\delta$  regulates COX-2 expression in other systems, future experiments should investigate how the expression and activity of PPARs is related to COX-2 expression

in U87C versus U87B cells. In light of the FABP7-dependent effects of AA and DHA on MG cells, future experiments should also include an analysis of how AA and DHA alter PPAR and COX-2 activity in FABP7-positive MG cells.

While FABP7 expression in U87 cells increases production of PGE<sub>2</sub>, the effects of PGE<sub>2</sub> on FABP7-negative versus FABP7-positive cells is still unknown. When we treated U87B cells with PGE<sub>2</sub> there were no apparent changes in the cells' behaviour, which suggests that the FABP7-dependent effects of PGE<sub>2</sub> on U87B cells is saturated. However, the effect of PGE<sub>2</sub> on U87C cells remains to be determined. U87B cells show increased cell migration compared to U87C cells, and this is dependent on COX-2 activity. The role of FABP7 in mediating this process could be further examined by testing the effects of PGE<sub>2</sub> on U87C cell migration and comparing these to U87B cell migration. If U87C cells treated with PGE<sub>2</sub> can reach a migration rate that is similar to those observed in U87B cells, this would suggest that FABP7 induces the COX-2/PGE<sub>2</sub> pathway to promote cell migration. One possibility is that FABP7 expression stabilizes the cellular environment in a manner that is conducive to the promotion of PGE<sub>2</sub> production. Should PGE<sub>2</sub> treatment have no effect on U87C cells, this will suggest that FABP7 is sensitizing MG cells to the effects of PGE<sub>2</sub>.

Our phospholipid analyses examined the steady state effects of fatty acid treatment on the phospholipid content of U87C and U87B cells.

For the most part, it appears as though FABP7 does not play a role in regulating the fatty acid content of phospholipids; however, our experiments were not designed to test the short term effects of FABP7 on phospholipid content. In order to fully characterize the effects of FABP7 on AA and DHA content of phospholipid classes, we need to examine the effect of AA and DHA supplementation over a time course ranging from 15 minutes up to 2 hours. This should shed light on the immediate effects of FABP7 on fatty acid incorporation, and may show that FABP7-positive cells are more efficient at changing the fatty acid composition of phospholipids.

#### *4.1.5 Conclusions*

FABPs have long been proposed to play a wide array of functional roles within the cell, and have been implicated in both health and disease. However, evidence for specific functional roles of FABPs is scarce. FABP7 has been shown to have a clear role in promoting cell migration in MG, and this may spark various new treatment strategies for MG tumours. In order to develop these treatments, we need to improve our understanding of the mechanisms by which FABP7 can mediate specific cellular processes. Here, we have shown that the effects of FABP7 on MG cell migration are mediated in part by the COX-2 pathway. We also provide evidence that links FABP7 expression with molecules associated with aggressive behavior in MG tumours. As a step towards manipulating

FABP7 function for treating MG tumours, we show that phosphatidylcholine in the nuclear membranes of FABP7-positive MG cells may be the most manipulatable in terms of altering its DHA and AA content. This may provide a specific means of altering MG cell behaviour and response to treatment.

#### 4.1.6 References

TCGA (2008). Comprehensive genomic characterization defines human glioblastoma genes and core pathways. *Nature* 455, 1061-1068.

Adam-Klages, S., Schwandner, R., Luschen, S., Ussat, S., Kreder, D., and Kronke, M. (1998). Caspase-mediated inhibition of human cytosolic phospholipase A2 during apoptosis. *J Immunol* 161, 5687-5694.

Akasaki, Y., Liu, G., Chung, N.H., Ehtesham, M., Black, K.L., and Yu, J.S. (2004). Induction of a CD4+ T regulatory type 1 response by cyclooxygenase-2-overexpressing glioma. *J Immunol* 173, 4352-4359.

Alcantara Llaguno, S., Chen, J., Kwon, C.H., Jackson, E.L., Li, Y., Burns, D.K., et al. (2009). Malignant astrocytomas originate from neural stem/progenitor cells in a somatic tumor suppressor mouse model. *Cancer Cell* 15, 45-56.

Alshareeda, A.T., Rakha, E.A., Nolan, C.C., Ellis, I.O., and Green, A.R. (2012). Fatty acid binding protein 7 expression and its sub-cellular localization in breast cancer. *Breast Cancer Res Treat* 134, 512-529.

Amirnia, M., Babaie-Ghazani, A., Fakhrjou, A., Khodaeiani, E., Alikhah, H., Naghavi-Behzad, M., et al. (2012). Immunohistochemical study of cyclooxygenase-2 in skin tumors. *J Dermatolog Treat*, doi:10.3109/09546634.2012.674191

Annabi, B., Laflamme, C., Sina, A., Lachambre, M.P., and Beliveau, R. (2009). A MT1-MMP/NF-kappaB signaling axis as a checkpoint controller of COX-2 expression in CD133+ U87 glioblastoma cells. *J Neuroinflammation* 6, 8.

Anthony, T.E., Mason, H.A., Gridley, T., Fishell, G., and Heintz, N. (2005). Brain lipid-binding protein is a direct target of Notch signaling in radial glial cells. *Genes Dev* 19, 1028-1033.

Arai, Y., Funatsu, N., Numayama-Tsuruta, K., Nomura, T., Nakamura, S., and Osumi, N. (2005). Role of Fabp7, a downstream gene of Pax6, in the maintenance of neuroepithelial cells during early embryonic development of the rat cortex. *J Neurosci* 25, 9752-9761.

Athanassiou, H., Synodinou, M., Maragoudakis, E., Paraskevaidis, M., Verigos, C., Misailidou, D., et al. (2005). Randomized phase II study of temozolomide and radiotherapy compared with radiotherapy alone in newly diagnosed glioblastoma multiforme. *J Clin Oncol* 23, 2372-2377.

Ayers, S.D., Nedrow, K.L., Gillilan, R.E., and Noy, N. (2007). Continuous nucleocytoplasmic shuttling underlies transcriptional activation of PPARgamma by FABP4. *Biochemistry* 46, 6744-6752.

Balendiran, G.K., Schnutgen, F., Scapin, G., Borchers, T., Xhong, N., Lim, K., et al. (2000). Crystal structure and thermodynamic analysis of human brain fatty acid-binding protein. *J Biol Chem* 275, 27045-27054.

Bao, S., Wu, Q., McLendon, R.E., Hao, Y., Shi, Q., Hjelmeland, A.B., et al. (2006). Glioma stem cells promote radioresistance by preferential activation of the DNA damage response. *Nature* 444, 756-760.

Barak, Y., Nelson, M.C., Ong, E.S., Jones, Y.Z., Ruiz-Lozano, P., Chien, K.R., et al. (1999). PPAR gamma is required for placental, cardiac, and adipose tissue development. *Mol Cell* 4, 585-595.

Beier, D., Hau, P., Proescholdt, M., Lohmeier, A., Wischhusen, J., Oefner, P.J., et al. (2007). CD133(+) and CD133(-) glioblastoma-derived cancer stem cells show differential growth characteristics and molecular profiles. *Cancer Res* 67, 4010-4015.

Belkind-Gerson, J., Carreon-Rodriguez, A., Contreras-Ochoa, C.O., Estrada-Mondaca, S., and Parra-Cabrera, M.S. (2008). Fatty acids and neurodevelopment. *J Pediatr Gastroenterol Nutr* 47 Suppl 1, S7-9.

Bennett, M.P., and Mitchell, D.C. (2008). Regulation of membrane proteins by dietary lipids: effects of cholesterol and docosahexaenoic acid acyl chain-containing phospholipids on rhodopsin stability and function. *Biophys J* 95, 1206-1216.

Bidwell, P., Joh, K., Leaver, H.A., and Rizzo, M.T. (2010). Prostaglandin E2 activates cAMP response element-binding protein in glioma cells via a signaling pathway involving PKA-dependent inhibition of ERK. *Prostaglandins Other Lipid Mediat* 91, 18-29.

Bility, M.T., Zhu, B., Kang, B.H., Gonzalez, F.J., and Peters, J.M. (2010). Ligand activation of peroxisome proliferator-activated receptor-beta/delta and inhibition of cyclooxygenase-2 enhances inhibition of skin tumorigenesis. *Toxicol Sci* 113, 27-36.

Biondo, P.D., Brindley, D.N., Sawyer, M.B., and Field, C.J. (2008). The potential for treatment with dietary long-chain polyunsaturated n-3 fatty acids during chemotherapy. *J Nutr Biochem* 19, 787-796.

Bisgrove, D.A., Monckton, E.A., Packer, M., and Godbout, R. (2000). Regulation of brain fatty acid-binding protein expression by differential

phosphorylation of nuclear factor I in malignant glioma cell lines. *J Biol Chem* 275, 30668-30676.

Bock, H.C., Puchner, M.J., Lohmann, F., Schutze, M., Koll, S., Ketter, R., et al. (2010). First-line treatment of malignant glioma with carmustine implants followed by concomitant radiochemotherapy: a multicenter experience. *Neurosurg Rev* 33, 441-449.

Bonala, S., Lokireddy, S., Arigela, H., Teng, S., Wahli, W., Sharma, M., et al. (2012). Peroxisome proliferator-activated receptor beta/delta induces myogenesis by modulating myostatin activity. *J Biol Chem* 287, 12935-12951.

Bonavia, R., Inda, M.M., Cavenee, W.K., and Furnari, F.B. (2011). Heterogeneity maintenance in glioblastoma: a social network. *Cancer Res* 71, 4055-4060.

Bonavia, R., Inda, M.M., Vandenberg, S., Cheng, S.Y., Nagane, M., Hadwiger, P., et al. (2011). EGFRvIII promotes glioma angiogenesis and growth through the NF-kappaB, interleukin-8 pathway. *Oncogene*, doi: 10.1038/onc.2011.563.

Bradova, V., Smid, F., Ledvinova, J., and Michalec, C. (1990). Improved one-dimensional thin-layer chromatography for the separation of phospholipids in biological material. *J Chromatogr* 533, 297-299.

Brun, M., Coles, J.E., Monckton, E.A., Glubrecht, D.D., Bisgrove, D., and Godbout, R. (2009). Nuclear factor I regulates brain fatty acid-binding protein and glial fibrillary acidic protein gene expression in malignant glioma cell lines. *J Mol Biol* 391, 282-300.

Bunimov, N., and Laneuville, O. (2010). Characterization of proteins associating with 5' terminus of PGHS-1 mRNA. *Cell Mol Biol Lett* 15, 196-214.

Bunimov, N., Smith, J.E., Gosselin, D., and Laneuville, O. (2007). Translational regulation of PGHS-1 mRNA: 5' untranslated region and first two exons conferring negative regulation. *Biochim Biophys Acta* 1769, 92-105.

Burczynski, F.J., Fandrey, S., Wang, G., Pavletic, P.A., and Gong, Y. (1999). Cytosolic fatty acid binding protein enhances rat hepatocyte [3H]palmitate uptake. *Can J Physiol Pharmacol* 77, 896-901.

Casas, J., Gijon, M.A., Vigo, A.G., Crespo, M.S., Balsinde, J., and Balboa, M.A. (2006). Overexpression of cytosolic group IVA phospholipase A2 protects cells from Ca<sup>2+</sup>-dependent death. *J Biol Chem* 281, 6106-6116.

Castillo, A., Ruzmetov, N., Harvey, K.A., Stillwell, W., Zaloga, G.P., and Siddiqui, R.A. (2005). Docosahexaenoic acid inhibits protein kinase C translocation/activation and cardiac hypertrophy in rat cardiomyocytes. *J Mol Genet Med* 1, 18-25.

Chan, J.L., Lee, S.W., Fraass, B.A., Normolle, D.P., Greenberg, H.S., Junck, L.R., et al. (2002). Survival and failure patterns of high-grade gliomas after three-dimensional conformal radiotherapy. *J Clin Oncol* 20, 1635-1642.

Chawla, A., Schwarz, E.J., Dimaculangan, D.D., and Lazar, M.A. (1994). Peroxisome proliferator-activated receptor (PPAR) gamma: adipose-predominant expression and induction early in adipocyte differentiation. *Endocrinology* 135, 798-800.

Chearwae, W., and Bright, J.J. (2008). PPARgamma agonists inhibit growth and expansion of CD133+ brain tumour stem cells. *Br J Cancer* 99, 2044-2053.

Chen, C.Y., and Shyu, A.B. (1994). Selective degradation of early-response-gene mRNAs: functional analyses of sequence features of the AU-rich elements. *Mol Cell Biol* 14, 8471-8482.

Chen, J., McKay, R.M., and Parada, L.F. (2012). Malignant glioma: lessons from genomics, mouse models, and stem cells. *Cell* 149, 36-47.

Choi, E.M., Heo, J.I., Oh, J.Y., Kim, Y.M., Ha, K.S., Kim, J.I., et al. (2005). COX-2 regulates p53 activity and inhibits DNA damage-induced apoptosis. *Biochem Biophys Res Commun* 328, 1107-1112.

Clandinin, M.T. (1999). Brain development and assessing the supply of polyunsaturated fatty acid. *Lipids* 34, 131-137.

Corcoran, C.A., He, Q., Huang, Y., and Sheikh, M.S. (2005). Cyclooxygenase-2 interacts with p53 and interferes with p53-dependent transcription and apoptosis. *Oncogene* 24, 1634-1640.

Corsico, B., Liou, H.L., and Storch, J. (2004). The alpha-helical domain of liver fatty acid binding protein is responsible for the diffusion-mediated transfer of fatty acids to phospholipid membranes. *Biochemistry* 43, 3600-3607.

D'Angelo, B., Benedetti, E., Di Loreto, S., Cristiano, L., Laurenti, G., Ceru, M.P., et al. (2011). Signal transduction pathways involved in PPARbeta/delta-induced neuronal differentiation. *J Cell Physiol* 226, 2170-2180.

Darimont, C., Gradoux, N., Persohn, E., Cumin, F., and De Pover, A. (2000). Effects of intestinal fatty acid-binding protein overexpression on fatty acid metabolism in Caco-2 cells. *J Lipid Res* 41, 84-92.

Das, U.N. (2006). Essential fatty acids: biochemistry, physiology and pathology. *Biotechnol J* 1, 420-439.

Dix, A.R., Brooks, W.H., Roszman, T.L., and Morford, L.A. (1999). Immune defects observed in patients with primary malignant brain tumors. *J Neuroimmunol* 100, 216-232.

Doller, A., Akool el, S., Huwiler, A., Muller, R., Radeke, H.H., Pfeilschifter, J., et al. (2008). Posttranslational modification of the AU-rich element binding protein HuR by protein kinase Cdelta elicits angiotensin II-induced stabilization and nuclear export of cyclooxygenase 2 mRNA. *Mol Cell Biol* 28, 2608-2625.

Domoto, T., Miyama, Y., Suzuki, H., Teratani, T., Arai, K., Sugiyama, T., et al. (2007). Evaluation of S100A10, annexin II and B-FABP expression as markers for renal cell carcinoma. *Cancer Sci* 98, 77-82.

Duquette, M., and Laneuville, O. (2002). Translational regulation of prostaglandin endoperoxide H synthase-1 mRNA in megakaryocytic MEG-01 cells. Specific protein binding to a conserved 20-nucleotide CIS element in the 3'-untranslated region. *J Biol Chem* 277, 44631-44637.

Easaw, J.C., Mason, W.P., Perry, J., Laperriere, N., Eisenstat, D.D., Del Maestro, R., et al. (2011). Canadian recommendations for the treatment of recurrent or progressive glioblastoma multiforme. *Curr Oncol* 18, e126-e136.

Esteller, M., Garcia-Foncillas, J., Andion, E., Goodman, S.N., Hidalgo, O.F., Vanaclocha, V., et al. (2000). Inactivation of the DNA-repair gene MGMT and the clinical response of gliomas to alkylating agents. *N Engl J Med* 343, 1350-1354.

Feng, L., Hatten, M.E., and Heintz, N. (1994). Brain lipid-binding protein (BLBP): a novel signaling system in the developing mammalian CNS. *Neuron* 12, 895-908.

Feng, L., and Heintz, N. (1995). Differentiating neurons activate transcription of the brain lipid-binding protein gene in radial glia through a novel regulatory element. *Development* 121, 1719-1730.

Franke, T.F., Kaplan, D.R., and Cantley, L.C. (1997). PI3K: downstream AKTion blocks apoptosis. *Cell* 88, 435-437.

Furnari, F.B., Fenton, T., Bachoo, R.M., Mukasa, A., Stommel, J.M., Stegh, A., et al. (2007). Malignant astrocytic glioma: genetics, biology, and paths to treatment. *Genes Dev* 21, 2683-2710.

Garcia, A.D., Doan, N.B., Imura, T., Bush, T.G., and Sofroniew, M.V. (2004). GFAP-expressing progenitors are the principal source of constitutive neurogenesis in adult mouse forebrain. *Nat Neurosci* 7, 1233-1241.

Gerstner, J.R., Vander Heyden, W.M., Lavaute, T.M., and Landry, C.F. (2006). Profiles of novel diurnally regulated genes in mouse hypothalamus: expression analysis of the cysteine and histidine-rich domain-containing, zinc-binding protein 1, the fatty acid-binding protein 7 and the GTPase, ras-like family member 11b. *Neuroscience* 139, 1435-1448.

Gerstner, J.R., Vanderheyden, W.M., LaVaute, T., Westmark, C.J., Rouhana, L., Pack, A.I., et al. (2012). Time of day regulates subcellular trafficking, tripartite synaptic localization, and polyadenylation of the astrocytic Fabp7 mRNA. *J Neurosci* 32, 1383-1394.

Gil-Ranedo, J., Mendiburu-Elicabe, M., Garcia-Villanueva, M., Medina, D., del Alamo, M., and Izquierdo, M. (2011). An off-target nucleostemin RNAi inhibits growth in human glioblastoma-derived cancer stem cells. *PLoS One* 6, e28753.

Gillilan, R.E., Ayers, S.D., and Noy, N. (2007). Structural basis for activation of fatty acid-binding protein 4. *J Mol Biol* 372, 1246-1260.

Giorgione, J., Epand, R.M., Buda, C., and Farkas, T. (1995). Role of phospholipids containing docosahexaenoyl chains in modulating the activity of protein kinase C. *Proc Natl Acad Sci U S A* 92, 9767-9770.

Godbout, R., Bisgrove, D.A., Shkolny, D., and Day, R.S., 3rd (1998). Correlation of B-FABP and GFAP expression in malignant glioma. *Oncogene* 16, 1955-1962.

Gorski, K., Carneiro, M., and Schibler, U. (1986). Tissue-specific in vitro transcription from the mouse albumin promoter. *Cell* 47, 767-776.

Goto, Y., Koyanagi, K., Narita, N., Kawakami, Y., Takata, M., Uchiyama, A., et al. (2010). Aberrant fatty acid-binding protein-7 gene expression in cutaneous malignant melanoma. *J Invest Dermatol* 130, 221-229.

Goto, Y., Matsuzaki, Y., Kurihara, S., Shimizu, A., Okada, T., Yamamoto, K., et al. (2006). A new melanoma antigen fatty acid-binding protein 7, involved in proliferation and invasion, is a potential target for immunotherapy and molecular target therapy. *Cancer Res* 66, 4443-4449.

Gravendeel, L.A., Kouwenhoven, M.C., Gevaert, O., de Rooij, J.J., Stubbs, A.P., Duijm, J.E., et al. (2009). Intrinsic gene expression profiles of gliomas are a better predictor of survival than histology. *Cancer Res* 69, 9065-9072.

Greaves, M., and Maley, C.C. (2012). Clonal evolution in cancer. *Nature* 481, 306-313.

Grommes, C., Conway, D.S., Alshekhlee, A., and Barnholtz-Sloan, J.S. (2010). Inverse association of PPARgamma agonists use and high grade glioma development. *J Neurooncol* 100, 233-239.

Hamilton, J.A., and Brunaldi, K. (2007). A model for fatty acid transport into the brain. *J Mol Neurosci* 33, 12-17.

Han, C., Demetris, A.J., Liu, Y., Shelhamer, J.H., and Wu, T. (2004). Transforming growth factor-beta (TGF-beta) activates cytosolic phospholipase A2alpha (cPLA2alpha)-mediated prostaglandin E2 (PGE)2/EP1 and peroxisome proliferator-activated receptor-gamma (PPAR-gamma)/Smad signaling pathways in human liver cancer cells. A novel mechanism for subversion of TGF-beta-induced mitoinhibition. *J Biol Chem* 279, 44344-44354.

Han, S., and Roman, J. (2004). Suppression of prostaglandin E2 receptor subtype EP2 by PPARgamma ligands inhibits human lung carcinoma cell growth. *Biochem Biophys Res Commun* 314, 1093-1099.

Hanahan, D., and Weinberg, R.A. (2011). Hallmarks of cancer: the next generation. *Cell* 144, 646-674.

Harizi, H., Juzan, M., Pitard, V., Moreau, J.F., and Gualde, N. (2002). Cyclooxygenase-2-induced prostaglandin e(2) enhances the production of endogenous IL-10, which down-regulates dendritic cell functions. *J Immunol* 168, 2255-2263.

Hatten, M.E. (1985). Neuronal regulation of astroglial morphology and proliferation in vitro. *J Cell Biol* 100, 384-396.

Hauerland, N.H., and Spener, F. (2004). Fatty acid-binding proteins--insights from genetic manipulations. *Prog Lipid Res* 43, 328-349.

Herrmann, O., Baumann, B., de Lorenzi, R., Muhammad, S., Zhang, W., Kleesiek, J., et al. (2005). IKK mediates ischemia-induced neuronal death. *Nat Med* 11, 1322-1329.

Hertzel, A.V., and Bernlohr, D.A. (2000). The mammalian fatty acid-binding protein multigene family: molecular and genetic insights into function. *Trends Endocrinol Metab* 11, 175-180.

Hohoff, C., Borchers, T., Rustow, B., Spener, F., and van Tilbeurgh, H. (1999). Expression, purification, and crystal structure determination of recombinant human epidermal-type fatty acid binding protein. *Biochemistry* 38, 12229-12239.

Hohoff, C., and Spener, F. (1998). Correspondence re: Y.E. Shi et al., Antitumor activity of the novel human breast cancer growth inhibitor, mammary-derived growth inhibitor-related gene, MRG. *Cancer Res.*, 57: 3084-3091, 1997. *Cancer Res* 58, 4015-4017.

Holmes, M.D., Chen, W.Y., Schnitt, S.J., Collins, L., Colditz, G.A., Hankinson, S.E., et al. (2011). COX-2 expression predicts worse breast cancer prognosis and does not modify the association with aspirin. *Breast Cancer Res Treat* 130, 657-662.

Hostetler, H.A., Kier, A.B., and Schroeder, F. (2006). Very-long-chain and branched-chain fatty acyl-CoAs are high affinity ligands for the peroxisome proliferator-activated receptor alpha (PPARalpha). *Biochemistry* 45, 7669-7681.

Hostetler, H.A., McIntosh, A.L., Atshaves, B.P., Storey, S.M., Payne, H.R., Kier, A.B., et al. (2009). L-FABP directly interacts with PPARalpha in cultured primary hepatocytes. *J Lipid Res* 50, 1663-1675.

Huang, H.S., Nagane, M., Klingbeil, C.K., Lin, H., Nishikawa, R., Ji, X.D., et al. (1997). The enhanced tumorigenic activity of a mutant epidermal growth factor receptor common in human cancers is mediated by threshold levels of constitutive tyrosine phosphorylation and unattenuated signaling. *J Biol Chem* 272, 2927-2935.

Huang, T.T., Sarkaria, S.M., Cloughesy, T.F., and Mischel, P.S. (2009). Targeted therapy for malignant glioma patients: lessons learned and the road ahead. *Neurotherapeutics* 6, 500-512.

Inoue, H., Tanabe, T., and Umesono, K. (2000). Feedback control of cyclooxygenase-2 expression through PPARgamma. *J Biol Chem* 275, 28028-28032.

Irwin, C., Hunn, M., Purdie, G., and Hamilton, D. (2007). Delay in radiotherapy shortens survival in patients with high grade glioma. *J Neurooncol* 85, 339-343.

Jacques, T.S., Swales, A., Brzozowski, M.J., Henriquez, N.V., Linehan, J.M., Mirzadeh, Z., et al. (2010). Combinations of genetic mutations in the adult neural stem cell compartment determine brain tumour phenotypes. *EMBO J* 29, 222-235.

Joki, T., Heese, O., Nikas, D.C., Bello, L., Zhang, J., Kraeft, S.K., et al. (2000). Expression of cyclooxygenase 2 (COX-2) in human glioma and in vitro inhibition by a specific COX-2 inhibitor, NS-398. *Cancer Res* 60, 4926-4931.

Jupp, O.J., Vandenabeele, P., and MacEwan, D.J. (2003). Distinct regulation of cytosolic phospholipase A2 phosphorylation, translocation, proteolysis and activation by tumour necrosis factor-receptor subtypes. *Biochem J* 374, 453-461.

Kaloshi, G., Mokhtari, K., Carpentier, C., Taillibert, S., Lejeune, J., Marie, Y., et al. (2007). FABP7 expression in glioblastomas: relation to prognosis, invasion and EGFR status. *J Neurooncol* 84, 245-248.

Kang, K.B., Zhu, C., Yong, S.K., Gao, Q., and Wong, M.C. (2009). Enhanced sensitivity of celecoxib in human glioblastoma cells: Induction of DNA damage leading to p53-dependent G1 cell cycle arrest and autophagy. *Mol Cancer* 8, 66.

Kannan-Thulasiraman, P., Seachrist, D.D., Mahabeleshwar, G.H., Jain, M.K., and Noy, N. (2010). Fatty acid-binding protein 5 and PPARbeta/delta are critical mediators of epidermal growth factor receptor-induced carcinoma cell growth. *J Biol Chem* 285, 19106-19115.

Kiefer, J.R., Pawlitz, J.L., Moreland, K.T., Stegeman, R.A., Hood, W.F., Gierse, J.K., et al. (2000). Structural insights into the stereochemistry of the cyclooxygenase reaction. *Nature* 405, 97-101.

Kim, B.S., Kang, K.S., Choi, J.I., Jung, J.S., Im, Y.B., and Kang, S.K. (2011). Knockdown of the potential cancer stem-like cell marker Rex-1

improves chemotherapeutic effects in gliomas. *Hum Gene Ther* 22, 1551-1562.

King, J.G., Jr., and Khalili, K. (2001). Inhibition of human brain tumor cell growth by the anti-inflammatory drug, flurbiprofen. *Oncogene* 20, 6864-6870.

Kliwer, S.A., Lenhard, J.M., Willson, T.M., Patel, I., Morris, D.C., and Lehmann, J.M. (1995). A prostaglandin J2 metabolite binds peroxisome proliferator-activated receptor gamma and promotes adipocyte differentiation. *Cell* 83, 813-819.

Kliwer, S.A., Umesono, K., Noonan, D.J., Heyman, R.A., and Evans, R.M. (1992). Convergence of 9-cis retinoic acid and peroxisome proliferator signalling pathways through heterodimer formation of their receptors. *Nature* 358, 771-774.

Kota, B.P., Huang, T.H., and Roufogalis, B.D. (2005). An overview on biological mechanisms of PPARs. *Pharmacol Res* 51, 85-94.

Kuhnt, D., Becker, A., Ganslandt, O., Bauer, M., Buchfelder, M., and Nimsky, C. (2011). Correlation of the extent of tumor volume resection and patient survival in surgery of glioblastoma multiforme with high-field intraoperative MRI guidance. *Neuro Oncol* 13, 1339-1348.

Kurumbail, R.G., Stevens, A.M., Gierse, J.K., McDonald, J.J., Stegeman, R.A., Pak, J.Y., et al. (1996). Structural basis for selective inhibition of cyclooxygenase-2 by anti-inflammatory agents. *Nature* 384, 644-648.

Lalier, L., Cartron, P.F., Pedelaborde, F., Olivier, C., Loussouarn, D., Martin, S.A., et al. (2007). Increase in PGE2 biosynthesis induces a Bax dependent apoptosis correlated to patients' survival in glioblastoma multiforme. *Oncogene* 26, 4999-5009.

Laneuville, O., Breuer, D.K., Dewitt, D.L., Hla, T., Funk, C.D., and Smith, W.L. (1994). Differential inhibition of human prostaglandin endoperoxide H synthases-1 and -2 by nonsteroidal anti-inflammatory drugs. *J Pharmacol Exp Ther* 271, 927-934.

Lehmann, J.M., Moore, L.B., Smith-Oliver, T.A., Wilkison, W.O., Willson, T.M., and Kliwer, S.A. (1995). An antidiabetic thiazolidinedione is a high affinity ligand for peroxisome proliferator-activated receptor gamma (PPAR gamma). *J Biol Chem* 270, 12953-12956.

Lehmann, J.M., Moore, L.B., Smith-Oliver, T.A., Wilkison, W.O., Willson, T.M., and Kliwer, S.A. (1995). An antidiabetic thiazolidinedione is a high

affinity ligand for peroxisome proliferator-activated receptor gamma (PPAR gamma). *J Biol Chem* 270, 12953-12956.

Lehrke, M., and Lazar, M.A. (2005). The many faces of PPARgamma. *Cell* 123, 993-999.

Lei, L., Sonabend, A.M., Guarnieri, P., Soderquist, C., Ludwig, T., Rosenfeld, S., et al. (2011). Glioblastoma models reveal the connection between adult glial progenitors and the proneural phenotype. *PLoS One* 6, e20041.

Li, A., Walling, J., Ahn, S., Kotliarov, Y., Su, Q., Quezado, M., et al. (2009). Unsupervised analysis of transcriptomic profiles reveals six glioma subtypes. *Cancer Res* 69, 2091-2099.

Liang, Y., Bollen, A.W., Aldape, K.D., and Gupta, N. (2006). Nuclear FABP7 immunoreactivity is preferentially expressed in infiltrative glioma and is associated with poor prognosis in EGFR-overexpressing glioblastoma. *BMC Cancer* 6, 97.

Liang, Y., Diehn, M., Watson, N., Bollen, A.W., Aldape, K.D., Nicholas, M.K., et al. (2005). Gene expression profiling reveals molecularly and clinically distinct subtypes of glioblastoma multiforme. *Proc Natl Acad Sci U S A* 102, 5814-5819.

Liou, H.L., and Storch, J. (2001). Role of surface lysine residues of adipocyte fatty acid-binding protein in fatty acid transfer to phospholipid vesicles. *Biochemistry* 40, 6475-6485.

Liu, C., Sage, J.C., Miller, M.R., Verhaak, R.G., Hippenmeyer, S., Vogel, H., et al. (2011). Mosaic analysis with double markers reveals tumor cell of origin in glioma. *Cell* 146, 209-221.

Liu, J.W., Almaguel, F.G., Bu, L., De Leon, D.D., and De Leon, M. (2008). Expression of E-FABP in PC12 cells increases neurite extension during differentiation: involvement of n-3 and n-6 fatty acids. *J Neurochem* 106, 2015-2029.

Liu, R.Z., Graham, K., Glubrecht, D.D., Germain, D.R., Mackey, J.R., and Godbout, R. (2011). Association of FABP5 expression with poor survival in triple-negative breast cancer: implication for retinoic acid therapy. *Am J Pathol* 178, 997-1008.

Liu, R.Z., Graham, K., Glubrecht, D.D., Lai, R., Mackey, J.R., and Godbout, R. (2012). A fatty acid-binding protein 7/RXRbeta pathway

enhances survival and proliferation in triple-negative breast cancer. *J Pathol*, doi: 10.1002/path.4001.

Liu, R.Z., Li, X., and Godbout, R. (2008). A novel fatty acid-binding protein (FABP) gene resulting from tandem gene duplication in mammals: transcription in rat retina and testis. *Genomics* 92, 436-445.

Liu, R.Z., Mita, R., Beaulieu, M., Gao, Z., and Godbout, R. (2010). Fatty acid binding proteins in brain development and disease. *Int J Dev Biol* 54, 1229-1239.

Liu, R.Z., Monckton, E.A., and Godbout, R. (2012). Regulation of the FABP7 gene by PAX6 in malignant glioma cells. *Biochem Biophys Res Commun* 422, 482-487.

Louis, D.N. (2006). Molecular pathology of malignant gliomas. *Annu Rev Pathol* 1, 97-117.

Louis, D.N., Ohgaki, H., Wiestler, O.D., Cavenee, W.K., Burger, P.C., Jouvet, A., et al. (2007). The 2007 WHO classification of tumours of the central nervous system. *Acta Neuropathol* 114, 97-109.

Luschen, S., Ussat, S., Kronke, M., and Adam-Klages, S. (1998). Cleavage of human cytosolic phospholipase A2 by caspase-1 (ICE) and caspase-8 (FLICE). *Biochem Biophys Res Commun* 253, 92-98.

Maher, E.A., Brennan, C., Wen, P.Y., Durso, L., Ligon, K.L., Richardson, A., et al. (2006). Marked genomic differences characterize primary and secondary glioblastoma subtypes and identify two distinct molecular and clinical secondary glioblastoma entities. *Cancer Res* 66, 11502-11513.

Martin, D.D., Robbins, M.E., Spector, A.A., Wen, B.C., and Hussey, D.H. (1996). The fatty acid composition of human gliomas differs from that found in nonmalignant brain tissue. *Lipids* 31, 1283-1288.

Mbonye, U.R., Wada, M., Rieke, C.J., Tang, H.Y., Dewitt, D.L., and Smith, W.L. (2006). The 19-amino acid cassette of cyclooxygenase-2 mediates entry of the protein into the endoplasmic reticulum-associated degradation system. *J Biol Chem* 281, 35770-35778.

Mbonye, U.R., Yuan, C., Harris, C.E., Sidhu, R.S., Song, I., Arakawa, T., et al. (2008). Two distinct pathways for cyclooxygenase-2 protein degradation. *J Biol Chem* 283, 8611-8623.

Mei, J., Bachoo, R., and Zhang, C.L. (2011). MicroRNA-146a inhibits glioma development by targeting Notch1. *Mol Cell Biol* 31, 3584-3592.

- Mita, R., Beaulieu, M.J., Field, C., and Godbout, R. (2010). Brain fatty acid-binding protein and omega-3/omega-6 fatty acids: mechanistic insight into malignant glioma cell migration. *J Biol Chem* 285, 37005-37015.
- Mita, R., Coles, J.E., Glubrecht, D.D., Sung, R., Sun, X., and Godbout, R. (2007). B-FABP-expressing radial glial cells: the malignant glioma cell of origin? *Neoplasia* 9, 734-744.
- Mroske, C., Plant, M.H., Franks, D.J., and Laneuville, O. (2000). Characterization of prostaglandin endoperoxide H synthase-1 enzyme expression during differentiation of the megakaryocytic cell line MEG-01. *Exp Hematol* 28, 411-421.
- Murphy, E.J., Owada, Y., Kitanaka, N., Kondo, H., and Glatz, J.F. (2005). Brain arachidonic acid incorporation is decreased in heart fatty acid binding protein gene-ablated mice. *Biochemistry* 44, 6350-6360.
- Nadjar, A., Tridon, V., May, M.J., Ghosh, S., Dantzer, R., Amedee, T., et al. (2005). NFkappaB activates in vivo the synthesis of inducible Cox-2 in the brain. *J Cereb Blood Flow Metab* 25, 1047-1059.
- Nakano, Y., Kuroda, E., Kito, T., Yokota, A., and Yamashita, U. (2006). Induction of macrophagic prostaglandin E2 synthesis by glioma cells. *J Neurosurg* 104, 574-582.
- Nieder, C., and Mehta, M.P. (2011). Advances in translational research provide a rationale for clinical re-evaluation of high-dose radiotherapy for glioblastoma. *Med Hypotheses* 76, 410-413.
- O'Brien, J.S., and Sampson, E.L. (1965). Lipid composition of the normal human brain: gray matter, white matter, and myelin. *J Lipid Res* 6, 537-544.
- Okudaira, S., Yukiura, H., and Aoki, J. (2010). Biological roles of lysophosphatidic acid signaling through its production by autotaxin. *Biochimie* 92, 698-706.
- Owada, Y., Abdelwahab, S.A., Kitanaka, N., Sakagami, H., Takano, H., Sugitani, Y., et al. (2006). Altered emotional behavioral responses in mice lacking brain-type fatty acid-binding protein gene. *Eur J Neurosci* 24, 175-187.
- Patten, B.A., Peyrin, J.M., Weinmaster, G., and Corfas, G. (2003). Sequential signaling through Notch1 and erbB receptors mediates radial glia differentiation. *J Neurosci* 23, 6132-6140.

Patten, B.A., Sardi, S.P., Koirala, S., Nakafuku, M., and Corfas, G. (2006). Notch1 signaling regulates radial glia differentiation through multiple transcriptional mechanisms. *J Neurosci* 26, 3102-3108.

Pawliczak, R., Logun, C., Madara, P., Lawrence, M., Woszczek, G., Ptasinska, A., et al. (2004). Cytosolic phospholipase A2 Group IValpha but not secreted phospholipase A2 Group IIA, V, or X induces interleukin-8 and cyclooxygenase-2 gene and protein expression through peroxisome proliferator-activated receptors gamma 1 and 2 in human lung cells. *J Biol Chem* 279, 48550-48561.

Perdiki, M., Korkolopoulou, P., Thymara, I., Agrogiannis, G., Piperi, C., Boviatsis, E., et al. (2007). Cyclooxygenase-2 expression in astrocytomas. Relationship with microvascular parameters, angiogenic factors expression and survival. *Mol Cell Biochem* 295, 75-83.

Perou, C.M., Sorlie, T., Eisen, M.B., van de Rijn, M., Jeffrey, S.S., Rees, C.A., et al. (2000). Molecular portraits of human breast tumours. *Nature* 406, 747-752.

Peters, J.M., Cattley, R.C., and Gonzalez, F.J. (1997). Role of PPAR alpha in the mechanism of action of the nongenotoxic carcinogen and peroxisome proliferator Wy-14,643. *Carcinogenesis* 18, 2029-2033.

Peters, J.M., Shah, Y.M., and Gonzalez, F.J. (2012). The role of peroxisome proliferator-activated receptors in carcinogenesis and chemoprevention. *Nat Rev Cancer* 12, 181-195.

Piccirillo, S.G., Reynolds, B.A., Zanetti, N., Lamorte, G., Binda, E., Broggi, G., et al. (2006). Bone morphogenetic proteins inhibit the tumorigenic potential of human brain tumour-initiating cells. *Nature* 444, 761-765.

Pyper, S.R., Viswakarma, N., Yu, S., and Reddy, J.K. (2010). PPARalpha: energy combustion, hypolipidemia, inflammation and cancer. *Nucl Recept Signal* 8, e002.

Reddy, J.K., Azarnoff, D.L., and Hignite, C.E. (1980). Hypolipidaemic hepatic peroxisome proliferators form a novel class of chemical carcinogens. *Nature* 283, 397-398.

Rose, D.P., Connolly, J.M., Rayburn, J., and Coleman, M. (1995). Influence of diets containing eicosapentaenoic or docosahexaenoic acid on growth and metastasis of breast cancer cells in nude mice. *J Natl Cancer Inst* 87, 587-592.

Rosen, E.D., Sarraf, P., Troy, A.E., Bradwin, G., Moore, K., Milstone, D.S., et al. (1999). PPAR gamma is required for the differentiation of adipose tissue in vivo and in vitro. *Mol Cell* 4, 611-617.

Rundhaug, J.E., and Fischer, S.M. (2010). Molecular Mechanisms of Mouse Skin Tumor Promotion. *Cancers (Basel)* 2, 436-482.

Salmena, L., Carracedo, A., and Pandolfi, P.P. (2008). Tenets of PTEN tumor suppression. *Cell* 133, 403-414.

Samadi, N., Gaetano, C., Goping, I.S., and Brindley, D.N. (2009). Autotaxin protects MCF-7 breast cancer and MDA-MB-435 melanoma cells against Taxol-induced apoptosis. *Oncogene* 28, 1028-1039.

Sampetean, O., Saga, I., Nakanishi, M., Sugihara, E., Fukaya, R., Onishi, N., et al. (2011). Invasion precedes tumor mass formation in a malignant brain tumor model of genetically modified neural stem cells. *Neoplasia* 13, 784-791.

Sanai, N., Polley, M.Y., McDermott, M.W., Parsa, A.T., and Berger, M.S. (2011). An extent of resection threshold for newly diagnosed glioblastomas. *J Neurosurg* 115, 3-8.

Schachtrup, C., Emmler, T., Bleck, B., Sandqvist, A., and Spener, F. (2004). Functional analysis of peroxisome-proliferator-responsive element motifs in genes of fatty acid-binding proteins. *Biochem J* 382, 239-245.

Schley, P.D., Brindley, D.N., and Field, C.J. (2007). (n-3) PUFA alter raft lipid composition and decrease epidermal growth factor receptor levels in lipid rafts of human breast cancer cells. *J Nutr* 137, 548-553.

Serini, S., Fasano, E., Piccioni, E., Monego, G., Cittadini, A.R., Celleno, L., et al. (2012). DHA induces apoptosis and differentiation in human melanoma cells in vitro: involvement of HuR-mediated COX-2 mRNA stabilization and beta-catenin nuclear translocation. *Carcinogenesis* 33, 164-173.

Shi, Y., Hon, M., and Evans, R.M. (2002). The peroxisome proliferator-activated receptor delta, an integrator of transcriptional repression and nuclear receptor signaling. *Proc Natl Acad Sci U S A* 99, 2613-2618.

Shi, Y.E., Ni, J., Xiao, G., Liu, Y.E., Fuchs, A., Yu, G., et al. (1997). Antitumor activity of the novel human breast cancer growth inhibitor, mammary-derived growth inhibitor-related gene, MRG. *Cancer Res* 57, 3084-3091.

Shono, T., Tofilon, P.J., Bruner, J.M., Owolabi, O., and Lang, F.F. (2001). Cyclooxygenase-2 expression in human gliomas: prognostic significance and molecular correlations. *Cancer Res* 61, 4375-4381.

Simons, K., and Toomre, D. (2000). Lipid rafts and signal transduction. *Nat Rev Mol Cell Biol* 1, 31-39.

Simons, K., and Vaz, W.L. (2004). Model systems, lipid rafts, and cell membranes. *Annu Rev Biophys Biomol Struct* 33, 269-295.

Singh, B., Berry, J.A., Vincent, L.E., and Lucci, A. (2006). Involvement of IL-8 in COX-2-mediated bone metastases from breast cancer. *J Surg Res* 134, 44-51.

Singh, S.K., Hawkins, C., Clarke, I.D., Squire, J.A., Bayani, J., Hide, T., et al. (2004). Identification of human brain tumour initiating cells. *Nature* 432, 396-401.

Slipicevic, A., Jorgensen, K., Skrede, M., Rosnes, A.K., Troen, G., Davidson, B., et al. (2008). The fatty acid binding protein 7 (FABP7) is involved in proliferation and invasion of melanoma cells. *BMC Cancer* 8, 276.

Smith, A.J., Sanders, M.A., Juhlmann, B.E., Hertzler, A.V., and Bernlohr, D.A. (2008). Mapping of the hormone-sensitive lipase binding site on the adipocyte fatty acid-binding protein (AFABP). Identification of the charge quartet on the AFABP/aP2 helix-turn-helix domain. *J Biol Chem* 283, 33536-33543.

Snowden, S., and Nelson, R. (2011). The effects of nonsteroidal anti-inflammatory drugs on blood pressure in hypertensive patients. *Cardiol Rev* 19, 184-191.

Sorlie, T., Perou, C.M., Tibshirani, R., Aas, T., Geisler, S., Johnsen, H., et al. (2001). Gene expression patterns of breast carcinomas distinguish tumor subclasses with clinical implications. *Proc Natl Acad Sci U S A* 98, 10869-10874.

Spencer, L., Mann, C., Metcalfe, M., Webb, M., Pollard, C., Spencer, D., et al. (2009). The effect of omega-3 FAs on tumour angiogenesis and their therapeutic potential. *Eur J Cancer* 45, 2077-2086.

Spite, M., Norling, L.V., Summers, L., Yang, R., Cooper, D., Petasis, N.A., et al. (2009). Resolvin D2 is a potent regulator of leukocytes and controls microbial sepsis. *Nature* 461, 1287-1291.

Stockhausen, M.T., Kristoffersen, K., and Poulsen, H.S. (2012). Notch signaling and brain tumors. *Adv Exp Med Biol* 727, 289-304.

Storch, J., and Corsico, B. (2008). The emerging functions and mechanisms of mammalian fatty acid-binding proteins. *Annu Rev Nutr* 28, 73-95.

Storch, J., and Thumser, A.E. (2010). Tissue-specific functions in the fatty acid-binding protein family. *J Biol Chem* 285, 32679-32683.

Strokin, M., Sergeeva, M., and Reiser, G. (2003). Docosahexaenoic acid and arachidonic acid release in rat brain astrocytes is mediated by two separate isoforms of phospholipase A2 and is differently regulated by cyclic AMP and Ca<sup>2+</sup>. *Br J Pharmacol* 139, 1014-1022.

Stupp, R., Hegi, M.E., Mason, W.P., van den Bent, M.J., Taphoorn, M.J., Janzer, R.C., et al. (2009). Effects of radiotherapy with concomitant and adjuvant temozolomide versus radiotherapy alone on survival in glioblastoma in a randomised phase III study: 5-year analysis of the EORTC-NCIC trial. *Lancet Oncol* 10, 459-466.

Sun, Y.P., Oh, S.F., Uddin, J., Yang, R., Gotlinger, K., Campbell, E., et al. (2007). Resolvin D1 and its aspirin-triggered 17R epimer. Stereochemical assignments, anti-inflammatory properties, and enzymatic inactivation. *J Biol Chem* 282, 9323-9334.

Takaoka, N., Takayama, T., Teratani, T., Sugiyama, T., Mugiya, S., and Ozono, S. (2011). Analysis of the regulation of fatty acid binding protein 7 expression in human renal carcinoma cell lines. *BMC Mol Biol* 12, 31.

Tan, N.S., Shaw, N.S., Vinckenbosch, N., Liu, P., Yasmin, R., Desvergne, B., et al. (2002). Selective cooperation between fatty acid binding proteins and peroxisome proliferator-activated receptors in regulating transcription. *Mol Cell Biol* 22, 5114-5127.

Tanabe, T., and Tohnai, N. (2002). Cyclooxygenase isozymes and their gene structures and expression. *Prostaglandins Other Lipid Mediat* 68-69, 95-114.

Tang, X.Y., Umemura, S., Tsukamoto, H., Kumaki, N., Tokuda, Y., and Osamura, R.Y. (2010). Overexpression of fatty acid binding protein-7 correlates with basal-like subtype of breast cancer. *Pathol Res Pract* 206, 98-101.

- Taniura, S., Kamitani, H., Watanabe, T., and Eling, T.E. (2002). Transcriptional regulation of cyclooxygenase-1 by histone deacetylase inhibitors in normal human astrocyte cells. *J Biol Chem* 277, 16823-16830.
- Thiel, A., Mrena, J., and Ristimaki, A. (2011). Cyclooxygenase-2 and gastric cancer. *Cancer Metastasis Rev* 30, 387-395.
- Thompson, B.R., Mazurkiewicz-Munoz, A.M., Suttles, J., Carter-Su, C., and Bernlohr, D.A. (2009). Interaction of adipocyte fatty acid-binding protein (AFABP) and JAK2: AFABP/aP2 as a regulator of JAK2 signaling. *J Biol Chem* 284, 13473-13480.
- Thorens, B. (2012). Sensing of glucose in the brain. *Handb Exp Pharmacol*, 277-294.
- Thureson, E.D., Lakkides, K.M., Rieke, C.J., Sun, Y., Wingerd, B.A., Micielli, R., et al. (2001). Prostaglandin endoperoxide H synthase-1: the functions of cyclooxygenase active site residues in the binding, positioning, and oxygenation of arachidonic acid. *J Biol Chem* 276, 10347-10357.
- Tsitlakidis, A., Foroglou, N., Venetis, C.A., Patsalas, I., Hatzisotiriou, A., and Selviaridis, P. (2010). Biopsy versus resection in the management of malignant gliomas: a systematic review and meta-analysis. *J Neurosurg* 112, 1020-1032.
- Tso, C.L., Freije, W.A., Day, A., Chen, Z., Merriman, B., Perlina, A., et al. (2006). Distinct transcription profiles of primary and secondary glioblastoma subgroups. *Cancer Res* 66, 159-167.
- Uhrbom, L., Kastemar, M., Johansson, F.K., Westermarck, B., and Holland, E.C. (2005). Cell type-specific tumor suppression by Ink4a and Arf in Kras-induced mouse gliomagenesis. *Cancer Res* 65, 2065-2069.
- Umemoto, T., and Fujiki, Y. (2012). Ligand-dependent nucleo-cytoplasmic shuttling of peroxisome proliferator-activated receptors, PPARAlpha and PPARgamma. *Genes Cells*, doi: 10.1111/j.1365-2443.2012.01607.
- Vecchio, A.J., Simmons, D.M., and Malkowski, M.G. (2010). Structural basis of fatty acid substrate binding to cyclooxygenase-2. *J Biol Chem* 285, 22152-22163.
- Verhaak, R.G., Hoadley, K.A., Purdom, E., Wang, V., Qi, Y., Wilkerson, M.D., et al. (2010). Integrated genomic analysis identifies clinically relevant subtypes of glioblastoma characterized by abnormalities in PDGFRA, IDH1, EGFR, and NF1. *Cancer Cell* 17, 98-110.

Wada, M., DeLong, C.J., Hong, Y.H., Rieke, C.J., Song, I., Sidhu, R.S., et al. (2007). Enzymes and receptors of prostaglandin pathways with arachidonic acid-derived versus eicosapentaenoic acid-derived substrates and products. *J Biol Chem* 282, 22254-22266.

Wagemakers, M., van der Wal, G.E., Cuberes, R., Alvarez, I., Andres, E.M., Buxens, J., et al. (2009). COX-2 Inhibition Combined with Radiation Reduces Orthotopic Glioma Outgrowth by Targeting the Tumor Vasculature. *Transl Oncol* 2, 1-7.

Wagner, K.D., Benchetrit, M., Bianchini, L., Michiels, J.F., and Wagner, N. (2011). Peroxisome proliferator-activated receptor beta/delta (PPARbeta/delta) is highly expressed in liposarcoma and promotes migration and proliferation. *J Pathol* 224, 575-588.

Wagner, K.D., and Wagner, N. (2010). Peroxisome proliferator-activated receptor beta/delta (PPARbeta/delta) acts as regulator of metabolism linked to multiple cellular functions. *Pharmacol Ther* 125, 423-435.

Wan, Z., Shi, W., Shao, B., Shi, J., Shen, A., Ma, Y., et al. (2011). Peroxisome proliferator-activated receptor gamma agonist pioglitazone inhibits beta-catenin-mediated glioma cell growth and invasion. *Mol Cell Biochem* 349, 1-10.

Wang, J., Wang, C., Meng, Q., Li, S., Sun, X., Bo, Y., et al. (2012). siRNA targeting Notch-1 decreases glioma stem cell proliferation and tumor growth. *Mol Biol Rep* 39, 2497-2503.

Watanabe, K., Tachibana, O., Sata, K., Yonekawa, Y., Kleihues, P., and Ohgaki, H. (1996). Overexpression of the EGF receptor and p53 mutations are mutually exclusive in the evolution of primary and secondary glioblastomas. *Brain Pathol* 6, 217-223; discussion 223-214.

Westphal, M., Hilt, D.C., Bortey, E., Delavault, P., Olivares, R., Warnke, P.C., et al. (2003). A phase 3 trial of local chemotherapy with biodegradable carmustine (BCNU) wafers (Gliadel wafers) in patients with primary malignant glioma. *Neuro Oncol* 5, 79-88.

Weylandt, K.H., Chiu, C.Y., Gomolka, B., Waechter, S.F., and Wiedenmann, B. (2012). Omega-3 fatty acids and their lipid mediators: towards an understanding of resolvins and protectin formation. *Prostaglandins Other Lipid Mediat* 97, 73-82.

Willson, T.M., Cobb, J.E., Cowan, D.J., Wiethe, R.W., Correa, I.D., Prakash, S.R., et al. (1996). The structure-activity relationship between

peroxisome proliferator-activated receptor gamma agonism and the antihyperglycemic activity of thiazolidinediones. *J Med Chem* 39, 665-668.

Wolfrum, C., Borrmann, C.M., Borchers, T., and Spener, F. (2001). Fatty acids and hypolipidemic drugs regulate peroxisome proliferator-activated receptors alpha - and gamma-mediated gene expression via liver fatty acid binding protein: a signaling path to the nucleus. *Proc Natl Acad Sci U S A* 98, 2323-2328.

Xu, K., Chang, C.M., Gao, H., and Shu, H.K. (2009). Epidermal growth factor-dependent cyclooxygenase-2 induction in gliomas requires protein kinase C-delta. *Oncogene* 28, 1410-1420.

Xu, K., and Shu, H.K. (2007). EGFR activation results in enhanced cyclooxygenase-2 expression through p38 mitogen-activated protein kinase-dependent activation of the Sp1/Sp3 transcription factors in human gliomas. *Cancer Res* 67, 6121-6129.

Xu, L., Han, C., Lim, K., and Wu, T. (2006). Cross-talk between peroxisome proliferator-activated receptor delta and cytosolic phospholipase A(2)alpha/cyclooxygenase-2/prostaglandin E(2) signaling pathways in human hepatocellular carcinoma cells. *Cancer Res* 66, 11859-11868.

Xu, L., Han, C., and Wu, T. (2006). A novel positive feedback loop between peroxisome proliferator-activated receptor-delta and prostaglandin E2 signaling pathways for human cholangiocarcinoma cell growth. *J Biol Chem* 281, 33982-33996.

Xu, L.Z., Sanchez, R., Sali, A., and Heintz, N. (1996). Ligand specificity of brain lipid-binding protein. *J Biol Chem* 271, 24711-24719.

Yang, H.Y., Lieska, N., Shao, D., Kriho, V., and Pappas, G.D. (1994). Proteins of the intermediate filament cytoskeleton as markers for astrocytes and human astrocytomas. *Mol Chem Neuropathol* 21, 155-176.

Yang, L., Olsson, B., Pfeifer, D., Jonsson, J.I., Zhou, Z.G., Jiang, X., et al. (2010). Knockdown of peroxisome proliferator-activated receptor-beta induces less differentiation and enhances cell-fibronectin adhesion of colon cancer cells. *Oncogene* 29, 516-526.

Yang, Y.P., Chien, Y., Chiou, G.Y., Cherng, J.Y., Wang, M.L., Lo, W.L., et al. (2012). Inhibition of cancer stem cell-like properties and reduced chemoradioresistance of glioblastoma using microRNA145 with cationic polyurethane-short branch PEI. *Biomaterials* 33, 1462-1476.

Yazaki, M., Kashiwagi, K., Aritake, K., Urade, Y., and Fujimori, K. (2012). Rapid degradation of cyclooxygenase-1 and hematopoietic prostaglandin D synthase through ubiquitin-proteasome system in response to intracellular calcium level. *Mol Biol Cell* 23, 12-21.

Yuan, C., Sidhu, R.S., Kuklev, D.V., Kado, Y., Wada, M., Song, I., et al. (2009). Cyclooxygenase Allosterism, Fatty Acid-mediated Cross-talk between Monomers of Cyclooxygenase Homodimers. *J Biol Chem* 284, 10046-10055.

Zaric, J., and Ruegg, C. (2005). Integrin-mediated adhesion and soluble ligand binding stabilize COX-2 protein levels in endothelial cells by inducing expression and preventing degradation. *J Biol Chem* 280, 1077-1085.

Zhang, H., Rakha, E.A., Ball, G.R., Spiteri, I., Aleskandarany, M., Paish, E.C., et al. (2010). The proteins FABP7 and OATP2 are associated with the basal phenotype and patient outcome in human breast cancer. *Breast Cancer Res Treat* 121, 41-51.

Zhao, C., Deng, W., and Gage, F.H. (2008). Mechanisms and functional implications of adult neurogenesis. *Cell* 132, 645-660.

Zhao, Y., Calon, F., Julien, C., Winkler, J.W., Petasis, N.A., Lukiw, W.J., et al. (2011). Docosahexaenoic acid-derived neuroprotectin D1 induces neuronal survival via secretase- and PPARgamma-mediated mechanisms in Alzheimer's disease models. *PLoS One* 6, e15816.

Zhou, Y.C., and Waxman, D.J. (1999). STAT5b down-regulates peroxisome proliferator-activated receptor alpha transcription by inhibition of ligand-independent activation function region-1 trans-activation domain. *J Biol Chem* 274, 29874-29882.

Zhu, Y., Guignard, F., Zhao, D., Liu, L., Burns, D.K., Mason, R.P., et al. (2005). Early inactivation of p53 tumor suppressor gene cooperating with NF1 loss induces malignant astrocytoma. *Cancer Cell* 8, 119-130.